Spike timing-dependent plasticity and basal synaptic transmission characterization at hippocampal Schaffer collateral –CA1 synapses of adult APP/PS1 Alzheimer's disease mice

Thesis

for the degree of

doctor rerum naturalium (Dr. rer. nat.)

approved by the Faculty of Natural Sciences of Otto von Guericke University Magdeburg

by M.Sc., Machhindra Garad

born on _ 04/06/1989 in Agalgaon Solapur, India

Examiner: Prof. Dr. Volkmar Leßmann

Prof. Dr. Clive Bramham

submitted on: 02/03/2021 defended on:

07/10/2021

Dedicated to my parents, Aai, and Nana, and two greatest minds of the century, Stephen Hawking, and APJ Abdul Kalam!

The greatest enemy of knowledge is not ignorance; it is the illusion of knowledge!

- Stephen Hawking

M.Sc. Garad, Machhindra

Spike timing-dependent plasticity and basal synaptic transmission characterization at hippocampal Schaffer collateral -CA1 synapses of adult APP/PS1 Alzheimer's disease mice

Abstract:

Spike timing-dependent plasticity (STDP) is a Hebbian form of synaptic plasticity, and a strong candidate to underlie learning and memory at single neuron level. STDP has been studied profoundly in 1-month old mice (juveniles) and 2-3 months old mice (young adults). However, to the best of our knowledge, STDP in mature adults, e.g. 6 months old mice, has not been described until today. Using whole cell patch clamp recordings in CA1 pyramidal neurons of acute transversal hippocampal slices, we investigated timing-dependent long-term potentiation (t-LTP) induced by distinct STDP paradigms at Schaffer collateral (SC)-CA1 synapses in 6 months old C57Bl/6J mice (fully developed system; adults). T-LTP was induced by pairing 1 presynaptic half maximal stimulation (subthreshold EPSP) with 1 postsynaptic action potential (AP) i.e. 1:1 STDP paradigm or 1 presynaptic stimulation paired with 4 postsynaptic APs i.e 1:4 STDP paradigm. Our results show that t-LTP can be induced even in fully developed adult mice with different and even low repeat STDP paradigms. Distinct STDP paradigms elicited significant t-LTP at hippocampal SC-CA1 synapses of adult animals with similar efficiency. In comparison to juveniles, hippocampal SC-CA1 synapses of 6 months old mice displayed decreased t-LTP magnitude in response to 6x 1:1 stimulation (+10 ms spike timing interval), while higher t-LTP magnitude in response to 6x 1:1 stimulation (-10 ms spike timing interval). While similar t-LTP magnitudes, induced by 6x 1:4 stimulation (+10 ms spike timing interval), were observed in adults and juveniles. Moreover, adult mice expressed significantly decreased intrinsic excitability of CA1 pyramidal neurons and decreased paired-pulse facilitation at SC-CA1 synapses in the hippocampus compared to the results obtained in juvenile animals. Adults showed substantially increased $GABA_B$ receptor mediated EPSP components at SC-CA1 synapses compared to juveniles. The results from this dissertation indicate that developmental maturation alters STDP, intrinsic excitability of CA1 neurons, and short-term plasticity at SC-CA1 synapses in the hippocampus of 6 months old mice.

Alzheimer’s disease (AD) is a multifaceted neurodegenerative disorder characterized by progressive and irreversible cognitive decline, with no disease-modifying therapy until today. Although several studies reported impaired LTP in AD mouse models, the impact of Amyloid β (Aβ) pathology on STDP in the hippocampus remains unknown. Henceforth, we investigated t-LTP at SC-CA1 synapses in the hippocampus of 6 months old (adult) APP/PS1 AD model mice. Adult APP/PS1 mice displayed intact t-LTP induced by low as well as high repeat 1:1 or 1:4 STDP paradigms when the position of Aβ plaques relative to the recorded CA1 neuron in the slice were not considered. However, when Aβ plaques were live stained with the fluorescent dye Methoxy-X04, we observed that in CA1 neurons with their somata <200 µm away from the border of the nearest Aβ plaque, t-LTP induced by 6x 1:4 stimulation was significantly impaired, while t-LTP was unaltered in CA1 neurons >200 µm away from plaques. Treatment of APP/PS1 mice with the anti-inflammatory drug fingolimod or voluntary running that we previously showed to alleviate synaptic deficits in this AD mouse model did not rescue the impaired t-LTP. Further, adult APP/PS1 mice expressed intact basal electrical properties of CA1 pyramidal neurons and spontaneous excitatory and inhibitory synaptic transmission at SC-CA1 synapses. Our data reveal that AD pathology in 6 months old APP/PS1 mice disrupts t-LTP in an Aβ plaque distance-dependent manner, and cannot be improved by fingolimod or voluntary running that have both been shown to rescue conventional LTP at SC-CA1 synapses in APP/PS1 mice. Finally, we observed that the Aβ pathology in adult APP/PS1 mice does not compromise basal electrical properties of CA1 pyramidal neurons and synaptic properties at SC-CA1 synapses.

M.Sc. Garad, Machhindra

Spike timing-dependent plasticity and basal synaptic transmission characterization at hippocampal Schaffer collateral -CA1 synapses of adult APP/PS1 Alzheimer's disease mice

Zusammenfassung:

Spike Timing-abhängige Plastizität (STDP) ist eine Hebbsche Form der synaptischen Plastizität und ein Kandidat, um Lernen und Gedächtnis auf Einzelzelleben zu untersuchen (Hebbsche Lernregel). Die STDP wurde bei einen Monat alten Mäusen (Jungtiere) und 2-3 Monate alten Mäusen (junge Erwachsene) eingehend untersucht. Jedoch ist die STDP in erwachsenen, (z.B. 6 Monate alten) Mäusen, nach unserem besten Wissen bisher nicht beschrieben worden. Unter Verwendung von Ganzzell-Patch-Clamp-Ableitungen in CA1-Pyramidenneuronen aus akuten transversalen Schnitten des Hippokampus untersuchten wir die zeitabhängige Langzeitpotenzierung (t-LTP), die durch unterschiedliche STDP-Paradigmen an Schaffer-Kollateral (SC)-CA1 Synapsen in 6 Monate alten C57Bl/6J-Mäusen (voll entwickelte erwachsene Tiere) induziert wird. Unsere Ergebnisse zeigen, dass die t-LTP bei voll entwickelten erwachsenen Mäusen mit unterschiedlichen STDP-Paradigmen induziert werden kann, die sich hinsichtlich der Anzahl und der Frequenz der synaptischen Stimulationen unterschieden. T-LTP konnte auch mit einem STDP-Paradigma ausgelöst werden, das aus nur sechs wiederholten prä- und postsynaptischen Stimulationen bestand (6x 1:1 bzw. 6x 1:4 t-LTP). Die verschiedenen STDP-Paradigmen zeigten dabei eine ähnliche Effizienz in der Induktion und Expression einer signifikanten t-LTP an den SC-CA1 Synapsen von 6 Monate alten Mäusen. Im Gegensatz zu den Resultaten in Jungtieren zeigten 6 Monate alte Mäuse eine geringere t-LTP als Reaktion auf 6x 1:1-Stimulation (+10 ms Spike-Timing-Intervall), während eine höhere t-LTP als Reaktion auf 6x 1:1-Stimulation (-10 ms Spike-Timing-Intervall) an den SC-CA1 Synapsen. Während ähnliche t-LTP, induziert durch 6x 1:4 Stimulation (+10 ms Spike-Timing-Intervall), bei Erwachsenen und Jungtieren beobachtet wurden. Darüber hinaus zeigten die adulten Tiere eine signifikant verminderte intrinsische Erregbarkeit in den CA1-Pyramiden-Neuronen und eine verminderte gepaarte Puls-Bahnung an SC-CA1 Synapsen des Hippocampus. Außerdem konnte an SC-CA1 Synapsen eine im Vergleich zu den juvenilen Mäusen deutlich erhöhte $GABA_{(B)}$-Rezeptor-vermittelte EPSP-Komponenten nachgewiesen werden. Insgesamt deuten die Ergebnisse der

vorliegenden Dissertation darauf hin, dass die intrinsische Erregbarkeit von CA1-Neuronen, die Entwicklung der STDP und die Kurzzeit-Plastizität an SC-CA1-Synapsen im Hippocampus in 6 Monate alten Mäusen gegenüber juvenilen Mäusen deutlich verändert sind.

Die Alzheimer-Krankheit (AD) ist eine vielschichtige neurodegenerative Erkrankung, die durch einen fortschreitenden und irreversiblen kognitiven Rückgang gekennzeichnet ist und für die es bisher keine krankheitsmodifizierende Therapie gibt. Obwohl mehrere Studien über LTP-Störungen im Hippocampus bei der AD-Pathologie berichten, war ihr Einfluss auf die STDP im Hippocampus bisher unbekannt. Aus diesem Grund untersuchten wir die t-LTP an SC-CA1 Synapsen im Hippocampus von 6 Monate alten APP/PS1 AD-Mäusen. Adulte APP/PS1 Tiere zeigten eine intakte t-LTP, die sowohl durch niedrige als auch hohe Wiederholungsraten von 1:1 oder 1:4 STDP-Paradigmen induziert werden konnte, wenn die Lokalisation von Amyloid-Plaques β (Aβ) in Relation zu der abgeleiteten CA1-Pyramidenzelle in den Schnitten unberücksichtigt blieben. Allerdings beobachteten wir, dass in CA1-Neuronen, deren Somata <200 µm vom Rand der nächstgelegenen Plaque Aβ entfernt waren, die durch 6x 1:4-Stimulation induzierte t-LTP in APP/PS1-Mäusen signifikant beeinträchtigt war, wohingegen die t-LTP in CA1-Neuronen >200 µm von den Plaques entfernt, unverändert war. Die chronische Behandlung von APP/PS1-Mäusen mit Fingolimod oder den freiwilligen Laufen auf einem Laufrad war nicht ausreichend, um die beeinträchtigte t-LTP in APP/PS1-Mäusen zu retten. Darüber hinaus zeigten APP/PS1-Mäuse intakte basale elektrische Eigenschaften der CA1-Pyramidenneurone und unveränderte spontane exzitatorische und inhibitorische synaptische Ströme in CA1-Neuronen. Insgesamt zeigen unsere Daten, dass in AD-Modellmäusen, die APP- und PS1-Proteinvarianten mit Mutationen überexprimieren, die in Patienten mit familärer AD vorkommen, die t-LTP, an SC-CA1 Synapsen in einer Aβ Plaque-distanzabhängigen Weise gestört wird. Die neuronale Erregbarkeit der CA1-Pyramidenzellen und die basala synaptische Transmission an SC-CA1 Synapsen des Hippocampus im von 6 Monate alten Mäusen ist in APP/PS1-Mäusen hingegen unbeeinträchtigt.

Abbreviations:

Δt	delta time, spike timing in ms
Aβ	amyloid beta
ACSF	artificial cerebrospinal fluid
AD	Alzheimer's disease
AMPAR	α-amino-3-hydroxy-5-methylisoxazole-4-propionic acid receptor
ANOVA	analysis of variance
AP	action potential
APP	amyloid precursor protein
bAP	backpropagating action potential
BDNF	brain-derived neurotrophic factor
CA1-CA3	*cornu ammonis 1-3* (regional differentiation within the hippocampus)
CaMKII	calcium/calmodulin-dependent protein kinase II
CNS	central nervous system
CREB	cAMP response element-binding protein
DG	dentate gyrus
DL-APV	DL-2-amino-5-phosphonopentanoic acid
DMSO	dimethyl sulfoxide
EC	entorhinal cortex
E(I)PSC	excitatory (inhibitory) postsynaptic current
EPSP	excitatory postsynaptic potential
GABA	gamma-aminobutyric acid
ISI	interstimulus interval
LJP	liquid junction potential
LTD	long-term depression
LTP	long-term potentiation
NMDAR	N-methyl- D-aspartate receptor
PPF	paired-pulse facilitation
PPR	paired-pulse ratio
Rin	input resistance
RMP	resting membrane potential
SC	Schaffer collateral
SC-CA1	Schaffer collateral - *Cornu Ammonis 1*
SEM	standard error of the mean

STDP	spike timing-dependent plasticity
t-LTP	timing-dependent long-term potentiation
WT	wild type

Pharmacological tools (chemicals):

Picrotoxin	(CAS Number 124-87-8)	Sigma Aldrich
Bicuculine	(CAS Number 485-49-4)	Sigma Aldrich
Tetrodotoxin	(CAS Number 4368-28-9)	TOCRIS
APV	(CAS Number 79055-68-8)	TOCRIS
DNQX	(CAS Number 2379-57-9)	TOCRIS

List of Figures:

19. SC-CA1 synapses in 6 months old APP/PS1 mice exhibited intact t-LTP induced by 6x 1:1 or 6x 1:4 stimulations
20. Pairing of one postsynaptic AP with one presynaptic stimulation for negative spike timings (6x 1:1, Δt=-10 ms) induced t-LTP at SC-CA1 synapses in adult APP/PS1 mice
21. High repeat STDP paradigm 100x 1:1 induced t-LTP at SC-CA1 synapses in 6 months old APP/PS1 mice
22. Six months old APP/PS1 mice expressed Aβ plaque distance-dependent t-LTP impairments at SC-CA1 synapses in the hippocampus
23. Impaired t-LTP at SC-CA1 synapses in 6 months old APP/PS1 mice could not be restored by chronic fingolimod or voluntary running treatments
24. Intact basal electrical and synaptic properties of CA1 pyramidal neurons in 6 months old APP/PS1 mice
25. Unaltered basal electrical and synaptic properties of CA1 pyramidal neurons in the vicinity of Aβ plaques in 6 months old APP/PS1 mice
26. Spontaneous and miniature excitatory synaptic transmission in CA1 neurons of 6 months old adult APP/PS1 mice
27. Spontaneous and miniature inhibitory synaptic transmission in CA1 neurons of adult APP/PS1 mice
28. Six months old APP/PS1 mice showed deficits in intrinsic excitability of CA1 neurons and synaptic signal integration at SC-CA1 synapses

Table of Contents:

Introduction

1 State of the art:

1.1 Synaptic plasticity: a cellular/synaptic substrate of learning and memory

Sensory and/or motor experiences are essential for the refinement of neuronal circuits during development and for learning and memory in the adult brain. Experiences that disrupt normal activity patterns can lead to largescale network remodeling and marked changes in neural response properties. How experience-dependent plasticity or learning and memory are achieved in the brain is a central question in neuroscience and likely to be mediated by activity-dependent synaptic modifications (Hughes, 1958).

Activity-dependent changes in synaptic strength, termed as synaptic plasticity, are believed to be crucial for the information processing in the mammalian brain. Furthermore, synaptic plasticity is one of the important foundations of learning and memory. In particular, synaptic plasticity plays a critical role in the formation of synapses, proper synaptic connections and mature neural circuitry during development (Bear & Malenka, 1994; Gaiarsa et al., 2002). Synaptic plasticity enables neuronal synapses to adapt to changing circumstances and encode information. The classical models for studying activity-dependent synaptic plasticity are long-term potentiation (LTP) and long-term depression (LTD), which represent an increase and a decrease in synaptic strength, respectively (Bear & Malenka, 1994).

1.1.1 Long-term potentiation

For the induction of long-lasting increase in synaptic strength (LTP), there are broad spectrums of experimental protocols. Theta burst stimulation (TBS), high-frequency stimulation (HFS) or pairing low-frequency presynaptic stimulation with postsynaptic depolarization are usually used to induce LTP (Larson and Munkacsy, 2015; Abrahamsson et al., 2016; Bliss & Lømo, 1973; Bliss & Collingridge, 1993). At the single cell level, LTP is classically induced by synchronous activation of pre- and postsynaptic components using theta-burst pairing and pairing protocols (Gustafsson et al., 1987; Liao et al.,1995). LTD, on the other hand, can be induced by different patterns of activity, such as prolonged low-frequency presynaptic stimulation (Kirkwood & Bear, 1994; Mulkey & Malenka, 1992). The LTP/LTD induction stimulation causes structural and functional modifications of pre- and

postsynaptic compartments which in turn results into induction and expression of LTP/LTD (compare Huang, 1998; Malenka and Bear, 2004; Citri and Malenka, 2008).

The theory of an ever-changing synapse offers an attractive framework for the regulation of synaptic strength. Changes in the probability of neurotransmitter released into the synaptic cleft and how effectively postsynaptic neurons respond to neurotransmitters, i.e., alteration of the neurotransmitter receptors, assist to accomplish synaptic plasticity (Gaiarsa et al., 2002; Gerrow & Triller, 2010). The postsynaptic calcium elevation is the most important aspect in the synaptic plasticity at both excitatory and inhibitory synapses (Gerrow & Triller, 2010). N-methyl D-aspartate (NMDA) receptor-dependent LTP and LTD in the *Cornu Ammonis* (CA) 1 region of the hippocampus remain the most extensively studied and therefore prototypic forms of synaptic plasticity (Bliss & Lømo, 1973; Bliss & Collingridge, 1993; Bosch et al., 2014).

Together, LTP and LTD allow activity-dependent bidirectional modification of synaptic strength, thus serving as promising candidates for the synaptic basis of learning and memory (Bliss & Collingridge, 1993; Ito, 2005; Siegelbaum & Kandel, 1991). The cellular and molecular mechanisms underlying the various forms of LTP and LTD, which can be elicited in the brain, promotes many functions including learning and memory. Two features of LTP-the associativity and input specificity-match the properties of some forms of learning and memory, suggesting that LTP may underlie these cognitive functions. However, it also should be noted that LTP and LTD are certainly not the only means by which the activity generated by experience can modify neural circuit behavior. As an example, metaplasticity, which manifests as a change in the ability to induce subsequent synaptic plasticity, and homeostatic plasticity mechanisms maintain average neuronal activity levels that dynamically adjust synaptic strengths and experience-driven changes in neuronal intrinsic excitability (compare reviews Abraham & Bear, 1996; Turrigiano & Nelson, 2004; Zhang & Linden, 2003). Given the importance of plastic changes in the brain, neurons likely use every type of plasticity mechanism at their disposal.

1.1.2 Spike timing-dependent plasticity

Mammalian neural circuits are modified during both development and adulthood through experience-dependent mechanisms (Buonomano & Merzenich, 1998; Gilbert, 1998; Wiesel & Hubel, 1965), and these modifications are thought to depend on activity-dependent synaptic

plasticity. The concept of synaptic plasticity signifies the key to today's research into information processing in the brain. To understand the causal relationship between the chain of events: sensory/motor experience → neuronal activity → synaptic changes → functional circuit modification, an important step is to characterize the synaptic learning rules, i.e., how the spatiotemporal patterns of neuronal activity determine the changes in synaptic strength. The best-known learning rule, which has successfully guided experimental and theoretical studies, was proposed by Donald Hebb. In his influential postulate on the cellular basis for learning, Hebb stated that-

"when an axon of cell A is near enough to excite a cell B and repeatedly or persistently takes part in firing it, some growth process or metabolic change takes place in one or both cells such that A's efficiency, as one of the cells firing B, is increased"

Donald Hebb (1949)

Hebb speculated that repeatedly and persistently co-active cells should increase connective strength among populations of interconnected neurons as a means of storing a memory trace, also known as an engram. Direct support for Hebb's rule came from the discovery of LTP (Bliss & Lømo, 1973) and LTD (Mulkey & Malenka, 1992).

Spike timing-dependent plasticity (STDP) is a Hebbian form of synaptic plasticity, and a strong candidate to underlie circuit remodeling during development, as well as for learning and memory. STDP consists of precisely timed (near) coincident activation of pre- and postsynaptic neurons in forward or backward sequence that induces bidirectional and timing-dependent changes in synaptic efficacy (reviewed in Feldman, 2012). It has been demonstrated that bi-directional changes in synaptic strength can be induced in the hippocampus by temporal correlations in low frequency stimulation according to a STDP rule (Bi & Poo, 1998; Debanne et al., 1998; Edelmann et al., 2015; Edelmann & Lessmann, 2011; Markram et al., 1997; Wang et al., 2005). Recent STDP studies illustrate that, in addition to the temporal correlation, the order of presynaptic and postsynaptic spiking is critical in defining the direction of synaptic change (Bell et al., 1997; Bi & Poo, 1998; Debanne et al., 1998b; Froemke & Dan, 2002; Levy & Steward, 1983).

The signaling cascades involved in timing-dependent LTP (t-LTP) and LTD (t-LTD) depend on the STDP stimulation (number of repeats and frequency) and developmental stage of animal. Similar to conventional LTP and LTD, t-LTP and t-LTD also depend on NMDA receptor activation and subsequent postsynaptic Ca^{2+} rise (Bi & Poo, 1998; Debanne et al.,

1998b; Feldman, 2000; Magee & Johnston, 1997; Sjöström et al., 2001). The main three signaling pathways that mediate STDP are as follows:

1. NMDA receptor (NMDAR)-dependent t-LTP
2. NMDAR-dependent t-LTD
3. Metabotropic glutamate receptor (mGluR)-dependent and/or cannabinoid type 1 receptor (CB1R)-dependent t-LTD

In the following sections we describe each signaling pathway implicated in STDP.

1. NMDAR-dependent t-LTP

The aforementioned three mechanisms mediate STDP, with postsynaptic spikes providing an important component of postsynaptic depolarization. T-LTP induction requires the presynaptic activation (generating excitatory postsynaptic potential (EPSP)) milliseconds before the backpropagating action potential (bAP) in postsynaptic dendrites (pre-post, positive interval). The bAP facilitates Mg^{2+} unblocking of NMDARs allowing Ca^{2+} influx and thus lead to t-LTP induction. In addition, other types of interactions between EPSP and bAP could shape the t-LTP. For example, an EPSP can cause changes in the dendritic conductance which in turn affects the action potential (AP) backpropagation into the dendrites. In the hippocampus, the distal dendrites of CA1 neurons express a high density of A-type K^+ channels, which play a crucial role in regulating bAP (Hoffman et al., 1997). An EPSP that depolarizes the dendrites and inactivates these channels, can boost bAP which arrive after tens of milliseconds (Magee & Johnston, 1997; Watanabe et al., 2002). Consequently, this bAP boosting can increase the Ca^{2+} influx through voltage-sensitive Ca^{2+} channels (VSCCs), which in turn determines the t-LTP magnitude (Bi & Poo, 1998; Froemke et al., 2006; Magee & Johnston, 1997). Furthermore, α-amino-3-hydroxy-5-methylisoxazole-4-propionic acid receptor (AMPAR)-mediated EPSP provide local depolarization that boosts the supralinear interaction between NMDAR currents and the bAP, which results in t-LTP induction (Fuenzalida et al., 2010; Holbro et al., 2010).

2. NMDAR- dependent t-LTD

T-LTP or t-LTD induction are primarily determined by the magnitude and time course of calcium change, with brief, high calcium elevation leading to t-LTP, sustained moderate calcium elevation resulting in t-LTD, and low calcium elevation- leading to no plasticity (Lisman, 1989; Yang et al., 1999). The interaction between the EPSP and the bAP can explain

t-LTD (post-pre, negative interval), provided the bAP contains an afterdepolarization which lasts tens of milliseconds and all relevant Ca^{2+} enters the postsynaptic cell through NMDARs. The EPSP overlapping with the afterdepolarization leads to a moderate Ca^{2+} influx, which then leads to t-LTD induction (Karmarkar & Buonomano, 2002; Shouval et al., 2002). In another model, the bAP preceding an EPSP causes Ca^{2+} influx through VSCCs, that inactivates the NMDARs (Froemke et al., 2005; Rosenmund et al., 1995; Tong et al., 1995). Consequently, the reduced Ca^{2+} influx through NMDARs results in t-LTD (Bender et al., 2006; Bi & Poo, 1998; Froemke et al., 2005; Nevian & Sakmann, 2006). Moreover, the pairing EPSPs and bAPs at negative intervals results into sublinear summation of Ca^{2+} influx (Koester & Sakmann, 1998; Nevian & Sakmann, 2004).

3. Metabotropic glutamate receptor (mGluR)-dependent and/or cannabinoid type 1 receptor (CB1R)-dependent t-LTD

In this model, t-LTD induction requires postsynaptic group I metabotropic glutamate receptors (mGluRs) activation and Ca^{2+} influx through VSCCs (Bi & Poo, 1998; Karmarkar & Buonomano, 2002). mGluRs signaling can lead to phospholipase C (PLC) activation, and Ca^{2+} influx through VSCCs can facilitate mGluR-dependent-PLC activation (Fino et al., 2010; Hashimotodani et al., 2005; Maejima et al., 2005). Thus, PLC serves as a potential coincidence detector for t-LTD. Subsequently, PLC may generate inositol 1,4,5-triphosphate (IP3), which triggers Ca^{2+} release from internal stores via IP3 receptors (IP3Rs) (Bender et al., 2006). PLC activation and Ca^{2+} influx (through VSCCs and/or NMDARs, or release from internal stores) can promote endocannabinoid synthesis and release (Hashimotodani et al., 2007). It has been reported that signaling through presynaptic endocannabinoid receptors (CB1R) is also required for t-LTD (Bender et al., 2006; Nevian & Sakmann, 2006; Tzounopoulos et al., 2007), apparently by inhibition of presynaptic transmitter release (Chevaleyre et al., 2006). The mGluR and/or CB1R-dependent t-LTD is independent of postsynaptic NMDARs but often depends on presynaptic NMDARs (preNMDAR) (Rodríguez-Moreno & Paulsen, 2008). In the presynaptic coincidence detector model, each presynaptic activation supplies glutamate and depolarization to activate preNMDARs, while each postsynaptic spike induces a brief eCB signal that in turn activates presynaptic CB1Rs. The precise coactivation of preNMDARs and CB1Rs is required to drive t-LTD (Duguid & Sjöström, 2006; Sjöström et al., 2003). In the postsynaptic coincidence detector model, presynaptic stimulation activates mGluRs, while postsynaptic spikes activate VSCCs. The integration of mGluR and VSCC-derived calcium signals in the postsynapse plays a crucial

role in computation of post-pre spike timing (Bender et al., 2006; Nevian & Sakmann, 2006). The eCB signal then diffuses retrogradely to activate CB1Rs on presynaptic terminals and thereby reduce release probability (Bender et al., 2006). Alternatively, the eCB can activate CB1Rs on astrocytes that in turn signal to presynaptic terminals, possibly through preNMDARs, and decrease transmitter release (Min & Nevian, 2012). In **Figure 1**, the major signaling pathways implicated in STDP are outlined.

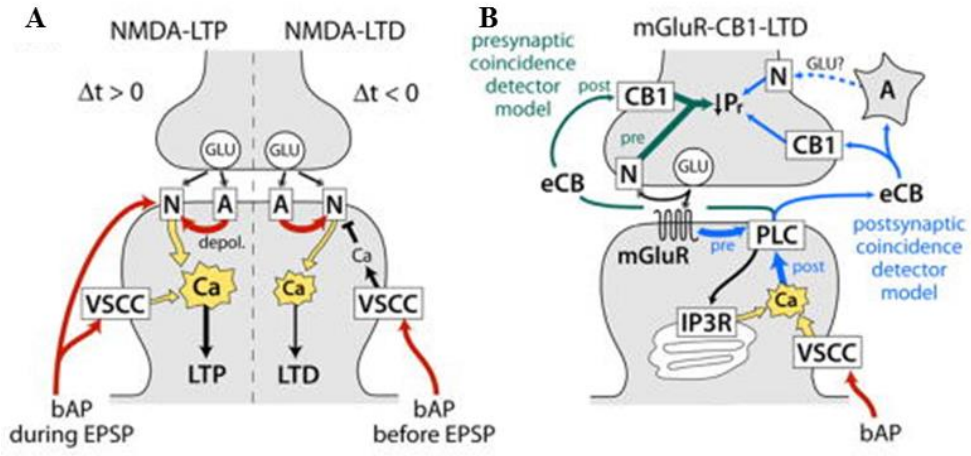

Figure 1. Cellular mechanisms for spike timing-dependent plasticity. (A) NMDA receptor-dependent t-LTP and t-LTD. N and A, NMDA and AMPA receptors. Red, depolarization. **(B)** mGluR and/or CB1R dependent t-LTD, the proposed presynaptic coincidence detector is shown in green, and the postsynaptic coincidence detector is displayed in blue. N- n-methyl d-aspartate (NMDA) receptor, A- α-amino-3-hydroxy-5-methylisoxazole-4-propionic acid (AMPA) receptor, GLU- glutamate, VSCC- voltage-sensitive Ca^{2+} channels, bAP- backpropagating action potential, mGluR- metabotropic glutamate receptor, PLC- phospholipase C, IP3R- inositol 1,4,5-triphosphate, eCB- endocannabinoids, CB1- endocannabinoid receptor 1, Pr- presynaptic neurotransmitter release probability, A- astrocyte; Figure modified after (Feldman, 2012).

In addition to the various intrinsic and extrinsic factors including the history of activity at the synapse (Larsen et al., 2014), dendritic location (Froemke et al., 2005; Sjöström & Häusser, 2006), and astrocytes (Valtcheva & Venance, 2016), availability of neuromodulators play a crucial role in STDP (Edelmann et al., 2017; Edelmann & Lessmann, 2011; Pawlak et al., 2010; Seol et al., 2007). Several studies have reported that STDP is under neuromodulatory control by acetylcholine, monoamines (dopamine, noradrenaline, serotonin), and other signaling molecules e.g. histamine (Edelmann et al., 2017; Gu, 2002; Pawlak et al., 2010; Seol et al., 2007)). Moreover, local signaling molecules, such as endocannabinoids (Cui et al.,

2016; Fino & Venance, 2010; Sjöström et al., 2003) and brain-derived neurotrophic factor (Edelmann et al., 2015; Lu et al., 2014), as well as blood-borne steroid hormones, can influence plasticity. Neuromodulation offers an attractive mechanism to understand the relationship between the millisecond-precision spike timing required for STDP and the much slower timescales of behavioral learning.

Compared with the traditional correlational forms of synaptic plasticity, STDP captures the importance of causality in determining the direction of synaptic modification, which is implied in Hebb's original postulate. STDP also opens up new avenues for understanding information coding and circuit plasticity that depend on the precise timing of neuronal spikes. Moreover, STDP has rapidly gained tremendous interest, perhaps because of its combination of elegant simplicity, biological plausibility, and computational power.

The hippocampus has been a key experimental system for synaptic plasticity studies concerning information processing mechanisms in the brain (Neves et al., 2008).

1.2 Hippocampal formation

The hippocampus is located in the medial temporal lobe, and belongs to the limbic system in the brain of humans and other mammals. It is a crucial structure for long-term memory, episodic memory and spatial navigation (spatial memory). The traditional excitatory trisynaptic pathway (entorhinal cortex (EC)- dentate gyrus (DG)- CA3- CA1) in the hippocampus constitutes major connectivity pathway thereby making it a perfect candidate to investigate the cellular principles of learning and memory. The laminated organization of the hippocampus is very useful for electrophysiological recordings, as it allows the stimulation of selective pathways and simultaneous recording of the evoked synaptic responses generated by a target population of neurons.

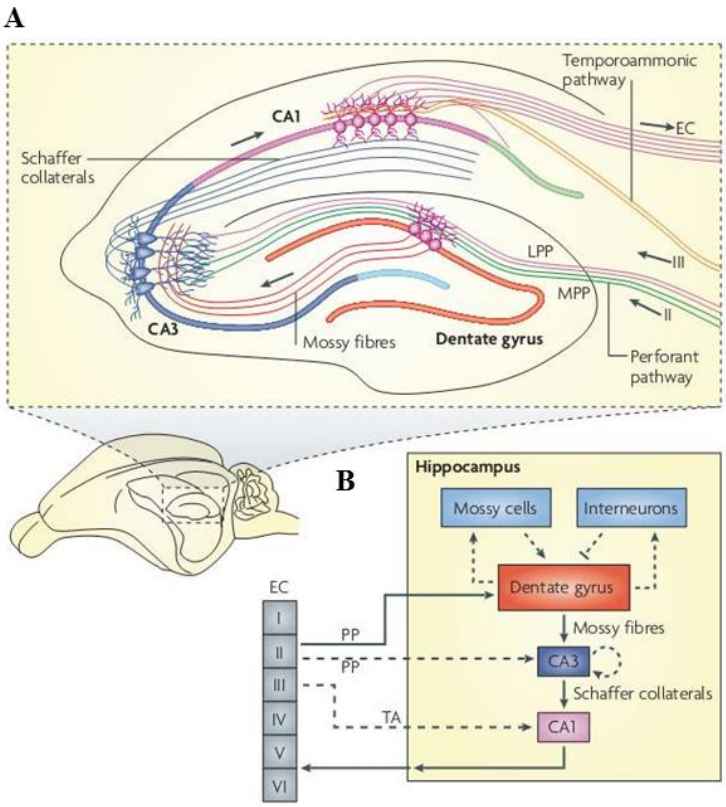

Figure 2. The neural circuitry representation in the hippocampus. (A) An illustration of the trisynaptic neural circuit and **(B)** the neural network in the hippocampus. The established trisynaptic circuit is presented by solid arrows. CA- *Cornu Ammonis 1-3*, EC- entorhinal cortex; LPP and MPP- lateral and medial perforant path, PP- perforant path, TA- temporoammonic path (Figure modified after Deng et al., 2010).

The basic anatomy of the hippocampal formation is illustrated in **Figure 2**. The neuronal network in the hippocampus is usually presented as a trisynaptic loop. The perforant pathway (lateral and medial) provides the major input which conveys polymodal sensory information from layer II neurons of the EC to the DG. The axons of perforant path form excitatory synaptic contacts with the granule cells of DG. The granule cells project to the proximal apical dendrites of CA3 pyramidal cells through the mossy fibers. The CA3 neurons send axons to ipsilateral CA1 pyramidal cells, which are designated as Schaffer collaterals (SC). The CA3 projections to contralateral CA3 and CA1 pyramidal cells termed as commissural connections. In addition to the sequential trisynaptic circuit, a dense associative network is present in the hippocampus which is responsible for interconnecting CA3 cells on the same side (i.e. associative fibers). CA3 pyramidal neurons also receive a direct input from layer II neurons of the EC, while distal apical dendrites of CA1 pyramidal cells receive a direct input from layer III neurons of the EC (temporoammonic pathway). CA1 neurons project to the

subiculum, are responsible for sending the hippocampal output back to the EC (layer V, VI) and therefore represent primary output of hippocampal network (Neves et al., 2008; Amaral & Lavenex, 2007).

1.3 Developmental maturation of central nervous system

Brain development is a remarkable process. As a fundamental developmental strategy, common to the mammalian central nervous system (CNS) including humans, primates and rodents, neurons present at birth increase synaptic density over a period through overproduction of their arborization and synaptic contacts, followed by an elimination or pruning phase of refinement (Andersen, 2003). In the rodent brain, synapses and receptors within most regions are overproduced during early postnatal life (till postnatal day (pnd) 20-21) and of these as much as 50% are eliminated during pnd 25-49. At pnd 60+, rodent brain represents adult levels of neurotransmitters and synaptic density (see review Semple et al., 2013). This activity-dependent pruning of excess synapses is assumed to play a crucial role in synaptic plasticity and serve as a mechanism for neuronal circuitry refinement, which in turn allows efficient processing of adult cognition. During development, the neurogenesis, synaptogenesis, gliogenesis and oligodendrocyte maturation coincide with developmentally regulated molecular and biochemical changes.

The synaptic plasticity rules change throughout many stages of brain development (Lohmann & Kessels, 2014). Postnatally, rodent hippocampus displays change from a period of excitatory synapses hyperplasticity to a mature stable level of plasticity (Lohmann & Kessels, 2014). Moreover, the induction and expression mechanisms underlying synaptic plasticity change with increasing postnatal age in the hippocampus (Buchanan & Mellor, 2007; Meredith et al., 2003; Yasuda et al., 2003). These developmental changes are correlated with the ability to perform hippocampal-dependent memory tasks (Dumas, 2005) as well as the maturation of NMDAR subunit complement (Barria & Malinow, 2002; Ritter et al., 2002).

Inhibition is crucial for neuronal signal integration and information processing (Brickley & Mody, 2012; Lovett-Barron et al., 2012). Inhibitory synaptic function undergoes profound transformation during postnatal development. In rodents, gamma-aminobutyric acid (GABA)-ergic inhibition is upregulated and does not mature until the second postnatal month in the hippocampus (Banks et al., 2002; Cohen et al., 2000; Danglot et al., 2006). In hippocampal

CA1 region, GABAergic inhibition plays a key role in network oscillations and synaptic plasticity (see reviews Mann & Paulsen, 2007; Mody, 2005). Groen et al., (2014) illustrate developmental regulation of dendritic excitability and STDP in CA1 pyramidal neurons through tonic GABAergic inhibition. The dendritic conductances have been reported to change with maturation of the hippocampus (Chen & Johnston, 2004; Kip et al., 2006; Santos et al., 1998).

The bAP carry information from the neuron soma to the dendrites and spines and play an important role in STDP (Campanac & Debanne, 2008). The bAP is modulated by different voltage-gated ion channels especially A-type potassium channels and hyperpolarization-activated channels, which change with developmental maturation (Andrásfalvy et al., 2008; Magee, 1998). It has been reported that a developmental increase in dendritic tonic $GABA_{(A)}$ receptors mediate modulation of bAP (Groen et al., 2014). Furthermore, the distinct ion channels expression changes during developmental maturation (Maletic-Savatic et al., 1995; Vasilyev & Barish, 2002). As example, the L-type voltage-gated calcium channel is completely matured by the second postnatal month in rodents (Glazewski et al., 1993; Kramer et al., 2012).

All of these postnatal developmental changes until 2 months illustrate significant differences on different levels in juveniles and young adult rodents and these differences affect the synaptic plasticity mechanisms. However, strikingly up-to-date developmental data from 2 months old onwards (elder) mice providing understanding of the ongoing maturation of CNS throughout the adulthood is unavailable. The aforementioned developmental changes in part may also continue to exist in matured adults (3-6 months old mice) and underline the necessity to use neurons from fully mature adults in the electrophysiological studies.

1.4 Alzheimer's disease

The better health care has led to longer lifespan. Concomitant with this longevity, the prevalence of aging-related neurodegenerative diseases (e.g., Alzheimer's, Parkinson's, etc.) is also on the rise. Alzheimer's disease (AD) is an age-related, multifaceted neurodegenerative disorder characterized by a progressive and irreversible cognitive decline. More than 35 million people worldwide have AD (Global Burden of Disease study, 2016). It is the most common cause of dementia and currently there is no disease-modifying therapy

("2020 Alzheimer's Disease Facts and Figures," 2020). The main pathological hallmarks in AD are the presence of extracellular amyloid beta (Aβ) plaques, consisting of Aβ protein oligomer aggregates (Aβo, residues 1-40/42) and the accumulation of neurofibrillary tangles within neurons, composed of abnormally hyper-phosphorylated tau protein (Alzheimer, 1907; Furcila et al., 2018; Goedert et al., 1988; Grundke-Iqbal et al., 1986; Querfurth & Laferla, 2010). The Aβ plaques induce microglial activation, cytokine release, reactive astrocytosis, and subsequently an induction of chronic neuroinflammation, leading to increased levels of pro-inflammatory cytokines, neurotoxic tryptophan metabolites (kynurenines), and anti-inflammatory cytokines (compare review Tanaka et al., 2020). Importantly, neuroinflammatory signals mediated by microglial cells and concomitant astrogliosis are major hallmarks of AD (Heneka et al., 2015; Sarlus and Heneka., 2017). Loss of neurons and white matter, congophilic (amyloid) angiopathy and oxidative damage also exists in AD.

Aβ peptides are natural products of metabolism composed of 36-43 amino acids. Aβ40 monomers are abundant than the aggregation-prone and damaging Aβ42 species. Aβ peptides originate from proteolysis of the amyloid precursor protein (APP) by the sequential enzymatic actions of beta-site amyloid precursor protein-cleaving enzyme 1 (BACE-1), a β-secretase, and γ-secretase, a protein complex with presenilin 1 at its catalytic core (Haass & Selkoe, 2007) (**Fig. 3**). An imbalance between production and clearance, and aggregation of peptides, causes Aβ to accumulate. This Aβ accumulation may be the initiating factor in AD. This idea, often termed as the "amyloid hypothesis," is based on genetic forms of AD studies, and evidence that Aβ42 is toxic to cells (Selkoe, 2001; Tanzi & Bertram, 2005). Spontaneously, Aβ self-aggregates into multiple coexisting physical forms. One contains 2-6 peptide oligomers, which merge into intermediate assemblies (Kayed et al., 2003; Klein et al., 2001). Aβ can also grow into fibrils that assemble themselves to form the insoluble fibers of advanced Aβ plaques.

Similar to Aβ oligomers, intermediate aggregates of abnormal tau molecules are cytotoxic (Khlistunova et al., 2006) and impair cognition (Oddo et al., 2006; Santacruz et al., 2005). Studies have described that Aβ accumulation precedes and drives tau aggregation (Götz et al., 2001; Lewis et al., 2001; Oddo et al., 2003). Increased oxidative stress, the impaired protein-folding function of the endoplasmic reticulum, and deficient proteasome-mediated and autophagic-mediated clearance of damaged proteins accelerate the buildup of amyloid and tau proteins in AD (Hoozemans et al., 2005; Salon et al., 2000).

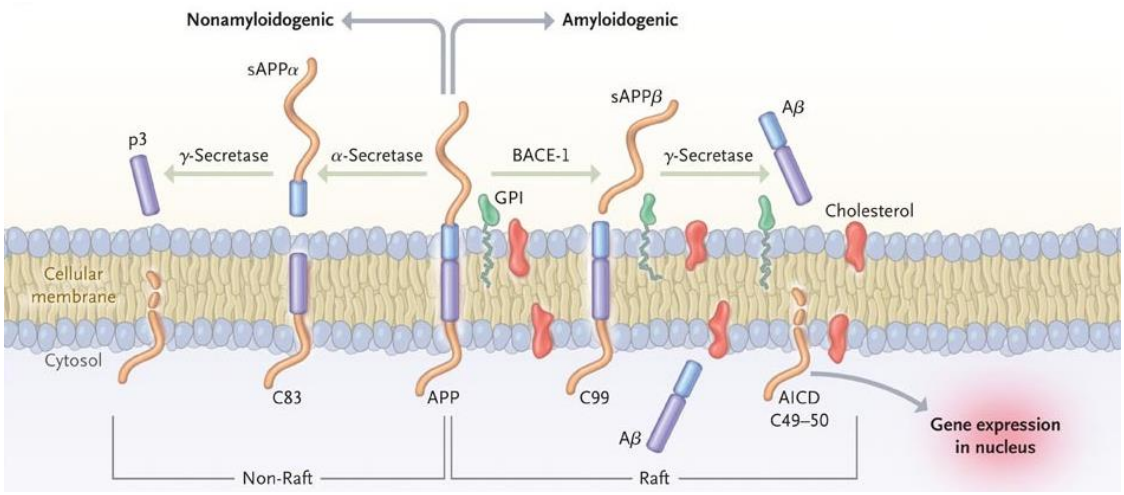

Figure 3: Processing of amyloid precursor protein (APP). Cleavage of the β-amyloid peptide (Aβ) interior sequence by α-secretase initiates nonamyloidogenic processing. A large amyloid precursor protein (sAPPα) ectodomain is released, leaving behind an 83-residue carboxy-terminal fragment. C83 is then digested by γ-secretase, liberating extracellular p3 and the amyloid intracellular domain (AICD). Amyloidogenic processing is initiated by β-secretase beta-site amyloid precursor protein–cleaving enzyme 1 (BACE-1), releasing a shortened sAPPα. The retained C99 is also a γ-secretase substrate, generating Aβ and AICD. γ-Secretase cleavage occurs within the cell membrane in a unique process termed "regulated intra- membranous proteolysis." Soluble Aβ is prone to aggregation. APP- amyloid precursor protein, GPI- glycophosphatidylinositol, AICD- amyloid intracellular domain, BACE-1- β-secretase beta-site amyloid precursor protein–cleaving enzyme 1 (modified after Querfurth & Laferla, 2010).

AD can be essentially a disorder of synaptic failure (Selkoe, 2002). In patients with mild cognitive impairments, hippocampal synapses show decline and compensatory increases in remaining synaptic profiles (Scheff et al., 2007). With disease progression, synapses are lost disproportionate to neurons, and this loss is correlated with dementia (DeKosky & Scheff, 1990; Terry et al., 1991). Basal synaptic transmission and LTP are disrupted in Aβ plaque-bearing AD mice (Larson et al., 1999; see review Mango et al., 2019; Walsh et al., 2005). Consequent to this impairment, signaling molecules which play important function in memory are reduced. Disruptions of presynaptic neurotransmitters release and postsynaptic glutamate-receptor ion currents occur partially as a consequence of NMDA and AMPA surface receptors endocytosis (Chapman et al., 1999; Hsieh et al., 2006; Shankar et al., 2007; Snyder et al., 2005) (**Fig. 4**).

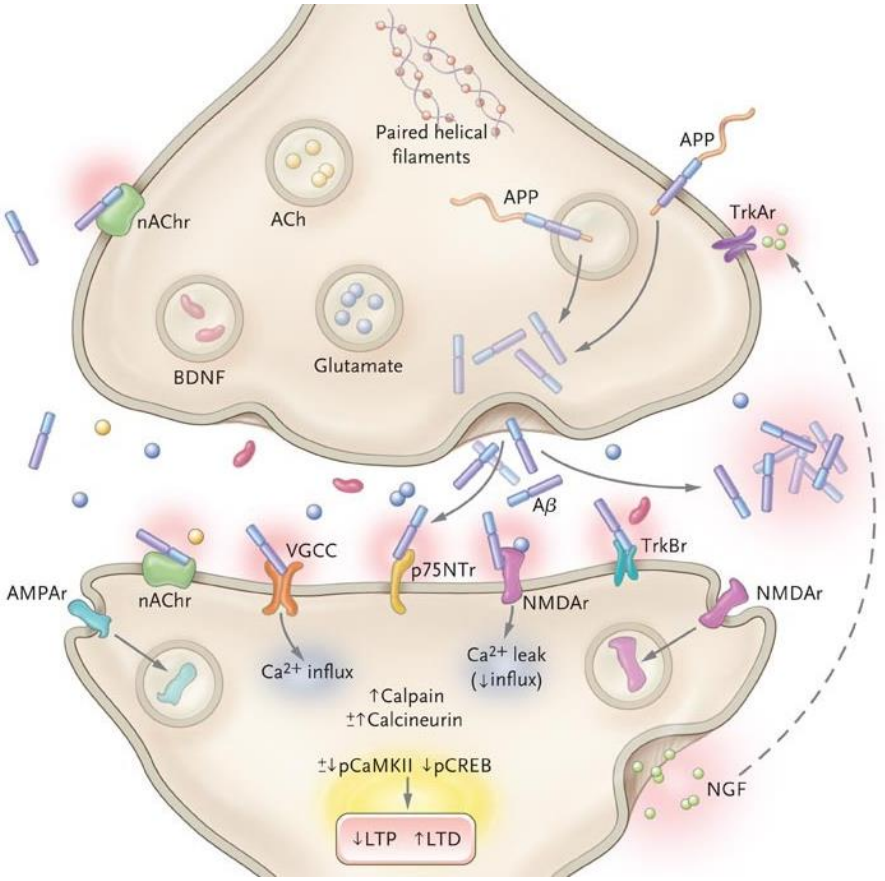

Figure 4: Synaptic impairments in Alzheimer's disease. In Alzheimer's disease, synaptic loss correlates with cognitive decline. Rings denote synaptic vesicles. Experimental application or expression of the β-amyloid (Aβ) oligomers disrupt synaptic plasticity by changing LTP and LTD balance and reduction of dendritic spines. At high concentrations, Aβ oligomers may suppress basal synaptic transmission. Aβ facilitates endocytosis of NMDA and AMPA receptors. Aβ binds with brain-derived neurotrophic factor (BDNF) receptors, p75NTR and TrkB, and exacerbates a situation where BDNF and nerve growth factor (NGF) levels are already suppressed. Aβ impairs nicotinic acetylcholine (ACh) receptor (nAChr) signaling and ACh release from the presynaptic terminal. Aβ- β-amyloid peptide, BDNF- brain-derived neurotrophic factor, Ach- acetylcholine, NGF- nerve growh factor, AMPAr- α-amino-3-hydroxy-5-methylisoxazole-4-propionic acid receptor, NMDAr- n-methyl d-aspartate receptor, nAChr- nicotinic acetylcholine receptor, p75NTR- p75 neurotrophin receptors, TrkB- tropomyosin related kinase, APP- amyloid precursor protein, pCaMKII- phosphorylated calcium–calmodulin–dependent protein kinase 2, pCREB- phosphorylated cyclic AMP response-element-binding protein, TrkAr- tropomyosin related kinase A receptor, and VGCC- voltage-gated calcium channel (adapted from after Querfurth & Laferla, 2010).

Degeneration of the medial temporal lobe, a critical brain region involved in memory formation, is a well-known indicator for AD (Beason-Held et al., 2020; Berron et al., 2020; Flores et al., 2020). The medial temporal lobe system comprises the hippocampal region and the adjacent entorhinal, perirhinal, and parahippocampal cortices (reviewed in Squire et al.,

2004). In the early stage of AD, the hippocampus is one of the first brain regions to suffer damage. Further, memory problems and disorientation appear among the first symptoms and are obvious in the early stage of AD (Asl et al., 2019; Palmer et al., 2007). The hippocampal CA1 region is crucial for spatial orientation, learning and different memory functions. It has been described that CA1 is one of the most affected regions in early stages of AD (Fouquet et al., 2012; Llorens- Martín et al., 2014).

1.4.1 APP/PS1 mouse model of Alzheimer's disease

A variety of transgenic mice have been generated to model cerebral amyloidosis, a hallmark of AD pathology. These models have been instrumental in studying the impact and mechanism of cerebral amyloidosis and to develop therapeutic strategies. Radde et al., (2006) generated a novel transgenic mouse model on a C57Bl/6J genetic background that coexpresses KM670/671NL mutated amyloid precursor protein (APP) and the L166P mutated presenilin 1 under the control of a neuron-specific Thy1 promoter element (APP/PS1 mice), which are characteristic for familial AD. Cerebral amyloidosis and human amyloid (A)β42 to Aβ40 ratio of 5 were observed in these 6-8 weeks old APP/PS1 mice. Amyloid-associated pathologies such as dystrophic synaptic boutons, hyperphosphorylated tau-positive neuritic structures and robust gliosis, with threefold increased neocortical microglia of 8 months old compared to 1 month old APP/PS1 mice were reported (Radde et al., 2006). Furthermore, behavioral analysis revealed learning impairments in APP/PS1 mice (Psotta et al., 2015; Radde et al., 2006). It has been reported that APP/PS1 mice exhibit significant impairments in LTP at SC-CA1 synapses and spine densities of CA1 pyramidal neurons in the vicinity of Aβ plaques in the hippocampus (Kartalou et al., 2020a, b). Because of the early onset of amyloid lesions, cognitive impairments, deficits in spine density and LTP; APPPS1 mice are well suited for studying the pathomechanism of amyloidosis in AD.

1.5 Objectives of the study

Up to date, STDP in the hippocampus has been profoundly studied in 1-month old mice (juveniles; Carlisle et al., 2008; Edelmann et al., 2015; Pang et al., 2019; Pérez-Rodríguez et al., 2019). Certain studies have described STDP in young adults (2-4 months old) with the use of robust STDP induction paradigms (Banerjee et al., 2009; Carlisle et al., 2008; Frey et al., 2009). However, whether STDP can be induced in the fully developed SC-CA1 synapses in the hippocampus, e.g. in mature adult mice (at least 6 months old), remains unanswered.

Henceforth the first objective in this dissertation was to-

Study STDP at SC-CA1 synapses and basal electrical properties of CA1 pyramidal neurons in the hippocampus of 6 months old mice (fully developed system, adults)

Alzheimer's disease (AD) is the most common cause of dementia and currently there is no disease-modifying therapy. Although several studies have described impaired LTP in the hippocampus of different mouse models of AD (compare review Mango et al., 2019), its impact on STDP in the hippocampus remains elusive.

Therefore, the second important objective in this dissertation was to-

Evaluate the influence of AD pathology on STDP at SC-CA1 synapses, basal electrical properties of CA1 pyramidal neurons and spontaneous synaptic transmission at SC-CA1 synapses in the hippocampus of adult APP/PS1 Alzheimer disease mouse model

2 Materials and Methods:

2.1 Animals

For all experiments, 1-6 months old male C57Bl/6J mice (Charles River, Sulzfeld, Germany), amyloid precursor protein/presenilin 1 (APP/PS1) double transgenic mice (Radde et al., 2006) and their WT littermates, derived from our own breeding colony were used. Animal's age and strain are mentioned in the respective results. APP/PS1 mice co-express KM670/671NL mutated amyloid precursor protein and L166P mutated presenilin 1 under the control of a neuron-specific Thy1 promoter element. These APP/PS1 animals are well suited for studying the pathomechanism of amyloidosis, a hallmark of Alzheimer's disease (AD) pathology. The animals were group housed in Makrolon cages at a temperature of 21 ± 2^{o} C and 12:12 hr light/dark cycle, lights on at 07:00 am. All experiments were conducted during the light phase of the animals. All animals had free access to food and water. Genotypes of APP/PS1 and their WT littermates were determined by PCR from ear punches before the STDP experiments and verified again by tail biopsies after performing and analyzing the experiments. All experimental procedures were performed in accordance with the ethical guidelines for the use of animals in experiments of the European Committees Council Directive (2010/63/EU), and were approved the local animal care committee (Landesverwaltungsamt Saxony-Anhalt, approval numbers: **IPHY**/G/01-1383/16 and **IPHY**/G/01-1492/18).

2.2 Hippocampal slice preparation and maintenance

All experiments were performed in the CA1 region of acute transversal hippocampal slices. The animal was anesthetized using isoflurane (Isofluran CP, cp-pharma, Germany). The loss of consciousness was confirmed by the absence of reflex activity following a toe pinch. The mouse was decapitated immediately, and the brain was separated from the skull. The brain was kept in an ice-cold artificial cerebrospinal fluid (aCSF) containing (in mM): 125 NaCl, 2.5 KCl, 26 $NaHCO_3$, 0.8 NaH_2PO_4, 25 glucose, 6 $MgCl_2$, 1 $CaCl_2$, saturated with 95% O_2 and 5% CO_2 (pH 7.2-7.4; 303-306 mOsmol/L, Fiske Micro-osmometer Model 210, Fiske associates, USA). The cerebellum, brainstem and one 3rd of the frontal brain were removed before brain slicing. Moreover, the ventral part of the brain was cut transversely at an angle of 11^{o} in order to obtain transversal slices. The brain was cut with a vibratome (LEICA VT1200S VIBRATOME, Leica Biosystems, Germany) and 350 µm thick acute hippocampal

slices were collected starting from the first slice that allowed clearly separated dentate gyrus and all *Cornu Ammonis* (CA) regions. These slices were used for all experiments and represent the intermediate and ventral region of the hippocampus. After slicing, the CA1 region was isolated from excessive CA3 input by a single cut between CA3 and CA2 to reduce spontaneous excitatory post-synaptic potentials (EPSPs; see **Fig. 5**). In all STDP recordings synaptic inhibition was blocked with γ-aminobutyric acid $(GABA)_A$ receptor antagonist picrotoxin (100 µM, dissolved in ethanol; Sigma Aldrich, Germany). Certain experiments were performed with exclusion of picrotoxin from the recording aCSF and acute slices with no CA3-CA1 cut (mentioned in relevant results section). About 6 slices were transferred onto a hydrophilic polytetrafluoroethylene (PTFE) cell culture insert with pore size of 0.4 µm (Millicell cell culture inserts, 30 mm diameter, PICMORG50, Merck Millipore Ltd., Germany) in the interface-style chamber. All slices were allowed for 25 min to incubate in carboxygenated (5% CO_2, 95% O_2) pre-warmed aCSF (200 mL, same composition as slice preparation medium mentioned above) at 34-35^oC to allow the slice surface to recover from blade trauma, followed by at least an hour of recovery at room temperature. The 25 min incubation at 34-35^oC and then at least an hour storage at room temperature helps to improve the slice viability (Cepeda-Prado et al., 2019; Edelmann et al., 2015). All slices were maintained in this interface chamber at room temperature (~22-25 ^oC) until being transferred to the recording chamber of an upright microscope for electrophysiological recording.

2.3 Electrophysiology in acute hippocampal slices

For all experiments, 350 µm thick acute, transversal hippocampal slices were used. Following 1 hr incubation at room temperature, one of the acute slices from interface-style chamber was transferred to submerged-style recording chamber. An anchor with parallel nylon threads was used to avoid any mechanical disturbance in the slice during the whole recording. Slices were incubated for 5-10 min in the submerged-style recording chamber before start of recording. For whole-cell recordings, pyramidal neurons in CA1 region of hippocampus were visualized with differential interference contrast (DIC) infrared video microscopy (VX45 Optronis camera, Optronis GmbH, Germany; Zeiss Examiner A1 microscope). For all STDP recordings, 100 µM picrotoxin (Sigma Aldrich, dissolved in ethanol) was added to the extracellular aCSF solution to block $GABA_A$ receptors. ACSF was composed of (in mM): 125 NaCl, 2.5 KCl, 25 $NaHCO_3$, 0.8 NaH_2PO_4, 25 glucose, 2 $CaCl_2$, 1 $MgCl_2$, saturated with 95% O_2 and 5% CO_2 (pH 7.2-7.4; 301–304 mOsmol/l). Certain experiments were performed with

exclusion of picrotoxin in the recording aCSF (mentioned in relevant results section). The slices in the recording chamber were continuously perfused with carboxygenated aCSF mentioned above (perfusion rate- 1.4-2 mL/min). The temperature of extracellular aCSF in the recording chamber was maintained at 28-31^{o}C with inline heater (Model SH-27B Inline Heater, Warner Instrument Corporation, USA) and continuously monitored with the help of heater controller (Model TC-324 Heater Controller, Warner Instrument Corporation, USA). Whole-cell recordings were performed with glass pipettes (pipette resistance 4-6 MΩ) filled with intracellular solution containing (in mM): 140 potassium gluconate, 10 HEPES, 20 KCl, 4 Mg-ATP, 0.3 Na-GTP, 10 Na-phosphocreatine; pH was adjusted to 7.2-7.4 using 1 M KOH (280-290 mOsmol/L). In the process of establishment of STDP in 6 months old mice, we tested four intracellular solutions composed of (in mM):

A. 140 potassium gluconate, 10 HEPES, 20 KCl, 4 Mg-ATP, 0.3 Na-GTP, 10 Na-phosphocreatine, 0.00075 $CaCl_2$; pH was adjusted to 7.2-7.4 using 1 M KOH (280-290 mOsmol/L).
B. 140 potassium gluconate, 10 HEPES, 20 KCl, 4 Mg-ATP, 0.3 Na-GTP, 10 Na-phosphocreatine; pH was adjusted to 7.2-7.4 using 1 M KOH (280-290 mOsmol/L).
C. 140 potassium gluconate, 10 HEPES, 20 KCl, 4 Mg-ATP, 0.3 Na-GTP, 10 Na-phosphocreatine, 1 EGTA; pH was adjusted to 7.2-7.4 using 1 M KOH (280-290 mOsmol/L).
D. 131.3 potassium gluconate, 10 HEPES, 8.75 KCl, 4 Mg-ATP, 0.4 Na-GTP, 10 NaCl, 0.5 EGTA; pH was adjusted to 7.2-7.4 using 1 M KOH (~300 mOsmol/L adjusted with sucrose; Personal communication with Smit Tamar, University of Amsterdam at 12th Göttingen meeting of the German Neuroscience Society (2017)).

The intracellular solution used in particular experiments is described in the relevant results.

Pipette capacitance, CA1 pyramidal cell capacitance and series resistance were compensated using EPC8 patch clamp amplifier in all voltage clamp and current clamp recordings. Cells were held in current or voltage clamp mode at -70 mV for different experimental approaches. The liquid junction potential of +10 mV observed before seal formation was corrected. For stimulation of presynaptic Schaffer collaterals (SC; stimulus duration 0.3 ms), a glass pipette (0.7-0.9 MΩ) filled with intracellular/recording aCSF solution was placed in stratum radiatum at a location where the SC axon bundles are located in the CA1 region (see **Fig. 5**). The glass pipettes used for stimulation and recording electrodes were pulled from the borosilicate glass

(diameter- outside 1.5 mm, inside 0.86 mm; Science Products GmbH, Germany) using a two-step puller (Model PP-830; Narishige Scientific Instrument Lab, Tokyo, Japan). The placements of stimulation and recording electrodes on the slice were executed with the help of micromanipulator system (Luigs & Neumann SM-5; **Fig. 5**). During control and test periods, EPSPs were evoked at 0.05 Hz in current clamp mode. Presynaptic stimulation which caused postsynaptic firing of action potential (AP) or the maximum EPSP amplitude observed was regarded as maximum stimulus intensity. Stimulus strength (µA) was adjusted to evoke 30–50% of maximal stimulation as optimal stimulation intensity and kept constant during the whole experiment. Input resistance was determined by injecting a 20 pA hyperpolarizing current through the recording electrode for a duration of 250 ms; 200 ms prior to each SC stimulation. Cells were accepted for analysis only if the resting membrane potential was between -50 and -70 mV at the start of the recording. Data were discarded if input resistance changed ±30 % throughout the recording or in case of a clear run- up or run- down of EPSP slopes during the first 10 min of a recording. The paired-pulse facilitation (PPF) was tested at 50 ms inter-stimulus interval (ISI) repeated 3 times at 0.05 Hz in voltage clamp mode.

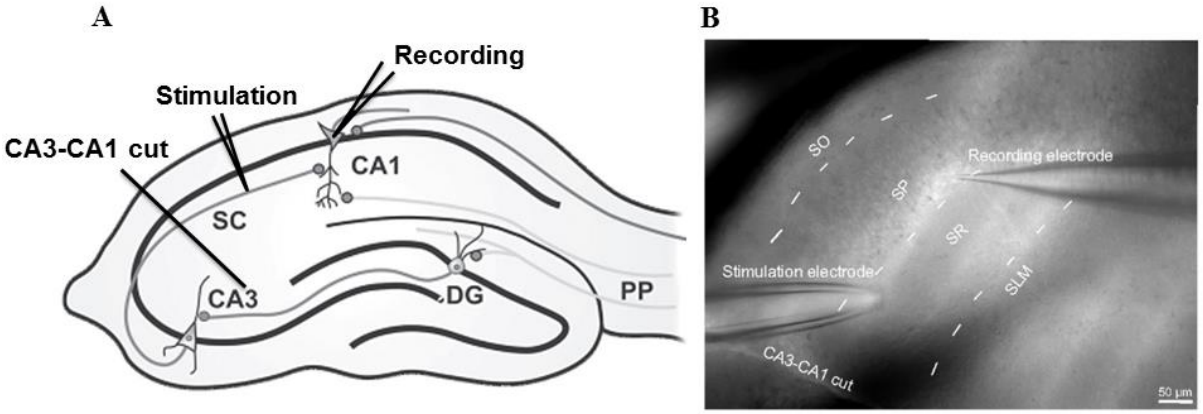

Figure 5: The stimulation, recording electrode placements and CA3-CA1 cut of acute hippocampal slice. (A) An illustration of the stimulation, recording electrode locations and CA3-CA1 cut of acute hippocampal slice. Figure A modified after (Biel et al., 2009)**. (B)** Live image of acute hippocampal slice displaying the placements of the stimulation and recording electrode at SC-CA1 synapses. SO: Stratum (S) oriens, SP: S. pyramidale, SR: S. radiatum, SLM: S. lacunosum moleculare.

STDP was induced by repeated pairings of an EPSP induced by single presynaptic stimulation, evoked by stimulation of SC input and one or four postsynaptic APs induced by 1x or 4x somatic current injections (2 ms, 1 nA) via the recording electrode. Paradigms using

either a 1 EPSP/1 AP sequence (indicated as 1:1) or a 1 EPSP/4 APs (specified as 1:4, 4 postsynaptic APs at a frequency of 200 Hz) sequence were used. Different numbers of pairings at 0.5 – 2 Hz were used depending on the stimulation protocol as mentioned in the results. STDP was induced by causal (pre-post) or anti-causal (post-pre) pairings at positive or negative spike timings. For each recorded cell, positive spike timing (i.e., Δt in ms) was determined between the onset of the EPSP and the peak of the first AP, while negative spike timing was measured between the peak of the AP and the onset of the EPSP. Baseline synaptic transmission was assessed during the first 10 min of EPSP recording (time point: -10 to 0 min) at hippocampal SC-CA1 synapses, followed by STDP induction (at 0 min) with respective pre-postsynaptic or post-presynaptic pairing protocol and afterwards EPSP recording was continued for next 30 min (0 to 30 min). As a (negative) control, recordings with ongoing synaptic stimulation for 40 min at 0.05 Hz, but without pairing with postsynaptic APs, were performed (indicated as 0:0).

2.4 Data acquisition and data analyses

Whole-cell recordings were performed using an EPC8 patch clamp amplifier connected to a LiH8+8 interface (HEKA, Germany) and acquired with Patchmaster software (HEKA, Germany). The stimulation parameters such as stimulation strength, inter-stimulus interval, etc. were controlled with a stimulator device (Model 2100, A-M Systems, USA). All electrical activity taking place in the acute hippocampal slice in the recording chamber was continuously monitored on an oscilloscope (Tektronix TDS210, Tektronix, Inc. Oregon, USA). Data were filtered at 3 kHz and digitized at 10 kHz. Data analyses were performed using FitMaster (HEKA, Germany). Synaptic signals were recorded in current clamp mode as EPSP, except for PPF, which was recorded in voltage clamp as excitatory postsynaptic currents (EPSCs). With the help of FitMaster, initial EPSP slopes (i.e. first 2-3 ms after EPSP onset) were determined. In control and t-LTP experiments, EPSP slopes were normalized to the respective mean baseline, i.e., recorded during the first 10 min prior to STDP stimulation, which was set to 100%. In all experiments, magnitude of synaptic changes (e.g. t-LTP) was determined as the normalized change in mean response size during the last 10 min of measurement (between 21-30 min after t-LTP induction). Further, the numbers of APs fired by a CA1 neuron, in response to different depolarizing somatic current injections (0-180 pA for 1000 ms, 20 pA increments) through the recording electrode, were determined to analyze intrinsic excitability. As another read-out of intrinsic excitability, the stimulation current

(depolarization step (10 ms) of 0-400 pA, 40 pA increments) required to elicit one AP in the recorded CA1 cell was determined as rheobase (Luque et al., 2017; Zhao et al., 2007). The intrinsic excitability characteristics of CA1 pyramidal neurons were recorded at the start and the end of every whole-cell recording. The PPF was estimated by paired pulse ratio (PPR), calculated as the normalized change in mean amplitudes of 2^{nd} divided by the 1^{st} EPSC. PPR measurements were conducted in every STDP experiment at the start and the end in order to understand change in presynaptic glutamate release before and after STDP induction. It composed of two consecutive presynaptic stimulations with an inter-stimulus interval (ISI) of 50 ms. The AP peak amplitude, after-depolarization and $GABA_B$ receptor mediated EPSP components were measured using FitMaster (demonstrated in **Fig. 24**). Input resistance was used to assess stability of prolonged recordings. Similar to EPSP slopes, input resistance was normalized to the respective mean baseline during the first 10 min of recording, which was set to 100%. Data were discarded if input resistance changed ±30 % throughout the measurement. Further, mean EPSP rise time and decay time was calculated using the Trace Fit function (low level - high level: 10-90%) for the 10 min long baseline in FitMaster (see **Fig. 24**).

2.5 Synaptic signal integration

Acute hippocampal slices were continuously perfused with same aCSF mentioned in **section 2.3**, with no picrotoxin (perfusion rate- 2.4 mL/min). Intact acute slices were used, with no CA3-CA1 cut. The temperature of recording chamber was maintained at 34-36^{o}C with inline heater and heater controller. The endogenous resting membrane potential was used as holding potential, and was unchanged during the entire measurement. At the start of experiment, intrinsic excitability of CA1 pyramidal neurons was assessed with the numbers of APs fired by CA1 neuron, in response to different somatic current injections/depolarization steps (0-450 pA for 500 ms, 50 pA increments) through recording electrode. Furthermore, we used another approach to evaluate intrinsic excitability, with the measurement of hyperpolarization peak (Ih peak, current clamp (mV)), in response to different somatic current injections/hyperpolarization steps (0-200 pA for 500 ms, 50 pA increments). The synaptic signal integration was studied at half maximal stimulation intensity. The EPSP response of CA1 neuron was recorded in response to train of stimulation composed of 5 pulses at 5, 10, 20, 50, 100 and 200 Hz frequencies; repeated 5x with ISI of 20 sec, with 2 min interval between two different frequencies. Mean number of synaptic driven action potentials (APs) were calculated from individual traces at different frequencies (FitMaster) to determine spike

probability which was used as a measure of synaptic signal integration differences at hippocampal SC-CA1 synapses in APP/PS1 mice and their WT littermates.

2.6 Aβ plaque staining with Methoxy-X04 in acute hippocampal slices

The blue fluorescent dye 1,4-bis-(4´-hydroxystyryl)-2-methoxybenzene (Methoxy-X04; Tocris) has been used previously as a live stain for Aβ plaques in AD mice (Kartalou et al., 2020a, b; Klunk et al., 2002; T. L. Spires-Jones et al., 2007). To localize Aβ plaques in recorded hippocampal slices, APP/PS1 mice were injected intraperitoneally (i.p.) 24 hr before slice preparation with Methoxy-X04 (dissolved in dimethyl sulfoxide (DMSO); stock solution: 10 mg/ml) at a concentration of 25 mg/kg body weight. After slice preparation on the day of t-LTP measurement and transfer of a recorded slice into the recording chamber of an upright fluorescence microcope (Zeiss Examiner A1), Aβ plaques were visualized using a 10x and 63x water immersion objectives. Fluorescence of Methoxy X04 was excited with a band pass filter (352-402 nm) and the emitted light was passed through a filter cube allowing to selectively detect blue fluorescence (dichroic mirror: 409 nm; bandpass filter: 417-477 nm). Live cell imaging of blue fluorescent Aβ plaques in the CA1 area (**Fig. 6**) and associated stratum radiatum was performed with a digital CCD camera Photometrics CoolSNAP ES^2 (Visitron Systems, GmbH, Germany). Using a digitized micromanipulator system (Luigs & Neumann SM-5), the distance (x,y,z coordinates) between the recorded CA1 neuron soma and the border of the nearest Aβ plaque was determined. The diagonal distance of Aβ plaque from the CA1 neuron soma (compare **Fig.6**) was calculated offline with the Pythagorean equation.

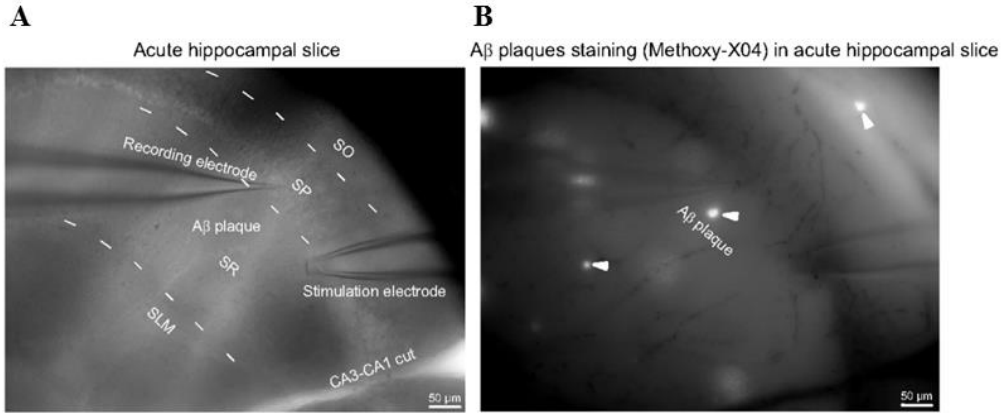

Figure 6: Methoxy-X04 staining of Amyloid-β (Aβ) plaque in acute hippocampal slices. (A) Live images of acute hippocampal slice with no methoxy-X04 staining of Aβ plaque and **(B)** with methoxy-X04 stained Aβ

plaque. Aβ: Amyloid-beta, SO: Stratum (S) oriens, SP: S. pyramidale, SR: S. radiatum, SLM: S. lacunosum moleculare.

2.7 Chronic fingolimod treatment of APP/PS1 mice

As a therapeutic strategy to rescue AD related deficits in t-LTP, we tested chronic fingolimod (Abcam, Germany) treatment in adult APP/PS1 mice (Deogracias et al., 2012; Fukumoto et al., 2014; Kartalou et al., 2020b). APP/PS1 animals and their WT littermates were injected intraperitoneally (i.p.) with a dose of 1 mg fingolimod /kg body weight (Fukumoto et al., 2014), every second day for a month. Fingolimod stock solution (200 mM in DMSO) was diluted with 0.9% saline and was stored in aliquots at -20^{o}C until use. On the day of administration, fingolimod solution was thawed at room temperature, and warmed in 37^{o}C water bath for 3-4 min before intraperitoneal injection.

2.8 Voluntary running

In another approach, voluntary running for 2 months was tested as a therapeutic strategy in adult APP/PS1 mice. Each cage of the exercising animals was exclusively equipped with two running wheels (**Fig. 7**), and running activity was voluntary. As a control, age-matched animals were housed in standard cages with no running wheels.

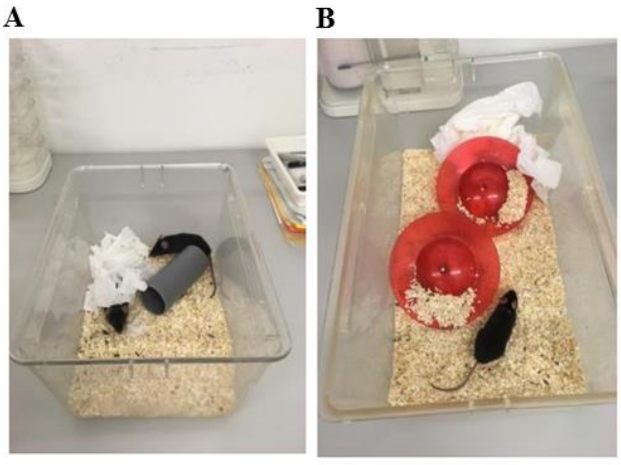

Figure 7: Voluntary running of APP/PS1 mice. (A) Standard cage; **(B)** Standard cage equipped with two running wheels for voluntary running. Figure (A) and (B) adapted from Edelmann, E. and Endres T., Progress report, CIRCPROT symposium 2019, Nizza.

2.9 Whole cell EPSC and IPSC recordings

Spontaneous and miniature EPSCs and inhibitory postsynaptic currents (IPSCs) were studied in hippocampal CA1 pyramidal neurons in acute slices with no CA3-CA1 cut, prepared from APP/PS1 and WT mice brains as described above. EPSCs were recorded with the intracellular solution containing (in mM): 140 potassium gluconate, 10 HEPES, 20 KCl, 4 Mg-ATP, 0.3 Na-GTP, 10 Na-phosphocreatine; pH was adjusted to 7.2 - 7.4 using 1 M KOH (280-290 mOsmol/L). Spontaneous EPSCs were studied in the presence of bicuculine (10 µM, Sigma Aldrich) in the extracellular aCSF solution and miniature EPSCs were examined in the presence of bicuculine (10 µM) and tetrodotoxin (TTX, 1 µM, Tocris) in the extracellular aCSF (Ju et al., 2016).

IPSCs were recorded with the intracellular solution containing the following (in mM): 125 Cs-methanosulfonate, 10 CsCl, 2 $MgCl_2$, 5 NaCl, 10 HEPES, 1 EGTA, 5 Mg-ATP and 0.3 Na3GTP; pH was adjusted to 7.2-7.4 using 1 M CsOH (Ju et al., 2016). Spontaneous IPSCs were examined in the presence of the N-methyl-d-aspartate receptor (NMDAR) antagonist D,L-2-amino-5-phosphonopentanoic acid (APV, 50 µM, Tocris) and the α-amino-3-hydroxy-5-methyl-4-isoxazolepropionic acid receptor (AMPAR) antagonist 6,7-dinitroquinoxaline-2,3-dione (DNQX, 10 µM, Tocris) in the extracellular aCSF. Miniature IPSCs were investigated in the presence of APV (50 µM), DNQX (10 µM) and TTX (1 µM) in the extracellular aCSF. EPSCs and IPSCs were recorded at -70 mV and -30 mV holding potentials respectively, for the period of 10 min; 250 events from each sweep were used for data analyses. The temperature of extracellular aCSF solution in the recording chamber was maintained at 34-36^{o}C (aCSF perfusion rate- 2.4 mL/min) for E(I)PSC recordings. Data were analyzed manually using the 'Mini Analysis program' (version 6.0.7, Synaptosoft, Decatur, GA, USA).

2.10 Statistics

Data are specified as mean ± standard error of mean (SEM), and experiments were combined from at least three different animals per group. Furthermore, the number of experiments (n) and number of animals (N) are indicated in the respective parts of the Results. Group size of 10 was determined by power analysis (G*Power, Heinrich-Heine University Düsseldorf, Germany). The distribution of variables was determined with Shapiro-Wilk test. Statistical

analyses were performed with one-sample t-test, paired or unpaired two-tailed Student's t-test, as applicable. Non-parametric data were analyzed by Mann-Whitney U-test. Multiple comparisons were performed with ANOVA and Kruskal-Wallis test for parametric and nonparametric data, respectively. In case of significant main effects, the ANOVA was followed by post hoc Dunnett/Tukey Test or Bonferroni adaptation for multiple comparisons. Pearson correlation coefficient was used to determine correlation between distance of CA1 cell from Aβ plaques and t-LTP magnitude. The Kolmogorov-Smirnov test was used to determine significance for cumulative frequency distributions. Significance levels are designated by *: $p<0.05$. The statistical procedures used in each experiment are also mentioned in the respective text passages. All data were analyzed using Origin 8.1G (Additive GmbH, Germany), GraphPad Prism 8 (GraphPad Software, California, USA), Mystat 12 (Systat, USA).

3 Results:

In the current dissertation, we were interested to understand whether developmental maturation or pathological aging impacts spike timing-dependent plasticity (STDP) in the hippocampus and thereby affects information storage at the single neuron level. To the best of our knowledge, STDP in the hippocampus has been profoundly studied in 1-month old mice (juveniles; Carlisle et al., 2008; Edelmann et al., 2015; Pang et al., 2019; Pérez-Rodríguez et al., 2019), while its role in mature animals was thus far poorly investigated. Most electrophysiological studies, including investigations of STDP, focus on 1 month old juvenile animals, although the brains of these mice are not fully matured in particular regarding the still ongoing synaptic pruning, experience-dependent refinement of synaptic circuits and myelination, which proceeds beyond 2 months of age (Semple et al., 2013). Therefore, in a first series of experiments we focused on establishing recording conditions and STDP induction paradigms to study STDP at hippocampal Schaffer collateral (SC) – *Cornu Ammonis* (CA) 1 synapses in 6 months old adult mice (fully developed system). To this aim, we used whole-cell patch clamp recordings in postsynaptic CA1 pyramidal neurons. We tested different STDP paradigms to induce synaptic plasticity by repeatedly pairing a single presynaptic stimulation with either 1 or 4 postsynaptic action potentials (APs) in the postsynaptic neuron. Moreover, we tested both positive and negative pairings with 10 ms interval between presynaptic stimulation and postsynaptic APs (spike timings, Δt). We observed that STDP can be successfully induced also in adult animals and subsequently compared the properties of this type of synaptic plasticity with STDP in juvenile animals. Furthermore, we compared basal electrical and synaptic properties of CA1 pyramidal neurons in adult and juvenile animals.

Next, we investigated whether STDP is altered in Alzheimer's disease (AD) mouse model. AD is the most common cause of dementia with no disease modifying therapy until today ("2020 Alzheimer's Disease Facts and Figures," 2020). Although synaptic dysfunctions such as impaired long-term potentiation (LTP) and long-term depression (LTD) of hippocampal synaptic transmission have been reported as an early event in AD (reviewed in Mango et al., 2019); properties of STDP in the hippocampal formation of AD mice have not been reported previously. Therefore, we investigated STDP in adult male APP/PS1 mice, expressing mutated (KM670/671NL) amyloid precursor protein (APP) and mutated (L166P) presenilin 1, a well-recognized AD mouse model (Radde et al., 2006). We tested different STDP

paradigms for their efficiency to induce synaptic plasticity at hippocampal SC-CA1 synapses in APP/PS1 mice in comparison to age-matched wildtype (WT) littermates. Further, we studied basal electrical properties of CA1 neurons and spontaneous excitatory and inhibitory synaptic transmission at SC synapses in this APP/PS1 mouse strain. The synaptic signal integration differences at SC-CA1 synapses in the hippocampus in APP/PS1 mice and their WT littermates were also investigated.

3.1 Six months old wildtype mice did not express t-LTP under recording conditions with intact GABAergic system

Since our ultimate goal was to record STDP properties in fully matured adult mice, in a first series of experiments we tested different aCSF and intracellular solution compositions to establish recording conditions in order to obtain viable acute hippocampal slices from fully mature mice that were suitable for STDP recordings in 6 months old WT mice. Therefore, we started with aCSF containing (in mM): 125 NaCl, 2.5 KCl, 26 $NaHCO_3$, 0.8 NaH_2PO_4, 25 glucose, 6 $MgCl_2$, 1 $CaCl_2$ for acute hippocampal slice preparation and incubation. The slices in the recording chamber were continuously perfused with carboxygenated aCSF containing (in mM): 125 NaCl, 2.5 KCl, 26 $NaHCO_3$, 0.8 NaH_2PO_4, 25 glucose, 1 $MgCl_2$, 2 $CaCl_2$. Cepeda-prado and coworkers (2020) reported t-LTP at SC-CA1 synapses in 1-month old mice with temperature of aCSF in the recording chamber maintained at 28-30°C, therefore temperature of aCSF in the recording chamber was maintained at 28-30°C in this set of experiments. Intact acute hippocampal slices (no CA3-CA1 cut) with GABAergic inhibition were used to allow physiological conditions. Tamar and colleagues observed successful t-LTP at hippocampal SC-CA1 synapses in 6-9 months old C57Bl/6J mice with intracellular solution that contained (in mM): 131.25 potassium gluconate, 10 HEPES, 8.75 KCl, 4 Mg-ATP, 0.4 Na-GTP, 10 NaCl, 0.5 EGTA (Personal communication with Smit Tamar, University of Amsterdam at 12th Göttingen meeting of the German Neuroscience Society (2017)). We used the same intracellular solution for these STDP experiments. The acute slices obtained with these conditions were viable, allowed whole cell patch clamp recording of CA1 pyramidal neurons, and recordings remained stable for ~1 hr, matching the duration of a typical STDP experiment. Here we argued that robust STDP paradigms might be necessary to induce STDP at fully mature SC-CA1 synapses in 6 months old mice. Therefore, we tested 100 or 60 pairings (Smit Tamar, University of Amsterdam) of a single presynaptic stimulation with single postsynaptic action potential (AP) in the postsynaptic neuron at 2 Hz (100x 1:1 or 60x

1:1; canonical stimulation) with 10 ms interval between presynaptic stimulation and postsynaptic AP (spike timings, Δt= +10 ms). As a (negative) control, recordings with ongoing synaptic stimulation for 40 min at 0.05 Hz, but without pairing with postsynaptic AP, were performed (indicated as 0:0). The hippocampal SC-CA1 synapses in 6 months old adults displayed no t-LTP induction with 100x 1:1 (2 Hz) or 60x 1:1 (0.14 Hz) stimulation (**Fig. 8A**; 0:0: 100.70 ± 7.9% (n=12/N=9); 100x 1:1, 2 Hz: 88.58 ± 11.8% (n=13/N=8); 60x 1:1, 0.14 Hz: 110.81 ± 13.8% (n=11/N=6), Kruskal-Wallis ANOVA H=1.077 p=0.5837). Since Tamar and coworkers observed t-LTP with 60x 1:1 (0.14 Hz) stimulation under these recording conditions – but at room temperature – whereas we routinely recorded at 28-30°C we next studied t-LTP at room temperature using 60x 1:1 (0.14 Hz) stimulation. We observed no t-LTP induction with 60x 1:1 (0.14 Hz) stimulation at room temperature (**Fig. 8B**; 60x 1:1, 28-30^{o}C: 110.81 ± 13.8% (n=11/N=6); 60x 1:1, RT: 107.14 ± 8.5% (n=11/N=5), Mann-Whitney U-test U=53.00 p=0.622). Under these recording conditions, the STDP paradigms 100x 1:1 (2 Hz) or 60x 1:1 (0.14 Hz), at room temperature or 28-30^{o}C in the recording chamber, were incapable to induce t-LTP at fully developed hippocampal SC-CA1 synapses.

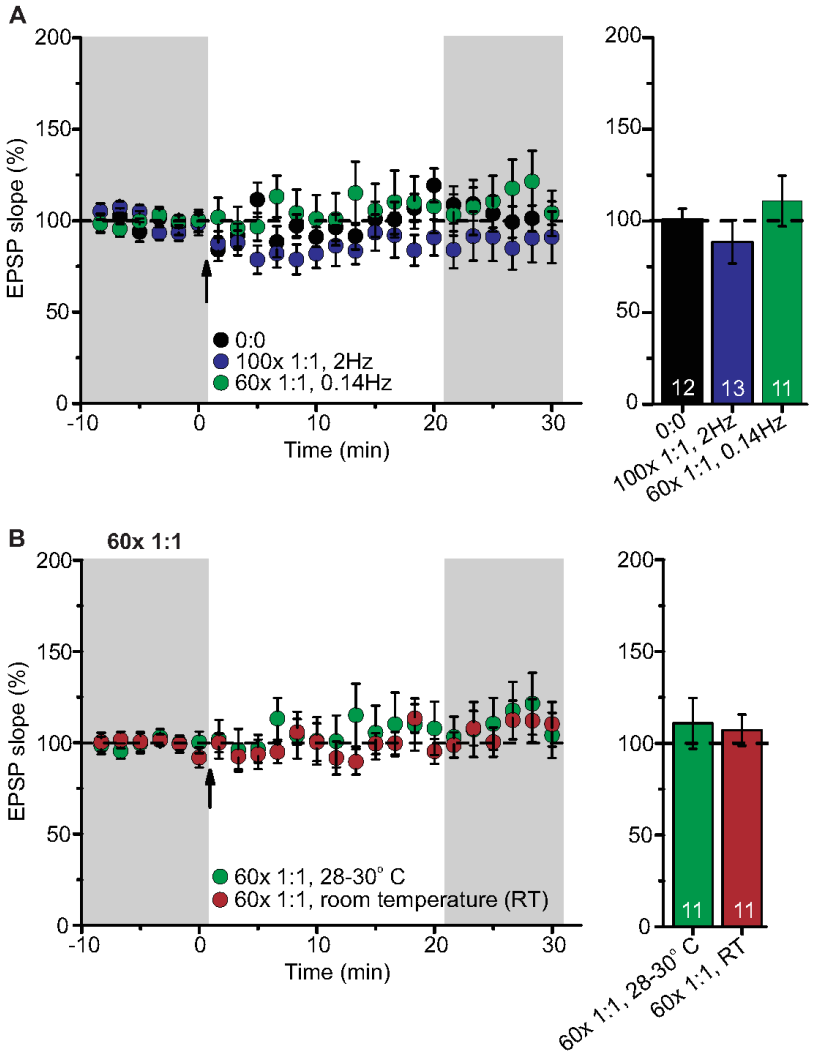

Figure 8: Different high repeat STDP paradigms did not induce t-LTP at SC-CA1 synapses in 6 months old mice, with intact GABAergic system. Patch clamp recordings from hippocampal CA1 pyramidal cells at a holding potential of -70 mV in current clamp mode. Left: Mean time-course of EPSP slopes for different STDP paradigms. Right: Averaged change in EPSP slopes (21-30 min) following t-LTP induction normalized to control before t-LTP induction. **(A)** The hippocampal SC-CA1 synapses in 6 months old mice did not express t-LTP with 100x 1:1 (2 Hz; blue circles, n=13/N=8) and 60x 1:1 (0.14 Hz; green circles, n=11/N=6) stimulations compared to control (black circles, n=12/N=9) at 28-30ºC temperature. **(B)** 60x 1:1 (0.14 Hz) STDP paradigm did not induce t-LTP at room temperature (brown circles, n=11/N=5) compared to 28-30ºC maintained of extracellular aCSF (green circles, n=11/N=6) in adult mice. Recording aCSF contained (in mM): 125 NaCl, 2.5 KCl, 26 NaHCO3, 0.8 NaH2PO4, 25 glucose, 1 MgCl2, 2 CaCl2. Intracellular solution contained (in mM): 131.25 potassium gluconate, 10 HEPES, 8.75 KCl, 4 Mg-ATP, 0.4 Na-GTP, 10 NaCl, 0.5 EGTA. Data displayed as mean ± SEM. Digits in the bars represent the number of recorded neurons per condition. *$p < 0.05$, nonparametric data were analyzed with Kruskal-Wallis ANOVA (A, multiple comparisons) and Mann-Whitney U-test (B).

3.2 Six months old mice did not express t-LTP with high repeat STDP paradigms, with inclusion of $CaCl_2$ in intracellular solution

Using recording aCSF and intracellular solution composition described in section 3.1, we did not observe successful t-LTP induction at hippocampal SC synapses in slices from 6 months old adult animals. Cepeda-Prado et al. (2020) described t-LTP at SC-CA1 synapses in 1 month old mice with extracellular aCSF containing (in mM): 125 NaCl, 2.5 KCl, 26 $NaHCO_3$, 0.8 NaH_2PO_4, 25 glucose, 1 $MgCl_2$, 2 $CaCl_2$, 0.1 picrotoxin for recording at 28-30°C and intracellular solution contained (in mM): 140 potassium gluconate, 10 HEPES, 20 KCl, 4 Mg-ATP, 0.3 Na-GTP, 10 Na-phosphocreatine, 0.00075 $CaCl_2$. In this series of experiments, we tested these recording conditions to investigate STDP at SC-CA1 synapses in 6 months old mice. In addition to 100x 1:1 canonical stimulation paradigm, here we investigated 35 pairings of a single presynaptic stimulation with four postsynaptic action potentials (APs) in the postsynaptic neuron at 1.66 or 0.5 Hz (35x 1:4; burst stimulation) with 10 ms interval between presynaptic stimulation and postsynaptic AP (spike timings, Δt= +10 ms). This is an important STDP paradigm since firing patterns that resemble burst stimulation were described in rodents during learning *in vivo* (compare Otto et al., 1991). Under these conditions, adult mice expressed no t-LTP with 35x 1:4 (1.66 Hz), 70-100x 1:1 (1.61 Hz) and 35x 1:4 (0.5 Hz) STDP stimulations (**Fig. 9**; 0:0: 116.04 ± 7.3% (n=18/N=15); 35x 1:4 (1.66 Hz): 144.77 ± 18.3% (n=9/N=8); 70-100x 1:1(1.61 Hz): 128.91 ± 9.7% (n=15/N=12); 35x 1:4 (0.5 Hz): 109.56 ± 10.9% (n=7/N=6), ANOVA $F_{(3,45)}$=1.572 p=0.2093). Nevertheless, 1-sample t-test revealed significant t-LTP induced with 35x 1:4 (144.77 ± 18.3%; t(8)=2.443 p=0.0404) and 70-100x 1:1 (128.91 ± 9.7%; t(14)=2.987 p=0.0098) stimulations. Here, we argued that the presence of $CaCl_2$ in intracellular solution could be responsible for spontaneous synaptic change/run-up in unpaired controls (0:0). Under these recording conditions, particularly the presence of $CaCl_2$ in intracellular solution, the hippocampal SC-CA1 synapses of 6 months old mice did not show t-LTP with different robust STDP paradigms (70-100x 1:1, 35 1:4). Henceforth, in further STDP experiments we tested different intracellular solutions, differing mainly in Ca-buffering capacity (amount of free calcium), in order to establish recording conditions where we observe successful t-LTP at hippocampal SC-CA1 synapses in adults.

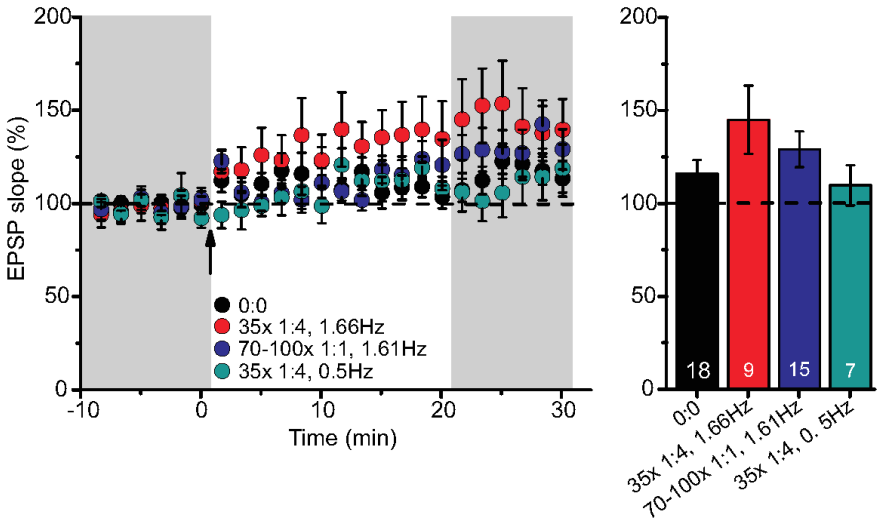

Figure 9: Adult 6 months old mice did not express t-LTP at SC-CA1 synapses in response to different STDP paradigms, with inclusion of $CaCl_2$ in intracellular solution. Patch clamp recordings from hippocampal CA1 pyramidal cells at a holding potential of -70 mV in current clamp mode. Left: Mean time-course of EPSP slopes for different STDP paradigms. Right: Averaged change in EPSP slopes (21-30 min) following t-LTP induction normalized to control before t-LTP induction. The hippocampal SC-CA1 synapses in 6 months old mice expressed no t-LTP with 35x 1:4 (1.66 Hz; red circles, n=9/N=8), 70-100x 1:1 (1.61 Hz; blue circles, n=15/N=12), 35x 1:4 (0.5 Hz; cyan circles, n=7/N=6) stimulations compared to control (black circles, n=18/N=15) when intracellular solution contained 0.75 µM $CaCl_2$. Recording aCSF contained (in mM): 125 NaCl, 2.5 KCl, 26 NaHCO3, 0.8 NaH2PO4, 25 glucose, 1 MgCl2, 2 CaCl2, 0.1 picrotoxin. Intracellular solution contained (in mM): 140 potassium gluconate, 10 HEPES, 20 KCl, 4 Mg-ATP, 0.3 Na-GTP, 10 Na-phosphocreatine, 0.00075 CaCl2. Data displayed as mean ± SEM. Digits in the bars represent the number of recorded neurons per condition. *p < 0.05, ANOVA.

3.3 SC-CA1 synapses in 6 months old mice expressed significant t-LTP with high repeat STDP paradigms when $CaCl_2$ was excluded from intracellular solution

Since the intracellular Ca^{2+} concentration is decisive for induction of synaptic plasticity and the fully matured GABAergic inhibition in adult mice might change STDP properties, in these series of experiments we examined three different intracellular solution compositions that differed primarily in amount of free calcium i.e. + 0.75 µM $CaCl_2$ (A), – $CaCl_2$ (B) and – $CaCl_2$ + 1 mM EGTA (C). Here, both 35x 1:4 and 100x 1:1 robust STDP stimulations were executed at a frequency of 2 Hz. Adult mice did not express t-LTP with 35x 1:4 and 100x 1:1 STDP paradigms compared to control, when 0.75 µM $CaCl_2$ was included in intracellular

solution (**Fig. 10**; 0:0: 116.04 ± 7.3% (n=18/N=15); 35x 1:4: 100.11 ± 10.0% (n=6/N=5); 100x 1:1: 112.68 ± 12.3% (n=9/N=8), ANOVA $F_{(2,30)}$=0.5631 p=0.5754).

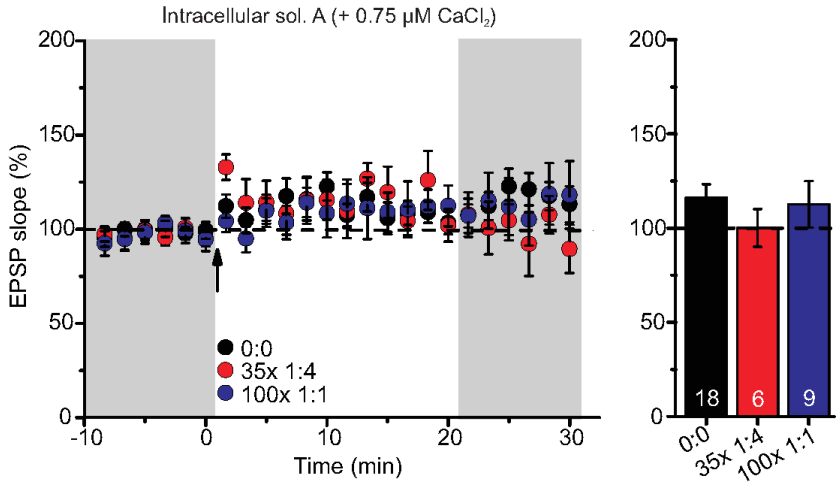

Figure 10: 35x 1:4 or 100x 1:1 stimulation did not induce t-LTP in 6 months old mice when $CaCl_2$ was included in intracellular solution. Patch clamp recordings from hippocampal CA1 pyramidal cells at a holding potential of -70 mV in current clamp mode. Left: Mean time-course of EPSP slopes for different STDP paradigms. Right: Averaged change in EPSP slopes (21-30 min) following t-LTP induction normalized to control before t-LTP induction. The hippocampal SC-CA1 synapses in 6 months old mice expressed no t-LTP when 0.75 µM $CaCl_2$ was included in intracellular solution with 35x 1:4 (2 Hz, red circles, n=6/N=5) or 100x 1:1 (2 Hz, blue circles, n=9/N=8) stimulations compared to control (black circles, n=18/N=15). Data displayed as mean ± SEM. Digits in the bar represent the number of recorded neurons per condition. *p < 0.05, data were analyzed with ANOVA (multiple comparisons).

The hippocampal SC-CA1 synapses in adult mice expressed significant t-LTP when $CaCl_2$ was excluded entirely from intracellular solution with 35x 1:4 and 100x 1:1 stimulations (**Fig. 11**; 0:0: 106.3 ± 11.0% (n=11/N=7); 35x 1:4: 139.1 ± 9.5% (n=10/N=10); 100x 1:1 WT: 142.0 ± 7.9% (n=13/N=12). ANOVA revealed a significant main effect ($F_{(2,31)}$=4.386 p=0.0210), and post hoc Dunnett's test showed p=0.0455 for 0:0 vs. 35x 1:4; p=0.0189 for 0:0 vs. 100x 1:1. Furthermore, t-LTP under these conditions can be induced and maintained successfully for 30 min.

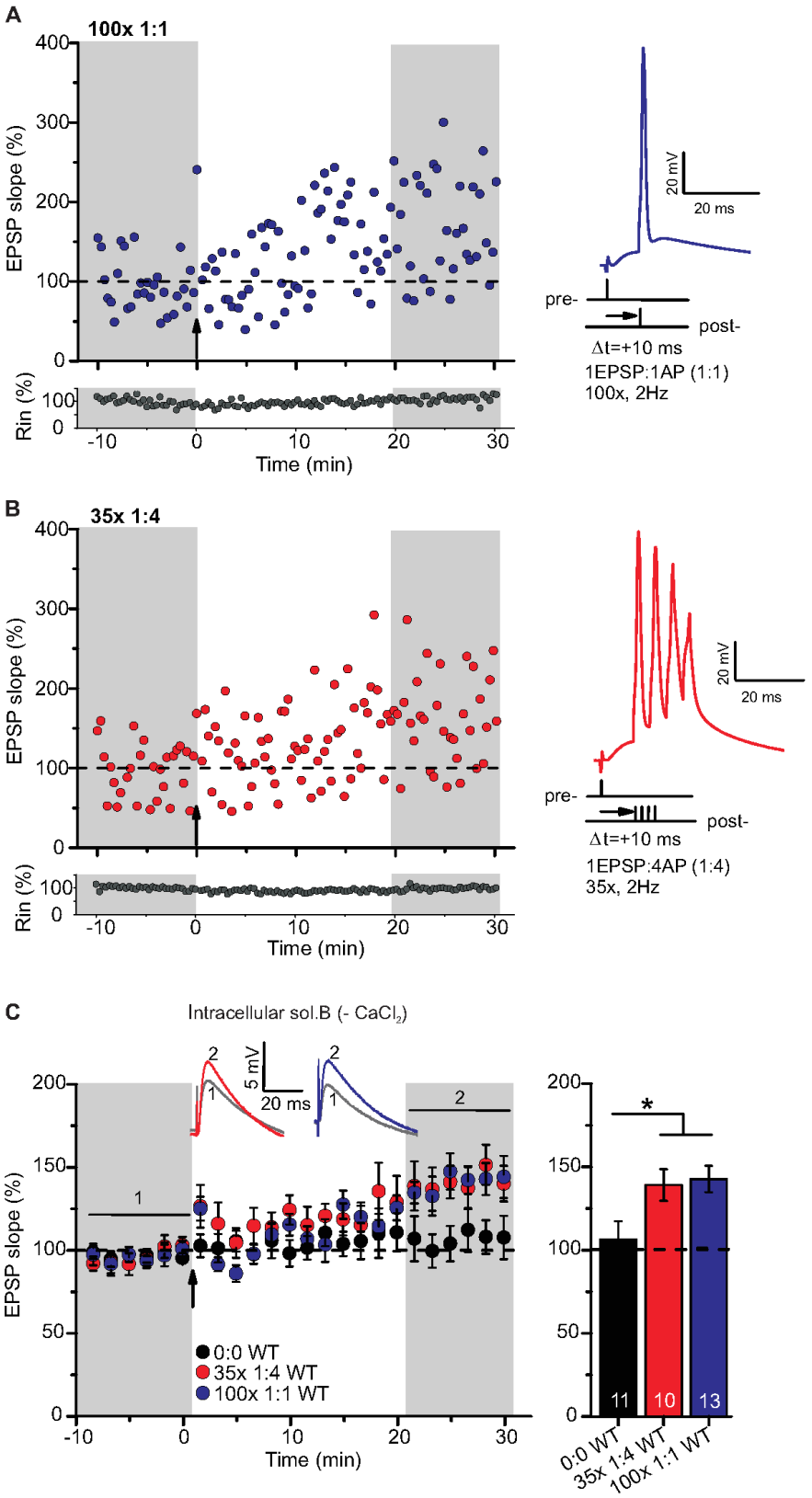

Figure 11: 35x 1:4 or 100x 1:1 STDP paradigms induced significant t-LTP at SC-CA1 synapses of 6 months old mice when $CaCl_2$ was excluded from intracellular solution. Patch clamp recordings from hippocampal CA1 pyramidal cells at a holding potential of -70 mV in current clamp mode. **(A)** Single experiment for t-LTP induced at SC-CA1 synapses in 6 months old mice (adults) with 1 presynaptic EPSP paired

with 1 postsynaptic action potential (AP, 100x 1:1) STDP paradigm. **(B)** Single experiment for 1 presynaptic EPSP paired with 4 postsynaptic APs (35x 1:4) STDP stimulation induced t-LTP at the hippocampal SC-CA1 synapses in adult animals. **(C)** Left: Mean time-course of EPSP slopes for different STDP paradigms. Right: Averaged change in EPSP slopes (21-30 min) following t-LTP induction normalized to control before t-LTP induction. Adult mice expressed significant t-LTP when $CaCl_2$ was excluded from intracellular solution with 35x 1:4 (2 Hz, red circles, n=10/N=10) or 100x 1:1 (2 Hz, blue circles, n=13/N=12) stimulations compared to control (black circles, n=11/N=7). Insets: average EPSP before (1) and after t-LTP induction (2). Scale bars are shown in the respective insets. Data displayed as mean ± SEM. Digits in the bar represent the number of recorded neurons per condition. *$p < 0.05$, data were analyzed with ANOVA (multiple comparisons). Modified after Garad et al., 2021.

We next asked whether t-LTP could still be elicited in the absence of added Ca^{2+} plus buffering the intracellular Ca^{2+} with EGTA. We observed that adult 6 months old mice expressed no t-LTP with 100x 1:1 stimulation compared to control, when $CaCl_2$ was excluded entirely and 1 mM EGTA was added in the intracellular solution (**Fig. 12A**; 0:0: 110.31 ± 6.9% (n=13/N=9); 100x 1:1: 129.24 ± 9.4% (n=9/N=6), two-tailed Student's t-test $t_{(20)}$=-1.6565 p=0.1132). Altogether, these results indicate that presence of a specific amount of $CaCl_2$ indeed is crucial to observe t-LTP at hippocampal SC-CA1 synapses in adults. **Figure 12B** recapitulates the influence of amount of free calcium in intracellular solution on t-LTP magnitude.

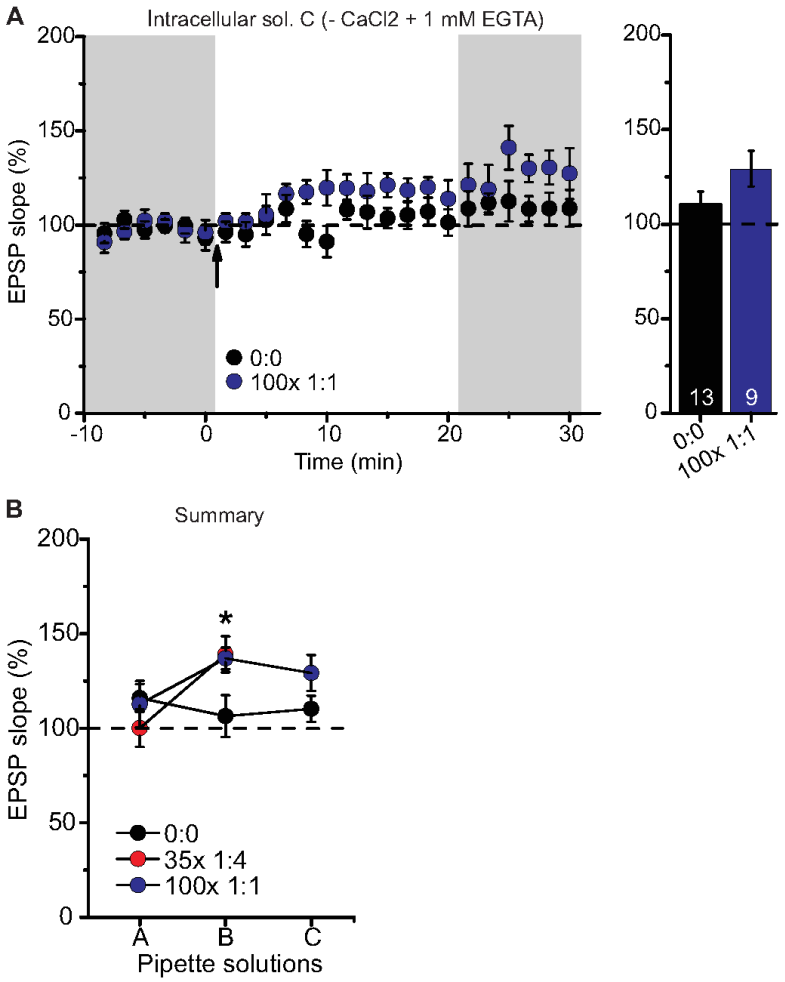

Figure 12: High repeat canonical stimulation (100x 1:1) did not induce t-LTP in adult mice with $CaCl_2$ excluded and EGTA (1 mM) included in the intracellular solution. Patch clamp recordings from hippocampal CA1 pyramidal cells at a holding potential of -70 mV in current clamp mode. **(A)** Left: Mean time-course of EPSP slopes for different STDP paradigms. Right: Averaged change in EPSP slopes (21-30 min) following t-LTP induction normalized to control before t-LTP induction. With 100x 1:1 (2 Hz, blue circles, n=9/N=6) stimulation, we observed no t-LTP in adult mice compared to control (black circles, n=13/N=9), with $CaCl_2$ excluded and 1 mM EGTA added to intracellular solution. Data displayed as mean ± SEM. Digits in the bar represent the number of recorded neurons per condition. *p < 0.05, two-tailed Student's t-test (A). **(B)** The plot summarizes the influence of amount of free calcium in intracellular solution on t-LTP expression efficiency. It shows t-LTP magnitude (EPSP slope %) for each intracellular solution with different STDP paradigms. +: inclusion, –: exclusion.

3.4 Low repeat STDP paradigms induced significant t-LTP at hippocampal SC-CA1 synapses in 6 months old mice

As described in the previous section, high repeat STDP paradigms at high frequency (2 Hz) induced t-LTP in 6 months old mice when Ca^{2+} and EGTA were absent from the intracellular

solution. To further characterize t-LTP in 6 months old mice, we next asked whether low repeat STDP paradigms at low frequency (0.5 Hz) can be successful in t-LTP induction at SC-CA1 synapses in the hippocampus of 6 months old mice (for low repeat STDP in juveniles, compare (Cepeda-Prado et al., 2019)). This is an important question since the low repeat paradigms rely on only 6 pairings of pre- and postsynaptic spiking occurring within 10 ms, thereby better resembling firing patterns that occur in rodents during learning *in vivo* (compare Otto et al., 1991). In fact, the hippocampal SC-CA1 synapses in adult mice showed significant t-LTP induced by 6x 1:4 stimulation, whereas the 6x 1:1 STDP paradigm induced synaptic change did not reach statistically significant t-LTP (**Fig. 13**; 0:0: 106.9 ± 7.7% (n=11/N=10); 6x 1:4: 157.9 ± 14.2% (n=11/N=8); 6x 1:1: 134.3 ± 7.5% (n=13/N=10)). ANOVA analyses showed a significant main effect ($F_{(2,32)}$=6.142 p=0.0055), and post hoc Dunnett's test revealed p=0.0027 for 0:0 vs. 6x 1:4, p=0.1041 for 0:0 vs 6x 1:1. Nevertheless, the 6x 1:1 STDP paradigm induced significant t-LTP in comparison to negative controls as well as its own baseline (two-tailed Student's t-test $t_{(22)}$=-2.5518 p=0.0182; one-sample t-test $t_{(12)}$=4.595 p=0.0006). While these results revealed that t-LTP can be induced in 6 months old WT mice with both low repeat STDP paradigms, a higher magnitude of t-LTP was observed in WT animals in response to the 6x 1:4 compared to the 6x 1:1 protocol.

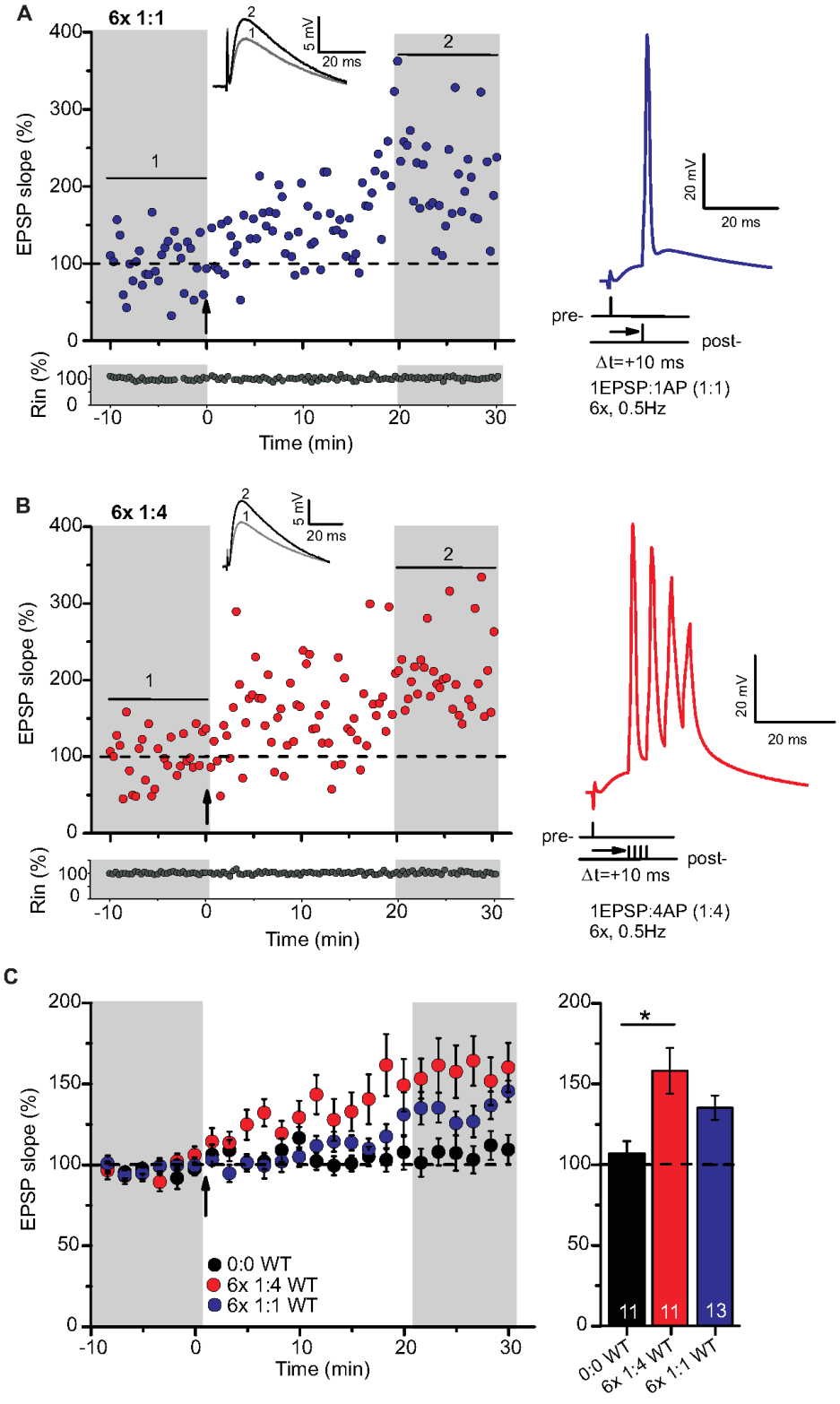

Figure 13: Low repeat STDP paradigms in forward fashion induced t-LTP at SC-CA1 synapses in 6 months old adult mice. Patch clamp recordings from hippocampal CA1 pyramidal cells at a holding potential of -70 mV in current clamp mode. **(A)** Single experiment for t-LTP induced at SC-CA1 synapses in 6 months old mice (adults) with 1 presynaptic EPSP paired with 1 postsynaptic AP (6x 1:1) STDP paradigm. **(B)** Single experiment for 1 presynaptic EPSP paired with 4 postsynaptic APs (6x 1:4) STDP stimulation induced t-LTP at

the hippocampal SC-CA1 synapses in adult animals. Insets: average EPSP before (1) and after t-LTP induction (2). **(C)** Left: Mean time-course of EPSP slopes with different STDP paradigms. Right: Averaged change in EPSP slopes (21-30 min) following t-LTP induction normalized to control before t-LTP induction. Adult mice expressed a significant t-LTP, induced by 6x 1:4 stimulation (red circles, n=11/N=8; p=0.003) while no t-LTP induced by 6x 1:1 STDP paradigm (blue circles, n=13/N=10; p=0.104) compared to unpaired control (black circles, n=11/N=10). Data displayed as mean ± SEM. Scale bars are presented in the respective insets. Digits in the bars represent the number of recorded neurons per condition. *: $p<0.05$, multiple comparisons were performed with ANOVA. Adapted from Garad et al., 2021.

Furthermore, we tested efficiency of negative spike timings (Δt=-10 ms) between presynaptic stimulation and postsynaptic AP, to investigate whether negative spike timings induce t-LTP or t-LTD in 6 months old adult mice. We observed that 6x 1:1 (Δt=-10 ms) STDP paradigm induced t-LTP at SC-CA1 synapses in 6 months old adult animals compared to unpaired control (**Fig. 14**; 0:0: 106.9 ± 7.7% (n=11/N=10); 6x 1:1: 137.4 ± 10.3% (n=18/N=11), two-tailed Student's t-test $t_{(27)}$=-2.0926 p=0.0459). Overall, under aforementioned recording conditions low or high repeat STDP paradigms at positive or negative spike timings (Δt= +10 or -10 ms) induced t-LTP at SC-CA1 synapses in 6 months old mice.

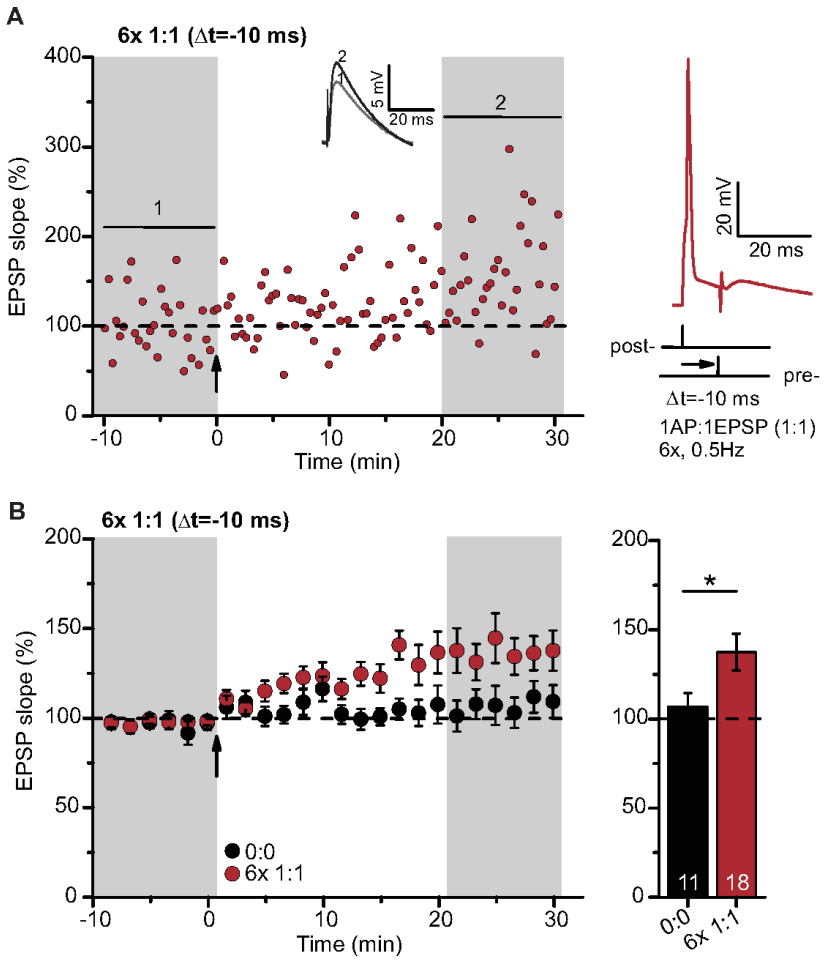

Figure 14: Low repeat STDP paradigm (6x 1:1) in backward fashion induced t-LTP at SC-CA1 synapses in 6 months old mice. Patch clamp recordings from hippocampal CA1 pyramidal cells at a holding potential of -70 mV in current clamp mode. **(A)** Single experiment for t-LTP induced at SC-CA1 synapses in adult mice using 1 postsynaptic AP paired with 1 presynaptic EPSP (6x 1:1, Δt=-10 ms) stimulation paradigm. Insets: average EPSP before (1) and after t-LTP induction (2). **(B)** Left: mean time course of EPSP slopes. Right: Averaged change in EPSP slopes (21-30 min) following t-LTP induction normalized to control before t-LTP induction. 6x 1:1 (Δt=-10 ms) STDP paradigm induced significant t-LTP in 6 months old mice (brown circles, n=18/N=11; p=0.04) in comparison to unpaired control (black circles, n=11/N=10). Data displayed as mean ± SEM. Scale bars are displayed in the inset. Digits in the bars represent the number of recorded neurons per condition. *: p<0.05, two-tailed Student's t-test.

3.5 T-LTP induced by 6x 1:4 stimulation in 6 months old mice involved NMDARs

The calcium elevation in the postsynaptic neuron is crucial for STDP. Therefore, we inspected whether NMDARs acts a Ca^{2+} source for t-LTP induced by 6x 1:4 stimulation in 6 months old mice. We observed that 6x 1:4 paradigm induced t-LTP at SC-CA1 synapses in 6 months old

adult animals is significantly impaired in the presence of APV compared to ACSF control (**Fig. 15**; ACSF: 157.3 ± 7.0% (n=8/N=6); APV: 105.6 ± 10.1% (n=9/N=5), two-tailed Student's t-test $t_{(15)}$=4.1014 p=0.0009). This indicate that 6x 1:4 t-LTP at fully matured hippocampal SC-CA1 synapses in 6 months old mice uses NMDARs as Ca^{2+} source for overall elevation in Ca^{2+} levels in the postsynaptic neuron.

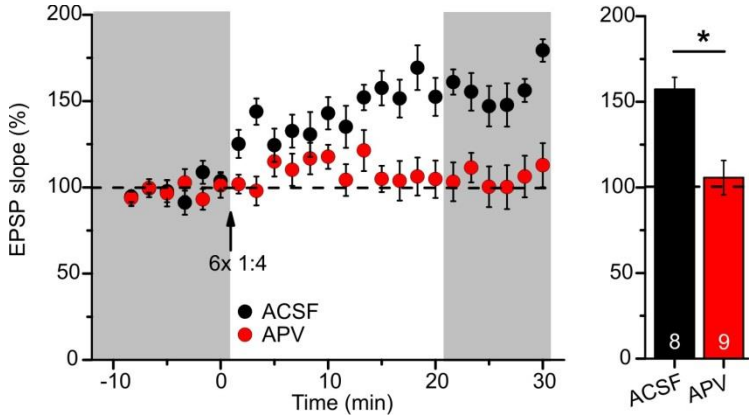

Figure 15: T-LTP induced by 6x 1:4 stimulation at SC-CA1 synapses in 6 months old mice is dependent on NMDARs. Patch clamp recordings from hippocampal CA1 pyramidal cells at a holding potential of -70 mV in current clamp mode. Left: mean time course of EPSP slopes. Right: Averaged change in EPSP slopes (21-30 min) following t-LTP induction normalized to control before t-LTP induction. 6x 1:4 stimulation induced t-LTP at hippocampal SC-CA1 synapses is significantly impaired in the presence of APV (red circles, n=9/N=5; p<0.001) in comparison to ACSF control (black circles, n=8/N=6) in adult mice. Data displayed as mean ± SEM. Digits in the bars represent the number of recorded neurons per condition. *: p<0.05, two-tailed Student's t-test.

In order to understand the impact of developmental maturation of mice on STDP, we used similar recording conditions in 1-month old mice (juveniles) and 6 months old adult mice (fully developed central nervous system) to study STDP at SC-CA1 synapses in the hippocampus. The results for STDP at SC-CA1 synapses and basal electrical and synaptic properties of CA1 pyramidal neurons in the hippocampus of adult compared to juvenile animals are described in the following sections.

3.6 T-LTP induced by 6x 1:1 stimulation was decreased in 6 months old adults compared to 1-month old juvenile mice

Under similar recording conditions, we investigated t-LTP at hippocampal SC-CA1 synapses in slices from 1-month old (juveniles) and 6 months old (adults) mice in order to understand the impact of developmental maturation on STDP. The SC-CA1 synapses in juvenile animals displayed significant t-LTP induced with 6x 1:4 or 6x 1:1 stimulations (**Fig. 16A**; 0:0: 106.19 ± 9.4% (n=11/N=7); 6x 1:4: 142.98 ± 7.9% (n=10/N=8); 6x 1:1: 165.15 ± 8.3% (n=9/N=7)). ANOVA analyses showed a significant main effect ($F_{(2,27)}$=11.96 p=0.0002), and post hoc Dunnett's test revealed p=0.0091 for 0:0 vs 6x 1:4, and p=0.0001 for 0:0 vs 6x 1:1. Six months old adult mice displayed comparable t-LTP, induced with 6x 1:4 stimulation, as juveniles (**Fig. 16B**; Juveniles: 142.98 ± 7.9% (n=10/N=8); Adults: 157.9 ± 14.2% (n=11/N=8), two-tailed Student's t-test $t_{(19)}$=-0.8954 p=0.3818; compare **Fig. 13**). Nevertheless, adult mice expressed significantly decreased t-LTP magnitude, induced with 6x 1:1 STDP stimulation, in comparison to juveniles (**Fig. 16C**; Juveniles: 165.15 ± 8.3% (n=9/N=7); Adults: 134.3 ± 7.5% (n=13/N=10), two-tailed Student's t-test $t_{(20)}$=2.7201 p=0.0132; compare **Fig. 13**). Altogether, 6x 1:4 STDP paradigm induced comparable t-LTP in juvenile and adults, while adults displayed decreased t-LTP induced by 6x 1:1 STDP paradigm compared to juveniles.

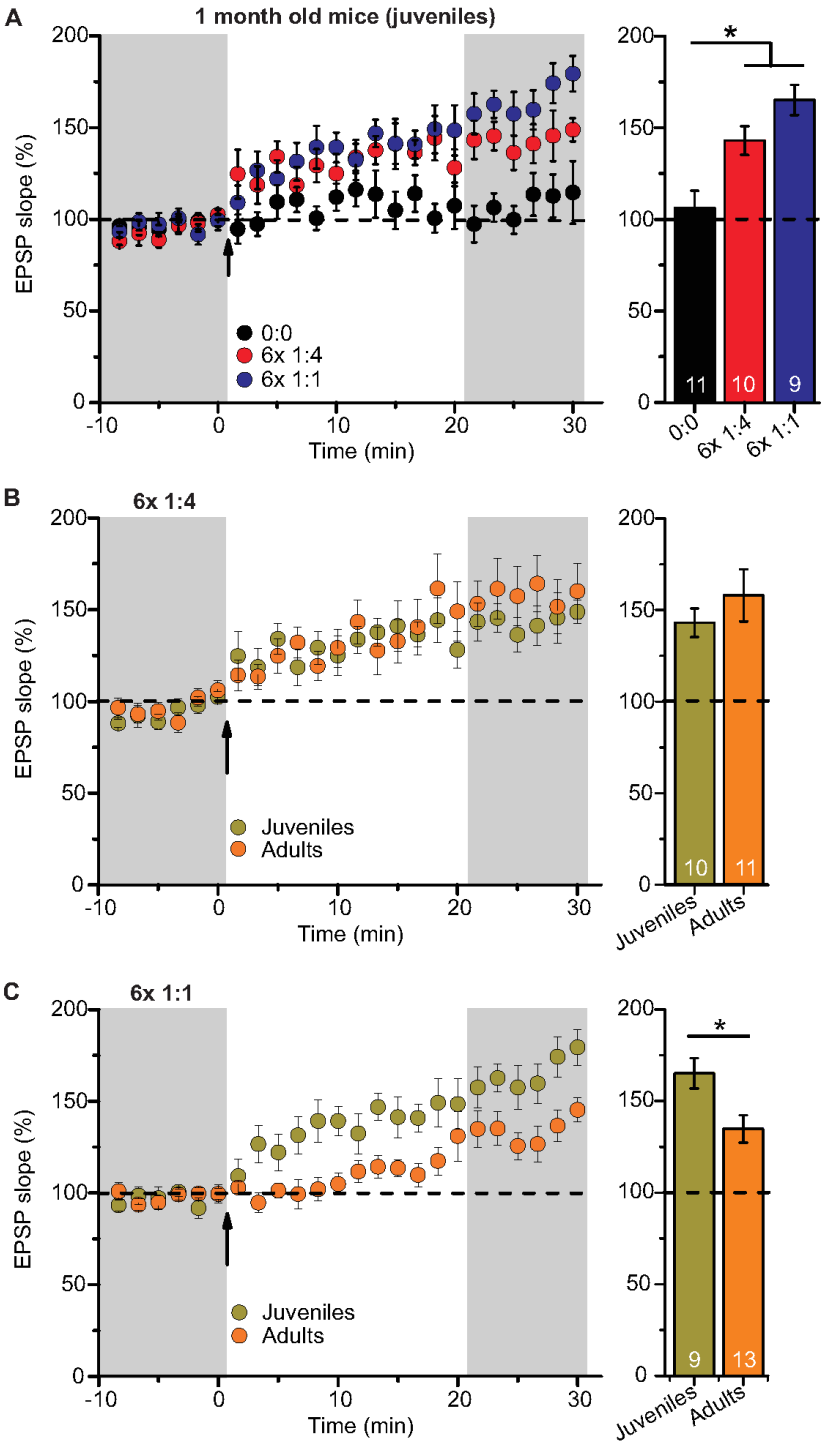

Figure 16: Six months old mice displayed similar 6x 1:4 t-LTP, while decreased 6x 1:1 t-LTP at SC-CA1 synapses compared to 1-month old juveniles. Patch clamp recordings from CA1 pyramidal cells at a holding potential of -70 mV in current clamp mode. Left: mean time course for EPSP slopes with different STDP paradigms. Right: Averaged change in EPSP slopes (21-30 min) following t-LTP induction normalized to control before t-LTP induction. **(A)** 6x 1:4 (red circles, n=10/N=8; p=0.0091) or 6x 1:1 stimulations (blue circles, n=9/N=7; p=0.0001) induced significant t-LTP in 1 month old juvenile mice in comparison to unpaired control (0:0; black circles, n=11/N=7). **(B)** 6 months old adult (orange circles, n=11/8) and 1 month old juvenile (dark yellow circles, n=10/8) mice displayed comparable 6x 1:4 t-LTP (p=0.38) (**C**) Adults (orange circles,

n=13/10) expressed decreased 6x 1:1 t-LTP in comparison to juveniles (dark yellow circles, n=9/7, p=0.01). Data shown as mean ± SEM. Digits in the bars indicate the number of recorded neurons per condition. *: p<0.05, parametric data were analyzed using ANOVA (A, multiple comparisons) and two-tailed Student's t-test (B and C).

3.7 Negative spike timing pairing of one postsynaptic AP with one presynaptic stimulation (6x 1:1, Δt= –10 ms) induced t-LTP in adults but not in juveniles

With positive spike timings, the 6x 1:4 STDP paradigm induced comparable t-LTP in juveniles and adults, while 6x 1:1 stimulation induced decreased t-LTP in adults compared to juveniles; both stimulations executed with positive spike timings (Δt= +10 ms). Henceforth, in a next approach we tested efficiency of negative spike timings (Δt= –10 ms) between postsynaptic AP and presynaptic stimulation, to investigate STDP in 6 months old adult mice compared to 1-month old juveniles. The 6x 1:1 (Δt= –10 ms) STDP paradigm did not induce t-LTP at SC synapses in juveniles (**Fig. 17A**; 0:0: 108.05 ± 10.4% (n=9/N=6); 6x 1:1: 107.78 ± 5.5% (n=8/N=4), two-tailed Student's t-test $t_{(15)}$=0.0216 p=0.9830). Six months old mice expressed a higher t-LTP magnitude, however it did not reach statistical significance compared to juvenile mice (**Fig. 17B**; Juveniles: 107.78 ± 5.5% (n=8/N=4); Adults: 137.4 ± 10.3% (n=18/N=11), two-tailed Student's t-test t(24)=1.8392 p=0.0783; compare **Fig. 14**). These results indicate that the 6x 1:1 (Δt= –10 ms) stimulation induced synaptic change (no t-LTP) transforms into significant t-LTP as animals mature from 1 month to 6 months, which highlights a developmental change in STDP. These results suggest a possible role of developmental maturation in STDP at hippocampal SC-CA1 synapses, in a STDP paradigm-dependent manner.

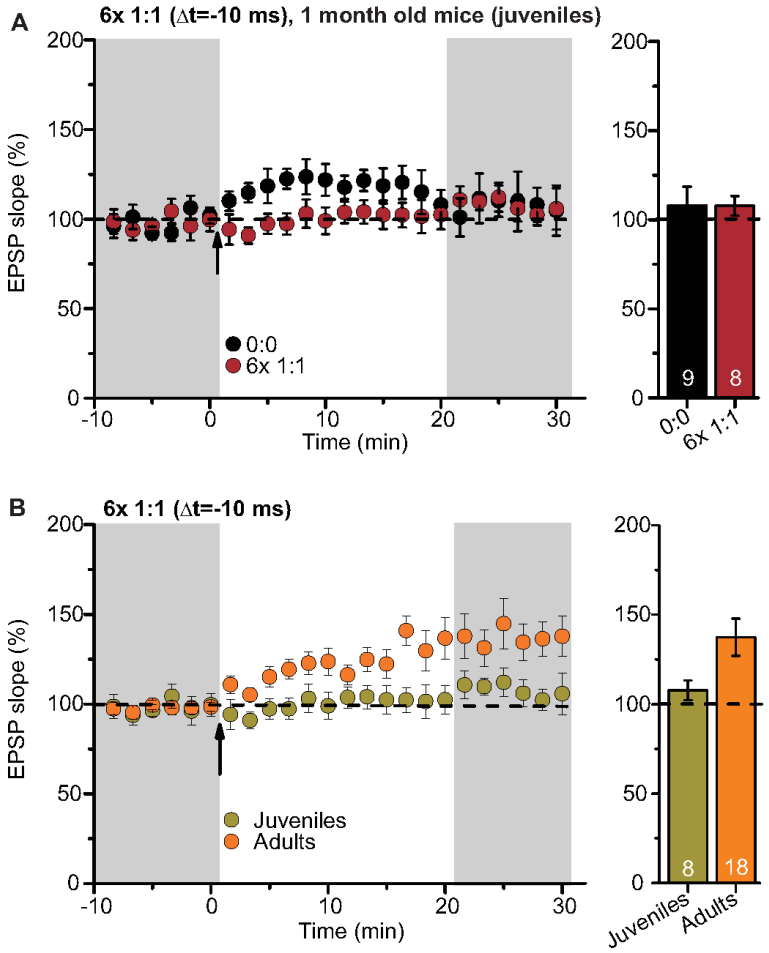

Figure 17: Negative pairing of one postsynaptic AP with one presynaptic stimulation (6x 1:1, Δt=-10 ms) induced t-LTP at SC-CA1 synapses in adults but no t-LTP in juveniles. Patch clamp recordings from hippocampal CA1 pyramidal cells at a holding potential of -70 mV in current clamp mode. Left: mean time course for EPSP slopes for 6x 1:1, Δt=-10 ms STDP paradigm. Right: Averaged change in EPSP slopes (21-30 min) following t-LTP induction normalized to control before t-LTP induction. **(A)** 6x 1:1 (Δt=-10 ms) did not induce t-LTP in 1-month old mice (brown circles, n=8/N=4; p=0.9830) in comparison to unpaired control (0:0; black circles, n=9/N=6). (**B**) Six months old adult mice (orange circles, n=18/N=11) displayed higher t-LTP magnitude, though does not reach statistical significance, compared to juveniles (dark yellow circles, n=8/N=4, p=0.07). Data displayed as mean ± SEM. Digits in the bars represent the number of recorded neurons per condition. *: p<0.05 (two-tailed Student's t-test).

3.8 Six months old mice exhibited decreased intrinsic excitability of CA1 pyramidal neurons and decreased paired-pulse facilitation at SC-CA1 synapses

Since we observed altered STDP induced with 6x 1:1 (Δt= + or –10 ms) paradigm at hippocampal SC-CA1 synapses in 6 months old adult compared to 1-month old juvenile

animals, we wanted to clarify whether such a developmental difference was also present for basal electrical and synaptic properties of CA1 pyramidal neurons in adults. The hippocampal CA1 neurons from adults displayed significantly decreased intrinsic excitability, measured in the form of somatic driven action potentials firing, (**Fig. 18A**; depolarization step 180 pA: Juveniles: 23.2 ± 0.87 Hz (n=15/N=12); Adults: 17.9 ± 0.85 Hz (n=16/N=14), ANOVA $F_{(1,290)}$=131.6 p<0.0001), and decreased AP amplitudes in comparison to juveniles (**Fig. 18E**; Juveniles: 82.5 ± 1.52 mV (n=15/N=12); Adults: 76.6 ± 1.61 mV (n=16/N=14), two-tailed Student's t-test $t_{(29)}$=2.6724 p=0.0122). Whereas, CA1 neurons in adult mice showed comparable rheobases (**Fig. 18D**; Juveniles: 216.0 ± 6.53 pA (n=15/N=12); Adults: 227.5 ± 9.46 pA (n=16/N=14), Mann-Whitney U-test U=95.50 p=0.297), and after-depolarizations (**Fig. 18F**; Juveniles: 13.3 ± 0.38 mV (n=15/N=12); Adults: 12.8 ± 0.41 mV (n=16/N=14), two-tailed Student's t-test $t_{(29)}$=0.8871 p=0.3823) as juveniles. Adults showed significantly decreased PPR (**Fig. 18B**; Juveniles: 1.88 ± 0.13 (n=15/N=12); Adults: 1.56 ± 0.08 (n=15/N=14), two-tailed Student's t-test $t_{(28)}$=2.0995 p=0.0449), increased $GABA_B$ inhibitory responses coinciding with the EPSP decay (**Fig. 18J**; Juveniles: 0.77 ± 0.1 mV (n=14/N=11); Adults: 1.09 ± 0.1 mV (n=16/N=14), two-tailed Student's t-test $t_{(28)}$=-3.4896 p=0.0016), while similar EPSP rise times (**Fig. 18H**; Juveniles: 4.8 ± 0.17 ms (n=15/N=12); Adults: 4.7 ± 0.12 ms (n=16/N=14), two-tailed Student's t-test $t_{(29)}$=0.4436 p=0.6606), and EPSP decay times (**Fig. 18I**; Juveniles: 52.4 ± 1.28 ms (n=15/N=12); Adults: 51.9 ± 1.35 ms (n=16/N=14), two-tailed Student's t-test $t_{(29)}$=0.2847 p=0.7779) at SC-CA1 synapses compared to juveniles. Hippocampal CA1 neurons from adult mice showed similar resting membrane potentials (**Fig. 18C**; Juveniles: -74.7 ± 0.71 mV (n=15/N=12); Adults: -74.9 ± 0.62 mV (n=16/N=14), two-tailed Student's t-test $t_{(29)}$=0.2224 p=0.8256) and higher input resistances, although this effect did not reach statistical significance (**Fig. 18G**; Juveniles: 165.7 ± 7.98 MΩ (n=15/N=12); Adults: 184.8 ± 7.21 MΩ (n=16/N=14), two-tailed Student's t-test $t_{(29)}$=-1.7790 p=0.0857) in comparison to juveniles. Overall, basal electrical properties such as intrinsic excitability in CA1 neurons and synaptic properties, e.g. short-term plasticity, measured in the form of PPR, at SC-CA1 synapses were altered as a result of developmental maturation in 6 months old mice compared to 1-month old mice. Furthermore, the $GABA_B$ inhibitory responses coinciding with the EPSP decay at hippocampal SC-CA1 synapses increased significantly during development as observed in 6 months old adult mice. These altered basal properties of CA1 pyramidal neurons, particularly increased $GABA_B$ inhibitory responses coinciding with the EPSP decay be the cause underlying 6x 1:1 (Δt= + or –10 ms) stimulation induced altered STDP in adults.

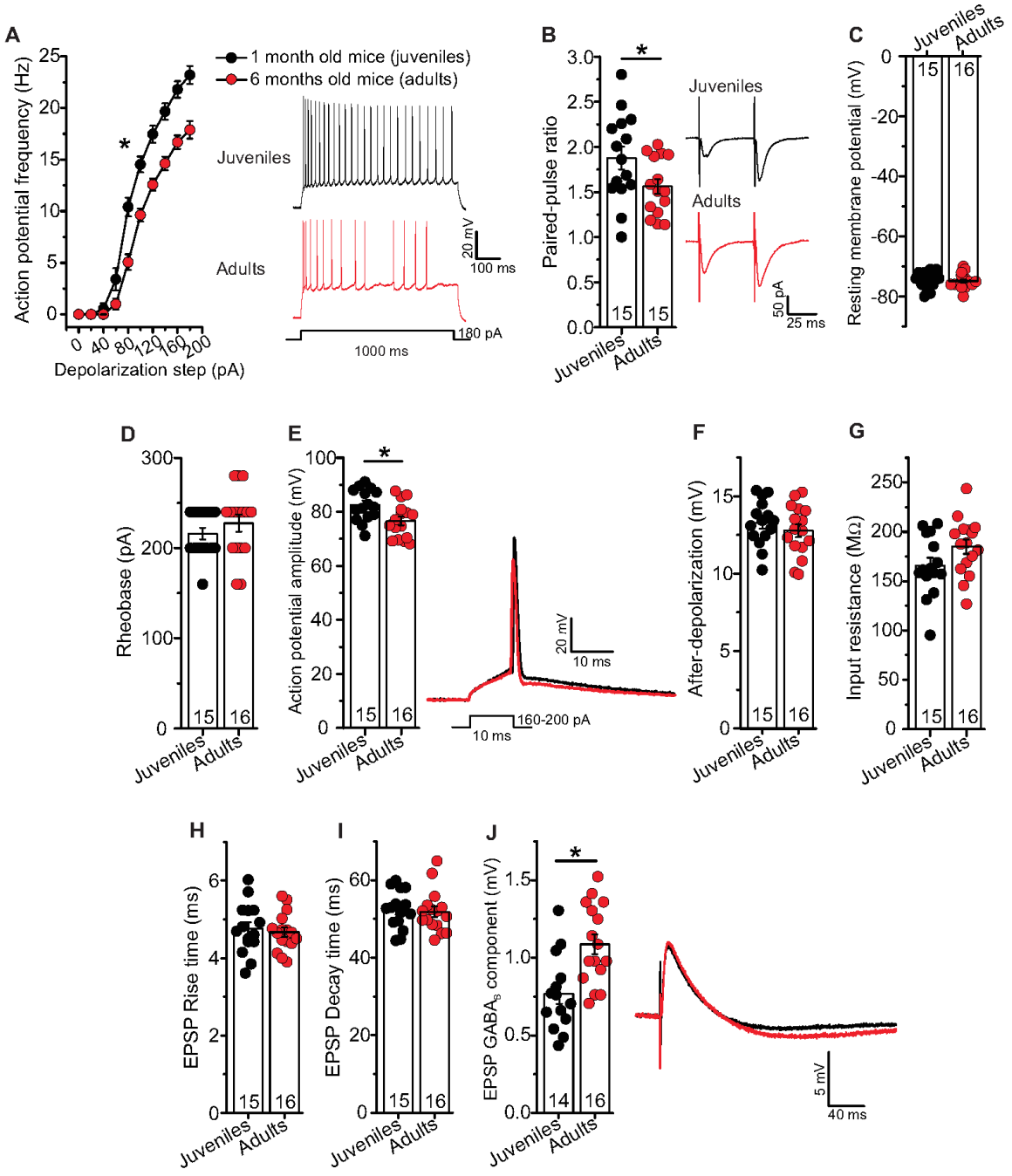

Figure 18: Six months old adult mice showed altered basal electrical and synaptic properties of hippocampal CA1 pyramidal neurons. Patch clamp recordings from hippocampal CA1 pyramidal cells at a holding potential of -70 mV in current clamp or voltage clamp mode. 6 months old mice (adults) specified by red circles, while 1-month old mice (juveniles) represented by black circles. **(A)** CA1 pyramidal neurons in adults displayed decreased intrinsic excitability compared to juveniles ($p<0.0001$, ANOVA). Insets: action potentials (APs) firing in CA1 neurons in response to 180 pA (for 1000 ms) somatic current injection from juveniles and adults. **(B)** Paired-pulse ratio (PPR) at SC-CA1 synapses in adults was significantly reduced compared to juveniles ($p=0.04$). Insets: PPR at inter-stimulus interval of 50 ms in juveniles and adults. Hippocampal CA1 neurons from adult mice showed similar resting membrane potentials (**C**; $p=0.83$), rheobases (**D**; $p=0.31$), after-depolarizations (**F**; $p=0.38$), EPSP rise times (**H**; $p=0.66$) and EPSP decay times (**I**; $p=0.78$) as juveniles. Adult

animals expressed significantly decreased AP amplitudes (**E**; p=0.01) compared to juveniles. Insets: Single AP firing in CA1 neurons in response to somatic current injection from juveniles (200 pA) and adults (160 pA). CA1 cells in adults displayed increased input resistances, though not statistically significant compared to juveniles (**G**; p=0.09). The hippocampal CA1 neurons from adults showed significantly increased $GABA_B$ inhibitory responses coinciding with the EPSP decay compared to juveniles (**J**; p=0.002). Insets: EPSP time-course from juveniles and adults. Scale bars are shown in the respective insets. Digits in the bars represent the number of recorded neurons per condition, at least from three different animals per group. Data expressed as mean ± SEM. *: $p<0.05$, parametric data were compared by two-tailed Student's t-test while non-parametric data were analyzed with Mann-Whitney U-test.

To sum up, SC-CA1 synapses in the hippocampus of 6 months old adult mice exhibited successful induction and expression of t-LTP, induced with low repeat (6x, 0.5 Hz) as well as high repeat (35x for 1:4, 70-100x for 1:1, 2 Hz) canonical and burst STDP paradigms under specified recording conditions (i.e., no added Ca^{2+} and no EGTA in the pipette solution). The 6x 1:4 STDP paradigm induced comparable t-LTP in 1-month old juvenile and 6 months old adult mice. As a consequence of developmental maturation, 6 months old mice exhibited decreased 6x 1:1 (Δt= +10 ms) t-LTP compared to juveniles. Furthermore, 6x 1:1 (Δt= –10 ms) stimulation induced t-LTP at hippocampal SC-CA1 synapses of 6 months old mice compared to no t-LTP induction in 1-month old mice. Moreover, adult mice showed changed basal electrical and synaptic properties of CA1 pyramidal neurons. In particular, intrinsic excitability, presynaptic release probability (short-term plasticity, PPR) and $GABA_B$ receptor mediated inhibitory responses coinciding with the EPSP decay differed, when compared to the respective properties in juvenile animals. Altogether, these results indicate that canonical stimulation (6x 1:1) induced t-LTP and basal electrical properties of CA1 pyramidal neurons show significant changes with developmental maturation from 1- to 6-months old in mice. In later parts of this dissertation, we investigated pathological aging influence, e.g., Alzheimer's disease, on STDP in 6 months old adult APP/PS1 mice.

3.9 Low repeat STDP paradigms induced t-LTP in 6 months old APP/PS1 mice when amyloid beta (Aβ) plaques location was not considered

To test whether Alzheimer's disease (AD) pathology has an effect on STDP at SC-CA1 synapses in the hippocampus, we investigated 6x 1:4 and 6x 1:1 induced t-LTP in 6 months old APP/PS1 mice. We observed unaltered 6x 1:4 t-LTP at hippocampal SC-CA1 synapses in

APP/PS1 mice in comparison to WT littermate mice (**Fig. 19A**; 6x 1:4 WT: 153.8 ± 13.5% (n=13/N=7); 6x 1:4 APP/PS1: 138.9 ± 8.7% (n=12/N=6), Mann-Whitney U-test U=87.0, p=0.624). However, the hippocampal SC-CA1 synapses in APP/PS1 animals displayed significant t-LTP compared to WT littermates (**Fig. 19B**; 6x 1:1 WT: 95.06 ± 8.5% (n=10/N=8); 6x 1:1 APP/PS1: 129.1 ± 11.9% (n=12/N=5), two-tailed Student's t-test $t_{(20)}$=-2.2325 p=0.0372). Surprisingly, 6x 1:1 STDP stimulation was unsuccessful to induce t-LTP in WT littermates suggesting gain of function in APP/PS1 mice. Together, these results indicate that hippocampal SC-CA1 synapses in APP/PS1 mice show comparable 6x 1:4 t-LTP, while 6x 1:1 t-LTP was observed in APP/PS1 mice but not in WT littermates.

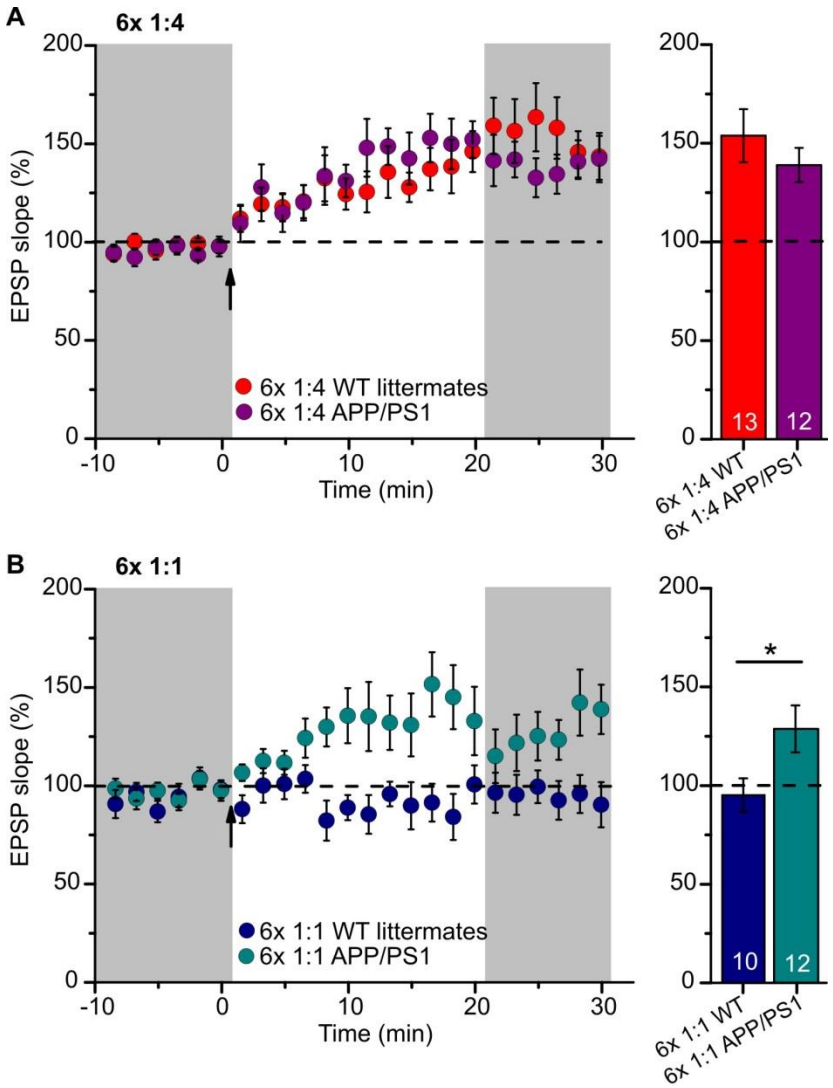

Figure 19: **SC-CA1 synapses in 6 months old APP/PS1 mice exhibited intact t-LTP induced by 6x 1:1 or 6x 1:4 stimulations.** Patch clamp recordings from hippocampal CA1 pyramidal cells at a holding potential of -70 mV in current clamp mode. Left: Mean time-course of EPSP slopes with either of the two different STDP

paradigms. Right: Averaged change in EPSP slopes (21-30 min) following t-LTP induction normalized to control before t-LTP induction. **(A)** The hippocampal SC-CA1 synapses in APP/PS1 mice showed unaltered 6x 1:4 t-LTP magnitude (purple circles, n=12/N=6; p=0.62) compared to t-LTP in WT littermate mice (red circles, n=13/N=7). **(B)** 6x 1:1 stimulation induced significant t-LTP in 6 months old APP/PS1 mice (cyan circles, n=12/N=5; p=0.037) but no t-LTP in WT littermates (blue circles, n=10/N=8). Data shown as mean ± SEM. Digits in the bars represent the number of recorded neurons per condition. *: p<0.05, Non-parametric data were analyzed using Mann-Whitney U-test (A), while parametric data were compared with two-tailed Student's t-test (B). Figure (A) adapted from Garad et al., 2021.

3.10 Negative spike timing pairing of one postsynaptic AP with one presynaptic stimulation (6x 1:1, Δt=-10 ms) induced intact t-LTP in 6 months old APP/PS1 mice

To test the efficiency of negative spike timing (Δt=-10 ms) between presynaptic stimulation and postsynaptic AP to induce t-LTP also in our AD mouse model, we compared slices from 6 months old APP/PS1 and WT littermate mice for 6x 1:1 (Δt=-10 ms) induced t-LTP (compare **Fig. 14**). Here we observed unimpaired t-LTP, induced by 6x 1:1 (Δt=-10 ms), at the hippocampal SC-CA1 synapses in APP/PS1 mice in comparison to WT littermate mice (**Fig. 20**; 6x 1:1 WT: 132.7 ± 19.2% (n=11/N=5); 6x 1:1 APP/PS1: 120.9 ± 8.4% (n=12/N=6), Mann-Whitney U-test: U=66.0, p=1.0). To sum up, these data show that negative spike timing (Δt=-10 ms) induced t-LTP is intact in the hippocampal CA1 neurons in the APP/PS1 mouse model of AD used in this study.

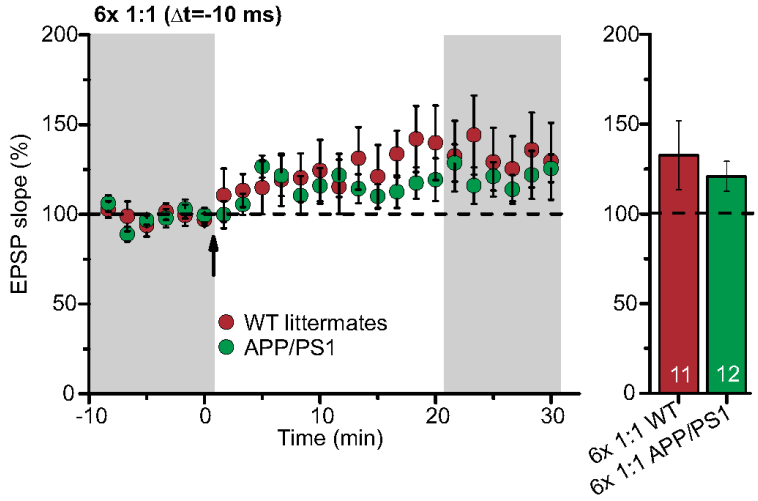

Figure 20: **Pairing of one postsynaptic AP with one presynaptic stimulation for negative spike timings (6x 1:1, Δt=-10 ms) induced t-LTP at SC-CA1 synapses in adult APP/PS1 mice.** Patch clamp recordings from hippocampal CA1 pyramidal cells at a holding potential of -70 mV in current clamp mode. Left: mean time course of EPSP slopes. Right: Averaged changes in EPSP slopes (21-30 min) following t-LTP induction

normalized to control before t-LTP induction. The hippocampal SC-CA1 synapses in APP/PS1 mice (green circles, n=12/N=6; p=1.0) displayed similar t-LTP, induced with 6x 1:1 (Δt=-10 ms)**,** as WT littermate mice (brown circles, n=11/N=5). Data displayed as mean ± SEM. Digits in the bars represent the number of recorded neurons per condition. *: p<0.05, Mann-Whitney U-test.

3.11 High repeat STDP paradigm (100x 1:1) induced t-LTP at hippocampal SC-CA1 synapses in 6 months old APP/PS1 mice

Since the low repeat STDP paradigms did not reveal a difference between WT littermate and APP/PS1 mice, we argued that in order to observe an AD pathology associated impact on t-LTP at single neuron level, it might be necessary to use more robust STDP induction stimuli. Since 100x 1:1 (2 Hz) STDP paradigm induced substantial t-LTP under our recording conditions in 6 months old adult mice (compare **Fig. 11**); we tested 100x 1:1 in APP/PS1 mice for t-LTP induction. Here, we also asked whether t-LTP induced with high repeat paradigms is different in magnitude or time-course compared to t-LTP induced with low repeat paradigms in 6 months old APP/PS1 mice. We observed no significant difference in t-LTP magnitudes at SC-CA1 synapses in APP/PS1 vs. WT lttermate mice, induced by 100x 1:1 stimulation (**Fig. 21**; 100x 1:1 WT: 130.9 ± 8.5% (n=11/N=5); 100x 1:1 APP/PS1: 157.3 ± 14.9% (n=9/N=5), two-tailed Student's t-test $t_{(18)}$=-1.6047 p=0.1259). This indicates that high repeat stimulation (100x 1:1) induced t-LTP is intact in adult APP/PS1 mice. Further, high repeat STDP stimulation protocol (100x 1:1: 157.3 ± 14.9%) yields more effective t-LTP than its low repeat paradigm (6x 1:1; 129.1 ± 11.9% compare **Fig. 19**), though did not reach statistical significance (two-tailed Student's t-test $t_{(19)}$=-1.4994 p=0.1502), at hippocampal SC-CA1 synapses in 6 months old APP/PS1 mice.

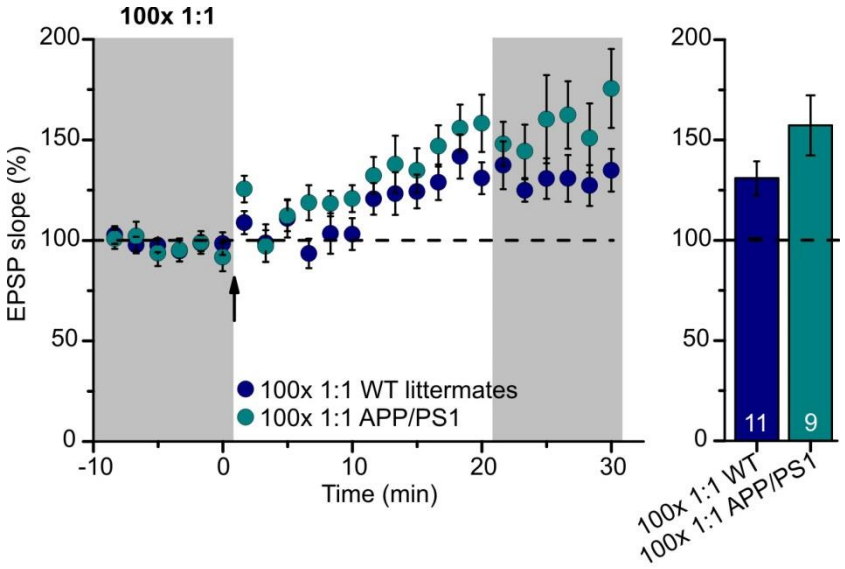

Figure 21: High repeat STDP paradigm 100x 1:1 induced t-LTP at SC-CA1 synapses in 6 months old APP/PS1 mice. Patch clamp recordings from hippocampal CA1 pyramidal cells at a holding potential of -70 mV in current clamp mode. Left: mean time course for EPSP slopes with 100x 1:1 (2 Hz) STDP paradigm. Right: Averaged changes in EPSP slopes (21-30 min) following t-LTP induction normalized to control before t-LTP induction. 100x, 1:1 stimulation induced comparable t-LTP in APP/PS1 mice (cyan circles, n=9/N=5; p=0.28) and WT littermates (blue circles, n=11/N=5). Data shown as mean ± SEM. Digits in the bars indicate the number of recorded neurons per condition. *: p<0.05, two-tailed Student's t-test. Adapted from Garad et al., 2021.

3.12 Six months old adult APP/PS1 mice expressed Aβ plaque distance-dependent t-LTP impairments

As described in earlier sections, adult APP/PS1 mice displayed intact t-LTP induced by different STDP paradigms when tested under conditions where the location of Aβ plaques relative to the recorded cell is not visualized. Henceforth, we argued that the proximity of Aβ plaques might be decisive to observe significant t-LTP deficits in APP/PS1 animals. Thus, we focused on t-LTP in CA1 neurons in the vicinity of Aβ plaques that were visualized by staining with the dye Methoxy-X04 (for staining procedure, compare Methods). Stained Aβ plaques in APP/PS1 mice were visible in stratum radiatum, stratum oriens, and in the pyramidal cell layer of the CA1 area, but at this age (6 months), the density of Aβ plaques is relatively sparse (compare Kartalou et al., 2020a, b). Thus, we decided to record t-LTP in CA1 pyramidal neurons in a Aβ plaque distance-dependent manner. To this aim we determined the distance between the recorded CA1 neuron soma and the nearest plaque. In Methoxy-X04 stained slices, we observed that in CA1 neurons with their somata <200 µm away from the border of the nearest Aβ plaque in APP/PS1 mice (AD near), t-LTP induced by

6x 1:4 stimulation was significantly impaired in comparison to t-LTP in Methoxy-X04 treated WT littermates (p=0.0093). Moreover, CA1 neurons >200 µm away from the border of the nearest Aβ plaques in APP/PS1 mice (AD distant) expressed comparable t-LTP as WT littermate mice (**Fig. 22A**; WT: 135.8 ± 10.6% (n=16/N=9); AD near: 92.4 ± 9.1% (n=12/N=9); AD distant: 129.6 ± 9.6% (n=8/N=4)). ANOVA analyses revealed a significant main effect ($F_{(2,33)}$=5.338 p=0.0098), and post hoc Tukey's test showed p=0.0093 for WT vs. AD near, p=0.9153 for WT vs. AD distant, and p=0.0762 for AD near vs. AD distant. Interestingly, when plotting t-LTP magnitude of recorded CA1 cells vs. distance to nearest Aβ plaque, we observed a moderate positive correlation between both parameters (**Fig. 22B**; r(18)=0.5105 p=0.0215, Pearson correlation coefficient).

Altogether, these results indicate that the proximity of CA1 pyramidal cell somata to Aβ plaques crucially regulates the extent of impairments in t-LTP at the single neuron level.

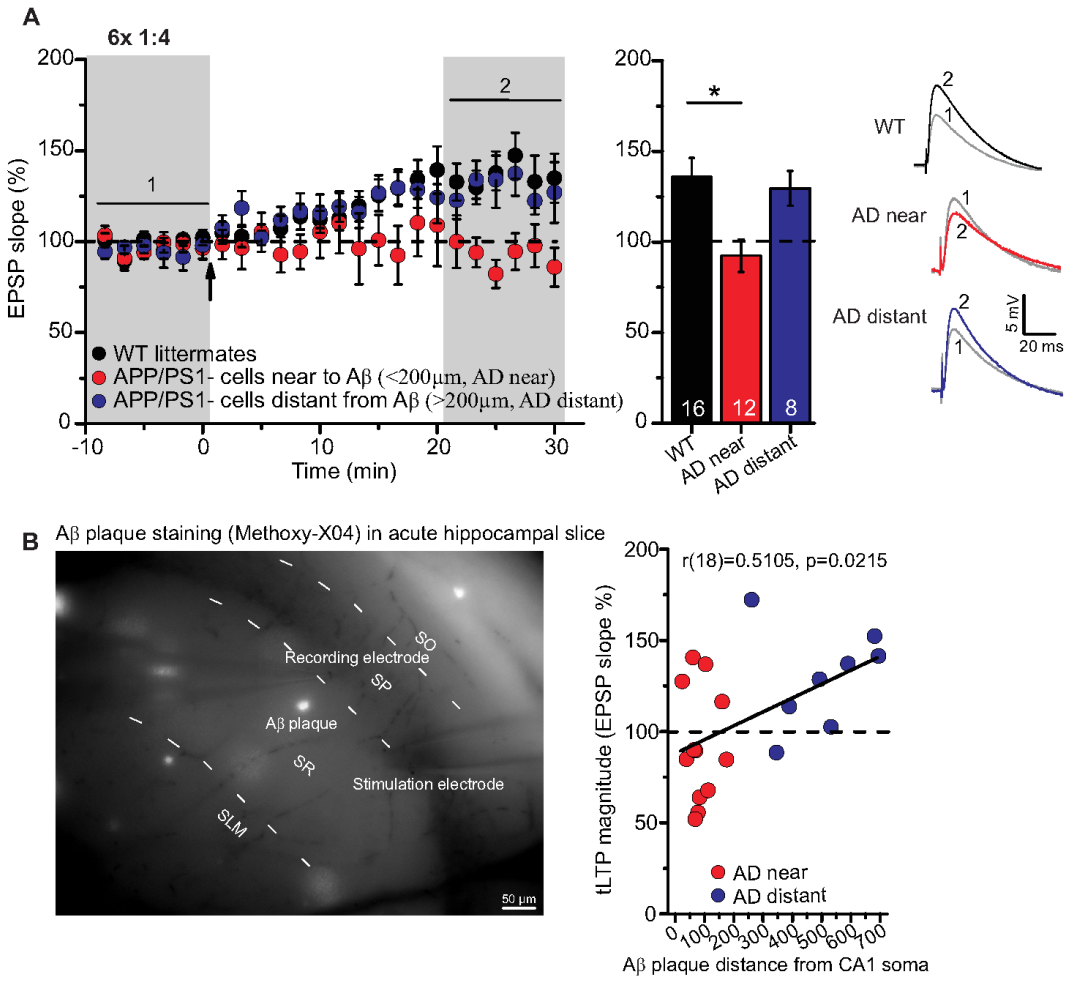

Figure 22: **Six months old APP/PS1 mice expressed Aβ plaque distance-dependent t-LTP impairments at SC-CA1 synapses in the hippocampus.** Patch clamp recordings from hippocampal CA1 pyramidal cells at a holding potential of -70 mV in current clamp mode. **(A)** Left: Mean time-course of EPSP slopes for 6x 1:4

paradigm. Right: Averaged change in EPSP slopes (21-30 min) following t-LTP induction normalized to control before t-LTP induction. APP/PS1 mice showed impaired t-LTP in CA1 neurons near to Aβ plaques (red circles, AD near, n=12/N=9; vs WT: p=0.009), while in CA1 neurons distant from Aβ plaques (blue circles, AD distant, n=8/N=4; vs WT: p=0.92), t-LTP magnitude was comparable to WT littermate mice (black circles, n=16/N=9). **(B)** Methoxy-X04 staining of Aβ plaques in acute hippocampal slices. APP/PS1 mice showed moderate positive correlation between CA1 cell soma distance from Aβ plaque and t-LTP magnitude (Pearson correlation coefficient r(18)=0.5105; p=0.02). Data are shown as mean ± SEM. Insets: average EPSP before (1) and after t-LTP induction (2). Scale bars are presented in the inset. Digits in the bars indicate the number of recorded neurons per condition. *: p<0.05, multiple comparisons were performed with ANOVA followed by post hoc Tukey's test (A). Modified from Garad et al., 2021.

3.13 The effect of treatment of APP/PS1 mice with fingolimod or voluntary running on impaired t-LTP in CA1 neurons in the vicinity of Aβ plaques

The FDA approved anti-multiple sclerosis drug fingolimod (FTY720) have been shown previously to ameliorate Aβ pathology, as well as associated deficits in synaptic plasticity and memory formation in AD mice (Fukumoto et al., 2013; Carreras et al., 2019; Kartalou et al., 2020b). Moreover, Deogracias and coworkers have reported, that the sphingosine-1 phosphate receptor modulator fingolimod, a drug that crosses the blood–brain barrier and increases brain-derived neurotrophic factor (BDNF) levels (Deogracias et al., 2012). Nagahara and colleagues reported broad neuroprotective effects of BDNF administration in animal models of AD (Nagahara et al., 2009). Based on these evidences, we tested the same regime of 1-month chronic fingolimod treatment (compare Methods) that we reported previously to rescue AD deficits in APP/PS1 mice (compare Kartalou et al., 2020b) for its potential to rescue 6x 1:4 t-LTP deficits in CA1 neurons near to Aβ plaques. We treated APP/PS1 and WT littermate mice with fingolimod for 1 month (for treatment regimens, compare Methods). Afterwards, we studied 6x 1:4 t-LTP in CA1 neurons with their somata <200 µm away from the border of the nearest Aβ plaque in the slices from APP/PS1 animals (AD near). We observed 6x 1:4 t-LTP was impaired in AD near group compared to respective WT littermates (**Fig. 23A**; WT+Fingolimod: 169.9 ± 20.1% (n=12/N=7); AD near+Fingolimod: 111.1 ± 10.2% (n=16/N=7), Mann-Whitney U-test: U=42.0, p=0.012). This suggests that the regime of chronic fingolimod treatment used in this experiment was not sufficient to restore t-LTP deficits in CA1 cells in APP/PS1 mice.

Human and animal studies have reported that exercise may prevent age-related diseases (Samorajski et al., 1985). Importantly, exercise mediates beneficial effects on brain function

and neural health, particularly in the hippocampus (Alaei et al., 2006; Berchtold et al., 2005; Radahmadi et al., 2016). It has been reported that voluntary running (VR) increases BDNF mRNA and protein expression in the hippocampus and thereby protects hippocampal neurons against neurodegeneration (Farmer et al., 2004; Gómez-Pinilla et al., 2002; Lin et al., 2015). Therefore, in a further approach to restore the impaired t-LTP at hippocampal SC synapses in the proximity of Aβ plaques, 4-5 months old APP/PS1 mice were placed in the standard cages exclusively equipped with running wheels (compare Methods) on which animals can run voluntarily for the period of 2 months. After 2 months of voluntary running, we investigated 6x 1:4 t-LTP in CA1 neurons with their somata <200 µm away from the border of the nearest Aβ plaque in the slices from 6-7 months old APP/PS1 animals (AD near) and respective WT littermates. We observed comparable magnitude of synaptic change in AD near group as WT littermates (**Fig. 23B**; WT+VR: 110.94 ± 9.6% (n=8/N=5); AD near+VR: 112.25 ± 8.8% (n=9/N=6), two-tailed Student's t-test $t_{(15)}$=-0.1002 p=0.9215). Contrary to our expectations, we observed absence of 6x 1:4 t-LTP in WT littermate animals following voluntary running suggesting that voluntary running impaired t-LTP in WT littermates by an unknown mechanism. T-LTP in APP/PS1 mice indicates that voluntary running did not ameliorate disrupted t-LTP at SC-CA1 synapses in the hippocampus of APP/PS1 animals.

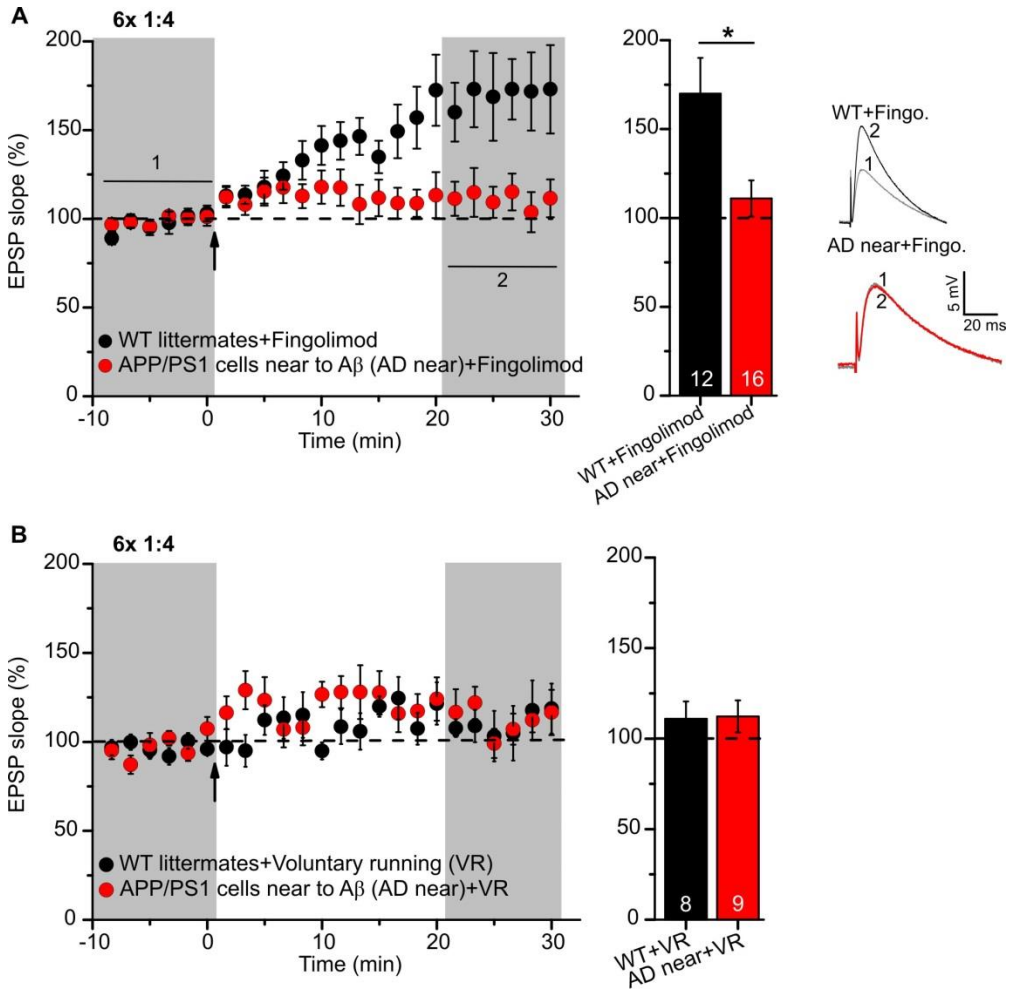

Figure 23: Impaired t-LTP at SC-CA1 synapses in 6 months old APP/PS1 mice could not be restored by chronic fingolimod or voluntary running treatments. Patch clamp recordings from hippocampal CA1 pyramidal cells at a holding potential of -70 mV in current clamp mode. Left: Mean time-course of EPSP slopes for 6x 1:4 paradigm. Right: Averaged change in EPSP slopes (21-30 min) following t-LTP induction normalized to control before t-LTP induction. **(A)** No rescue of impaired t-LTP in 6 months old APP/PS1 mouse CA1 neurons near to plaques after chronic fingolimod treatment (red circles, n=16/N=7; p=0.01), compared to fingolimod treated WT littermates (black circles, n=12/N=7). **(B)** Adult APP/PS1 animals (n=9/N=6; p=0.92) showed comparable magnitude of synaptic change in CA1 neurons near to plaques as age-matched WT littermates (n=8/N=5) after 2 months voluntary running. Data displayed as mean ± SEM. Insets: average EPSP before (1) and after t-LTP induction (2). Scale bars are shown in the inset. Digits in the bars indicate the number of recorded neurons per condition. *: p<0.05, Mann-Whitney U-test (A), two-tailed Student's t-test (B). Figure (A) adapted from Garad et al., 2021.

Altogether, the APP/PS1 mouse model of AD pathology (6 months old) used in our experiments exhibited clearly impaired 6x 1:4 t-LTP in CA1 pyramidal neurons in the vicinity of Aβ plaques (<200 µm). This indicates that AD pathology impacts t-LTP in the

hippocampal formation in an Aβ distance-dependent manner. Further, this impaired t-LTP was not restored by the fingolimod treatment or voluntary running regimes used in our study.

3.14 CA1 pyramidal neurons in adult APP/PS1 animals showed intact basal electrical and synaptic properties irrespective of Aβ plaques location

In the aforementioned results, we observed clear deficit in t-LTP at single CA1 neuron level in APP/PS1 mice close to Aβ plaques (<200 µm: AD near); therefore, we investigated whether the AD pathology also affects the basal electrical and synaptic properties of hippocampal CA1 neurons. First, we focus on general differences between the genotypes irrespective of Aβ plaques location. The hippocampal CA1 neurons in 6 months old adult APP/PS1 and WT littermate animals showed similar intrinsic excitability, measured in the form of somatic driven action potentials firing, (**Fig. 24A**; depolarization step 180 pA: WT: 17.8 ± 1.2 Hz (n=20/N=10); APP/PS1: 17.4 ± 1.2 Hz (n=17/N=8), ANOVA $F_{(1,350)}$=0.1830 p=0.6690), rheobases (**Fig. 24D**; WT: 260.0 ± 14.1 pA (n=20/N=10); APP/PS1: 254.7 ± 11.9 pA (n=19/N=9), two-tailed Student's t-test $t_{(37)}$=0.2839 p=0.7780), action potential amplitudes (**Fig. 24E**; WT: 76.3 ± 1.8 mV (n=20/N=10); APP/PS1: 77.0 ± 2.1 mV (n=19/N=9), Mann-Whitney U-test U=200.5, p=0.768), and after-depolarizations (**Fig. 24F**; WT: 13.5 ± 0.5 mV (n=18/N=10); APP/PS1: 12.7 ± 0.5 mV (n=19/N=9), two-tailed Student's t-test $t_{(35)}$=1.0097 p=0.3196). Moreover, we observed comparable PPR (**Fig. 24B**; WT: 1.63 ± 0.1 (n=20/N=10); APP/PS1: 1.48 ± 0.1 (n=19/N=9), two-tailed Student's t-test $t_{(37)}$=1.1941 p=0.2401), EPSP rise times (**Fig. 24H**; WT: 4.6 ± 0.1 ms (n=19/N=10); APP/PS1: 4.9 ± 0.1 ms (n=18/N=9), two-tailed Student's t-test $t_{(35)}$=-1.6256 p=0.1130), EPSP decay times (**Fig. 24I**; WT: 53.7 ± 1.5 ms (n=20/N=10); APP/PS1: 51.9 ± 1.5 ms (n=19/N=9), two-tailed Student's t-test $t_{(37)}$=0.8450 p=0.4036), and higher $GABA_B$ inhibitory responses coinciding with the EPSP decay, though did not reach statistical significance (**Fig. 24J**; WT: 0.95 ± 0.07 mV (n=20/N=10); APP/PS1: 1.15 ± 0.09 mV (n=19/N=9), two-tailed Student's t-test $t_{(37)}$=-1.8232 p=0.0764) at SC-CA1 synapses in APP/PS1 animals compared to WT littermates. The hippocampal CA1 neurons in APP/PS1 mice showed similar resting membrane potentials (**Fig. 24C**; WT: -75.1 ± 0.9 mV (n=20/N=10); APP/PS1: -74.2 ± 0.7 mV (n=19/N=9), two-tailed Student's t-test $t_{(37)}$=-0.7305 p=0.4697), and reduced input resistances, though did not reach statistical significance, in comparison to WT littermate mice (**Fig. 24G**; WT: 187.3 ± 7.5 MΩ (n=20/N=10); APP/PS1: 165.9 ± 8.2 MΩ (n=19/N=9), two-tailed Student's t-test $t_{(37)}$=1.9195 p=0.0627).

Altogether, adult APP/PS1 mice displayed intact neuronal excitability and basic synaptic properties in postsynaptic hippocampal CA1 pyramidal neurons.

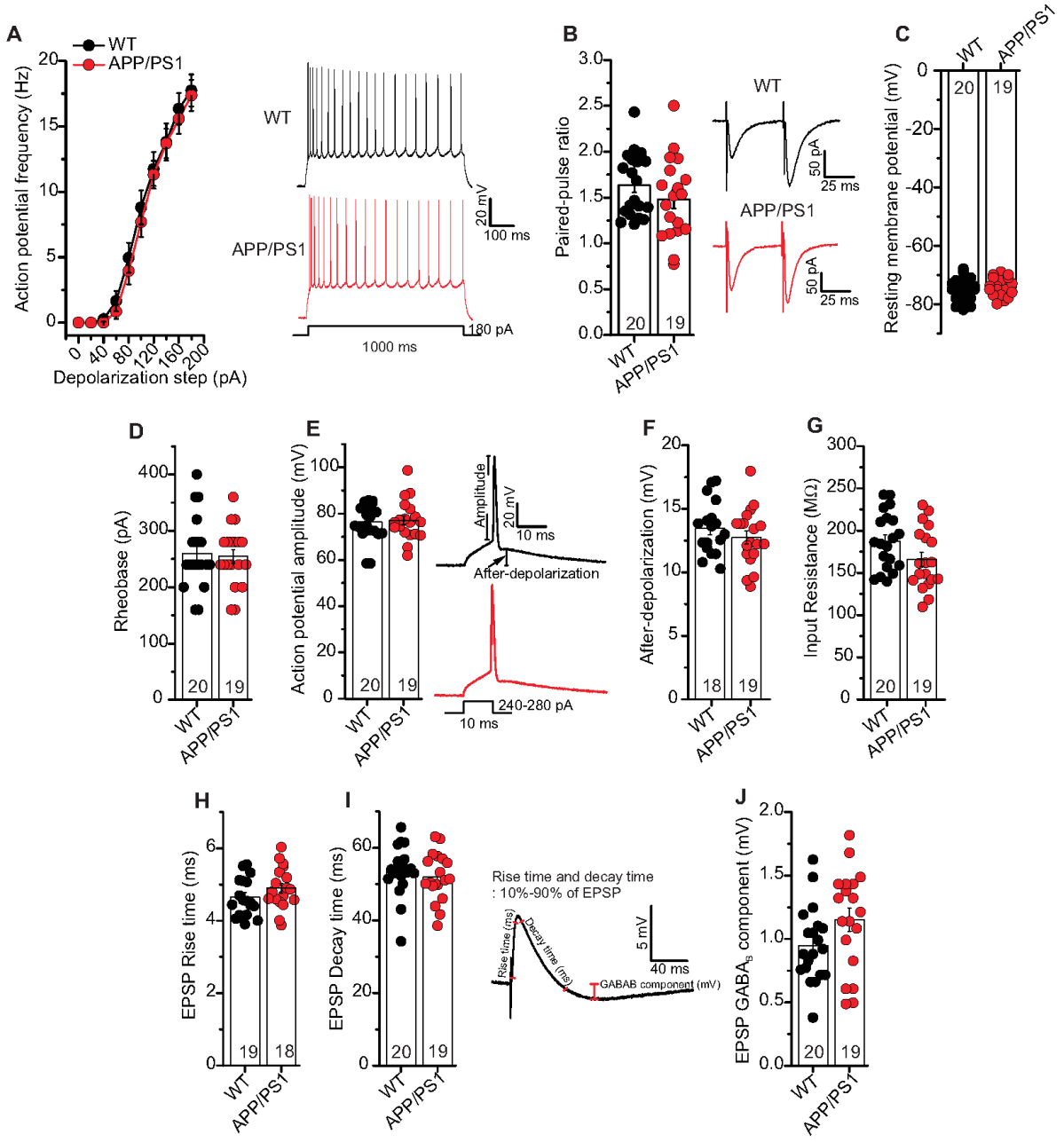

Figure 24: Intact basal electrical and synaptic properties of CA1 pyramidal neurons in 6 months old APP/PS1 mice. Patch clamp recordings from hippocampal CA1 pyramidal cells at a holding potential of -70 mV in current clamp or voltage clamp mode. APP/PS1 mice specified by red circles, while WT mice represented by black circles. **(A)** CA1 pyramidal neurons in APP/PS1 mice displayed similar intrinsic excitability as WT littermates (ANOVA p=0.67). Insets: action potentials (APs) firing in CA1 neurons in response to 180 pA (for 1000 ms) somatic current injection from APP/PS1 and WT littermate mice. **(B)** Paired-pulse ratio (PPR) at SC-

CA1 synapses in APP/PS1 animals was comparable to WT littermate animals (p=0.24). Insets: PPR at inter-stimulus interval of 50 ms in APP/PS1 and WT littermates. Hippocampal CA1 neurons from APP/PS1 mice showed similar resting membrane potentials (**C**; p=0.47), rheobases (**D**; p=0.78) and AP amplitudes (**E**; p=0.77) as WT littermate mice. Insets: Single AP firing in CA1 neurons in response to 240-280 pA (for 10 ms) somatic current injection from WT littermate and APP/PS1 animals. Measurements of AP amplitude and after-depolarization. In addition, CA1 cells from adult APP/PS1 mice expressed similar after-depolarizations (**F**; p=0.32), input resistances (**G**; p=0.06), EPSP rise times (**H**; p=0.11) and EPSP decay times (**I**; p=0.40) compared to WT littermates. Insets: EPSP time-course, 10%-90% EPSP trace fit for measurement of EPSP rise time and decay time, and measurement of $GABA_B$ receptor mediated EPSP component (FitMaster). The hippocampal CA1 neurons from APP/PS1 animals showed comparable $GABA_B$ inhibitory responses coinciding with the EPSP decay compared to WT littermate animals (J; p=0.08). Digits in the bars represent the number of recorded neurons per condition, at least from three different animals per group. Scale bars are displayed in the respective insets. Data expressed as mean ± SEM. *: p<0.05, Parametric data were compared by two-tailed Student's t-test while non-parametric data were compared by Mann-Whitney U-test.

Since we observed no general differences between APP/PS1 and WT littermate hippocampal CA1 neurons, when compared for genotypes; we investigated whether any such differences were evident when comparing CA1 neurons located near vs. distant to Aβ plaques of APP/PS1 animals. When testing basal electrical and synaptic properties of SC inputs to CA1 neurons we did not observe any significant differences between properties of neurons near plaques (AD near) compared to CA1 cells with their somata distant from plaques (AD distant). Likewise, both groups showed no significant differences in all these parameters compared to WT littermate controls. Thus AP frequency (**Fig. 25A**; AP frequency in response to a 180 pA depolarizing current step: WT: 21.6 ± 0.9 Hz (n=16/N=9); AD near: 20.3 ± 1.4 Hz (n=12/N=9); AD distant: 19.9 ± 1.0 Hz (n=8/N=4), $ANOVA_{(2,330)}$=2.7340 p=0.0664), rheobases (**Fig. 25D**; WT: 232.5 ± 07.5 pA (n=16/N=9); AD near: 223.3 ± 14.3 pA (n=12/N=9); AD distant: 230.0 ± 10.0 pA (n=8/N=4), $ANOVA_{(2,33)}$=0.2105 p=0.8113), after-depolarizations (**Fig. 25E**; WT: 12.3 ± 0.4 mV (n=16/N=9); AD near: 11.5 ± 0.8 mV (n=12/N=9); AD distant: 11.7 ± 0.5 mV (n=8/N=4), $ANOVA_{(2,33)}$=0.5997 p=0.5549) and action potential amplitudes (**Fig. 25F**; WT: 79.4 ± 1.4 mV (n=16/N=9); AD near: 77.9 ± 1.8 mV (n=12/N=9); AD distant: 81.4 ± 2.2 mV (n=8/N=4), $ANOVA_{(2,33)}$=0.8169 p=0.4505) were comparable between the groups. In addition, PPR at inter-stimulus interval of 50 ms (**Fig. 25B**; WT: 1.54 ± 0.1 (n=16/N=9); AD near: 1.38 ± 0.1 (n=12/N=9); AD distant: 1.45 ± 0.1 (n=8/N=4), $ANOVA_{(2,33)}$=0.4812 p=0.6223), EPSP rise times (**Fig. 25H**; WT: 4.47 ± 0.16 ms (n=16/N=9); AD near: 4.71 ± 0.21 ms (n=12/N=9); AD distant: 4.97 ± 0.24 ms

(n=8/N=4), $ANOVA_{(2,33)}$=1.552 p=0.2270), EPSP decay times (**Fig. 25I**; WT: 51.4 ± 1.5 ms (n=16/N=9); AD near: 48.2 ± 1.1 ms (n=12/N=9); AD distant: 52.8 ± 2.0 ms (n=8/N=4), $ANOVA_{(2,33)}$=2.083 p=0.1407), and $GABA_B$ inhibitory responses coinciding with the EPSP decay (**Fig. 25J**; WT: 1.00 ± 0.08 mV (n=16/N=9); AD near: 0.83 ± 0.07 mV (n=12/N=9); AD distant: 1.09 ± 0.11 mV (n=8/N=4), $ANOVA_{(2,33)}$=2.244 p=0.1220) were not significantly different between the groups. Further, the hippocampal CA1 neurons in WT, AD near and AD distant groups showed similar resting membrane potentials (**Fig. 25C**; WT: -76.3 ± 0.8 mV (n=16/N=9); AD near: -76.8 ± 1.0 mV (n=12/N=9); AD distant: -78.5 ± 0.6 mV (n=8/N=4), $ANOVA_{(2,33)}$=1.387 p=0.2641), and input resistances (**Fig. 25G**; WT: 167.9 ± 9.9 MΩ (n=16/N=9); AD near: 161.7 ± 9.5 MΩ (n=12/N=9); AD distant: 156.2 ± 8.9 MΩ (n=8/N=4), $ANOVA_{(2,33)}$=0.3197 p=0.7286).

These results revealed that the observed impairment in t-LTP in APP/PS1 mice cannot be accounted for by differences of neuronal excitability or basic synaptic properties in postsynaptic CA1 pyramidal cells of this AD mouse model.

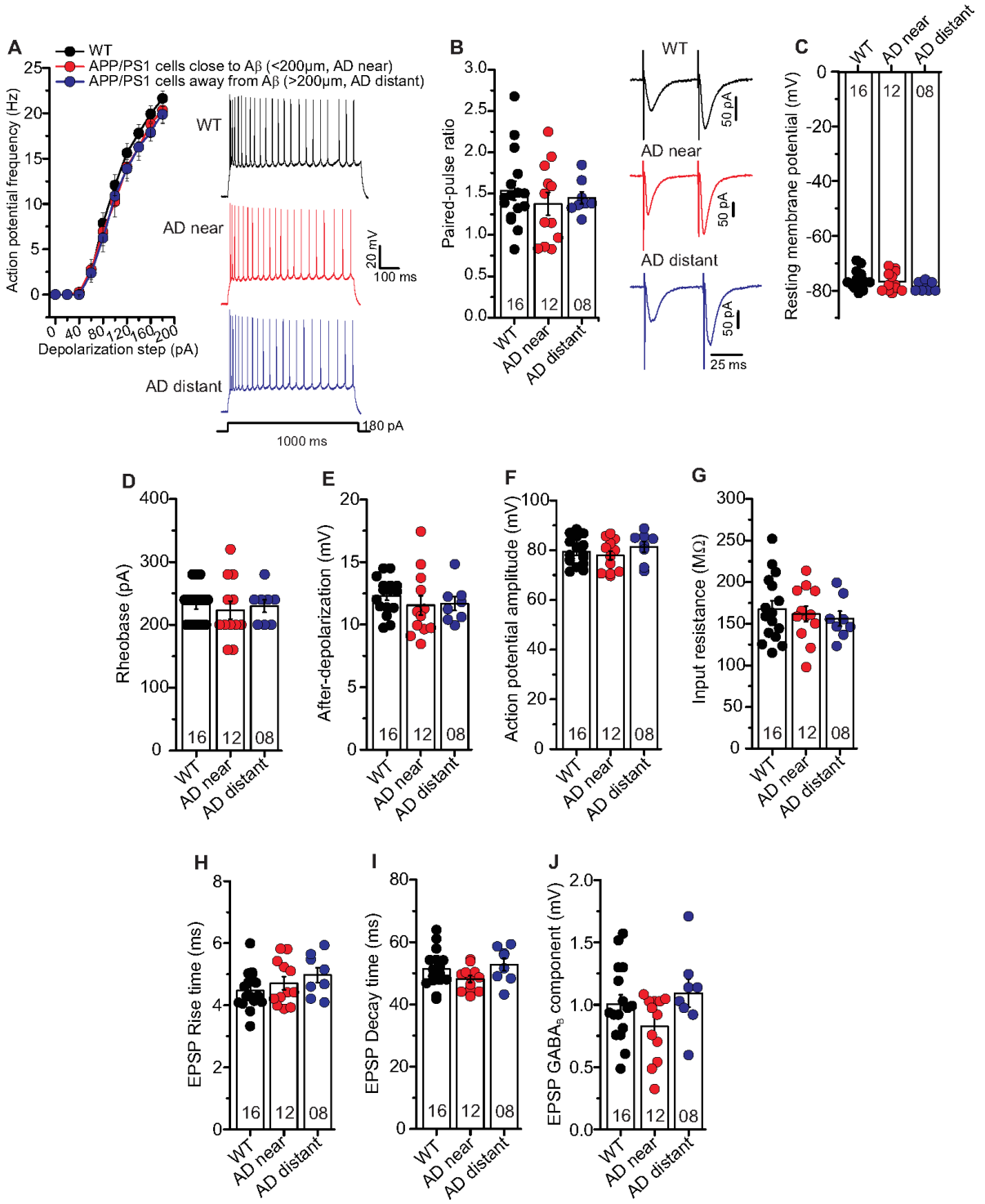

Figure 25: Unaltered basal electrical and synaptic properties of CA1 pyramidal neurons in the vicinity of Aβ plaques in 6 months old APP/PS1 mice. Patch clamp recordings from hippocampal CA1 pyramidal cells at a holding potential of -70 mV in current clamp or voltage clamp mode. The hippocampal CA1 neurons close to Aβ plaques in APP/PS1 mice (<200µm, AD near) shown by red circles, CA1 cells away from Aβ plaques in APP/PS1 mice (>200µm, AD distant) designated by blue circles and CA1 neurons from WT littermates specified by black circles. **(A)** The AD near and AD distant groups showed comparable intrinsic excitability compared to age-matched WT littermates (p=0.07). Insets: action potentials (APs) firing in CA1 neurons in response to 180

pA (for 1000 ms) somatic current injection from WT, AD near and AD distant groups. **(B)** Paired-pulse ratio (PPR) at SC-CA1 synapses in AD near and AD distant group was similar to PPR in WT littermate mice (p=0.62). Insets: PPR at inter-stimulus interval of 50 ms at SC-CA1 synapses from WT, AD near and AD distant groups. Hippocampal CA1 neurons from AD near, AD distant group showed similar resting membrane potentials (**C**; p=0.26), rheobases (**D**; p=0.81), AP amplitudes (**E**; p=0.45), after-depolarizations (**F**; p=0.55), input resistances (**G**; p=0.73), EPSP rise times (**H**; p=0.23) and EPSP decay times (**I**; p=0.14) compared to WT littermates. Moreover, the hippocampal CA1 neurons exhibited comparable $GABA_B$ inhibitory responses coinciding with the EPSP decay in slices of WT littermate animals, AD near and AD distant groups (**J**; p=0.12). Digits in the bars represent the number of recorded neurons per condition, at least from three different animals per group. Scale bars are presented in the respective insets. Data displayed as mean ± SEM. *: $p<0.05$, Multiple comparisons were performed with ANOVA. Modified after Garad et al., 2021.

3.15 Adult APP/PS1 mice showed distinct excitatory and inhibitory postsynaptic currents (EPSCs and IPSCs)

Although APP/PS1 mice show memory deficit in CA1 neurons close to Aβ plaques, we observed no impairments in basal properties of CA1 neurons in APP/PS1 animals. Therefore, in a final set of experiments, we were interested to learn whether Aβ pathology in AD mice has an influence on spontaneous/network driven or miniature excitatory and inhibitory synaptic transmission in contrast to evoked synaptic transmission. To address this question, we studied spontaneous (s) and miniature (m) excitatory and inhibitory postsynaptic currents (EPSCs and IPSCs) in hippocampal CA1 neurons in 6 months old APP/PS1 Alzheimer's disease mice and respective WT littermates. The hippocampal CA1 neurons in APP/PS1 mice showed significantly higher mean sEPSC amplitudes (**Fig. 26C**; WT: 11.17 ± 0.37 pA (n=12/N=4); APP/PS1: 13.08 ± 0.56 pA (n=7/N=3), two-tailed Student's t-test $t_{(17)}$=-2.9871 p=0.0083) and a different cumulative sEPSC amplitude distribution compared to WT littermates (**Fig. 26C**; Kolmogorov-Smirnov test D=0.1290 p<0.0001). Mean sEPSC frequencies in CA1 neurons were decreased in APP/PS1 mice compared to WT littermates, although this effect did not reach statistical significance (**Fig. 26D**; WT: 1.07 ± 0.14 Hz (n=12/N=4); APP/PS1: 0.76 ± 0.09 Hz (n=7/N=3), Mann-Whitney U-test U=61.0, p=0.108), whereas the sEPSC inter-event interval (IEI) distribution differed between the two groups (**Fig. 26D**; Kolmogorov-Smirnov test D=0.0518 p=0.0046). When synaptic events were recorded in the presence of 1 µM tetrodotoxin (TTX) to block firing of APs, recorded mEPSCs, as a measure for different quantal release probabilities showed comparable mean mEPSC amplitudes (**Fig. 26E**; WT: 11.43 ± 0.68 pA (n=11/N=4); APP/PS1: 12.64 ± 0.86 pA (n=8/N=3), two-tailed Student's t-test $t_{(17)}$=-1.1133 p=0.2811), while significantly different

cumulative mEPSC amplitudes (**Fig. 26E**; Kolmogorov-Smirnov test D=0.0843 p<0.0001) were evident between APP/PS1 and WT littermate mice. Moreover, we observed similar mean mEPSC frequencies (**Fig. 26F**; WT: 0.72 ± 0.07 Hz (n=11/N=4); APP/PS1: 0.62 ± 0.09 Hz (n=8/N=3), Mann-Whitney U-test U=58.0, p=0.248) and comparable distribution of mEPSC IEIs at hippocampal CA1 cells in WT littermate and APP/PS1 animals (**Fig. 26F**; Kolmogorov-Smirnov test D=0.0256 p=0.5174).

Taken together, the spontaneous and miniature EPSC analyses in CA1 neurons revealed that in APP/PS1 mice, sEPSC amplitudes are increased whereas sEPSC frequencies are decreased, although this effect did not reach statistical significance, compared to WT littermates. On the other hand, APP/PS1 and WT littermate mice express comparable mEPSC amplitudes and frequencies.

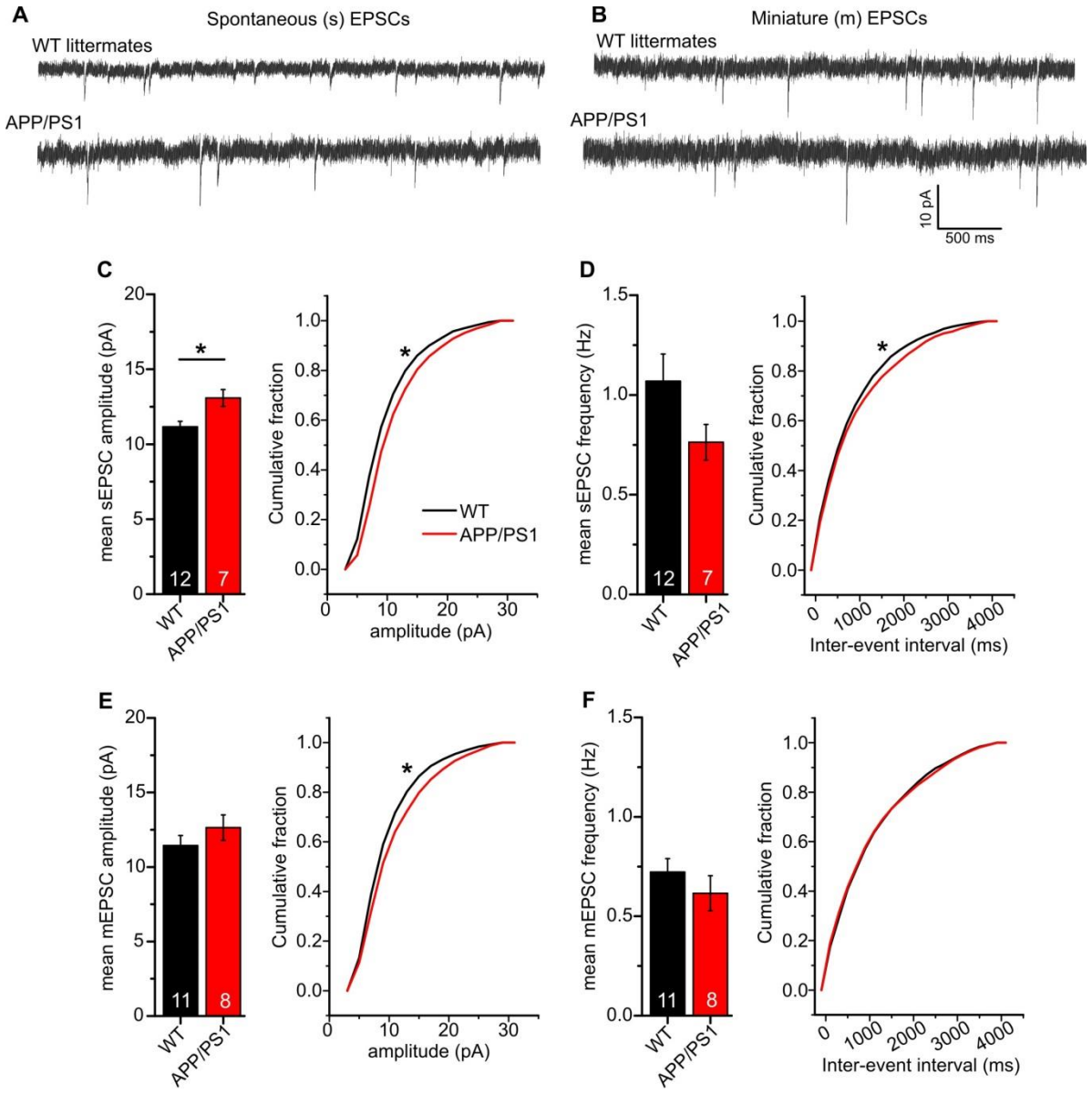

Figure 26: Spontaneous and miniature excitatory synaptic transmission in CA1 neurons of 6 months old adult APP/PS1 mice. Patch clamp recordings from hippocampal CA1 pyramidal cells at a holding potential of -70 mV in volatge clamp mode. APP/PS1 mice specified by red symbols, while WT littermate mice represented by black symbols. **(A)** and **(B)** spontaneous (s) and miniature (m) EPSCs from WT littermate and APP/PS1 mice, respectively. Scale bars are shown in the inset. **(C)** Hippocampal CA1 pyramidal neurons from APP/PS1 mice showed significantly higher mean sEPSC amplitudes (p=0.008) and significantly different cumulative sEPSC amplitude distribution (p<0.0001). **(D)** CA1 cells from APP/PS1 animals displayed comparable mean sEPSC frequencies as WT littermate animals (p=0.11), however significantly different distribution of sEPSC inter-event intervals (IEIs; p=0.005). **(E)** CA1 neurons from WT littermate and APP/PS1 mice showed similar mean mEPSC amplitudes (p=0.28), but significantly different cumulative mEPSC amplitude distribution (p<0.0001). **(F)** CA1 neurons from APP/PS1 animals displayed similar mean mEPSC frequencies (p=0.25) and distribution of mEPSC IEIs as WT littermates (p=0.52). Digits in the bars show the number of recorded neurons per condition, at least from three different animals per group. Data shown as mean ± SEM. *: p<0.05, statistical analyses were performed with two-tailed Student's t-test (parametric data) and Mann-Whitney U-test (non-

parametric data). Cumulative frequency distributions were analyzed with Kolmogorov-Smirnov test. Adapted from Garad et al., 2021.

Furthermore, hippocampal CA1 cells in APP/PS1 mice displayed decreased mean sIPSC amplitudes, though did not reach statistical significance (**Fig. 27C**; WT: 17.06 ± 2.13 pA (n=6/N=2); APP/PS1: 13.53 ± 2.02 pA (n=5/N=2), two-tailed Student's t-test $t_{(9)}$=1.1846 p=0.2665), while a different cumulative sIPSC amplitude distribution compared to WT littermates (**Fig. 27C**; Kolmogorov-Smirnov test D=0.2080 p<0.0001). Mean sIPSC frequencies were decreased in APP/PS1 mice compared to WT littermates, although this effect did not reach statistical significance (**Fig. 27D**; WT: 6.81 ± 1.96 Hz (n=6/N=2); APP/PS1: 3.55 ± 0.61 Hz (n=5/N=2), Mann-Whitney U-test U=23.0, df=1, p=0.144), whereas the sIPSC IEIs distribution differed between the two groups (**Fig. 27D**; Kolmogorov-Smirnov test D=0.1619 p<0.0001). In addition, we studied mIPSCs, as a measure for different quantal release probabilities, in APP/PS1 mice. The hippocampal CA1 cells in WT littermate and APP/PS1 animals showed similar mean mIPSC amplitudes (**Fig. 27E**; WT: 10.86 ± 1.15 pA (n=6/N=2); APP/PS1: 10.37 ± 1.01 pA (n=5/N=2), Mann-Whitney U-test U=18.0, p=0.584) and cumulative mIPSC amplitudes (**Fig. 27E**; Kolmogorov-Smirnov test D=0.0446 p=0.1342). In addition, CA1 neurons in APP/PS1 mice showed similar mean mIPSC frequencies as WT littermates (**Fig. 27F**; WT: 3.70 ± 0.90 Hz (n=6/N=2); APP/PS1: 3.36 ± 0.65 Hz (n=5/N=2), two-tailed Student's t-test $t_{(9)}$=0.3011 p=0.7703), nonetheless different distribution of mIPSC IEIs (**Fig. 27F**; Kolmogorov-Smirnov test D=0.0572 p=0.0253).

Overall, sIPSCs are slightly decreased in amplitude and frequency in APP/PS1 mice compared to WT littermates, but also this effect did not reach statistical significance. Moreover, mIPSC properties are indistinguishable between the genotypes.

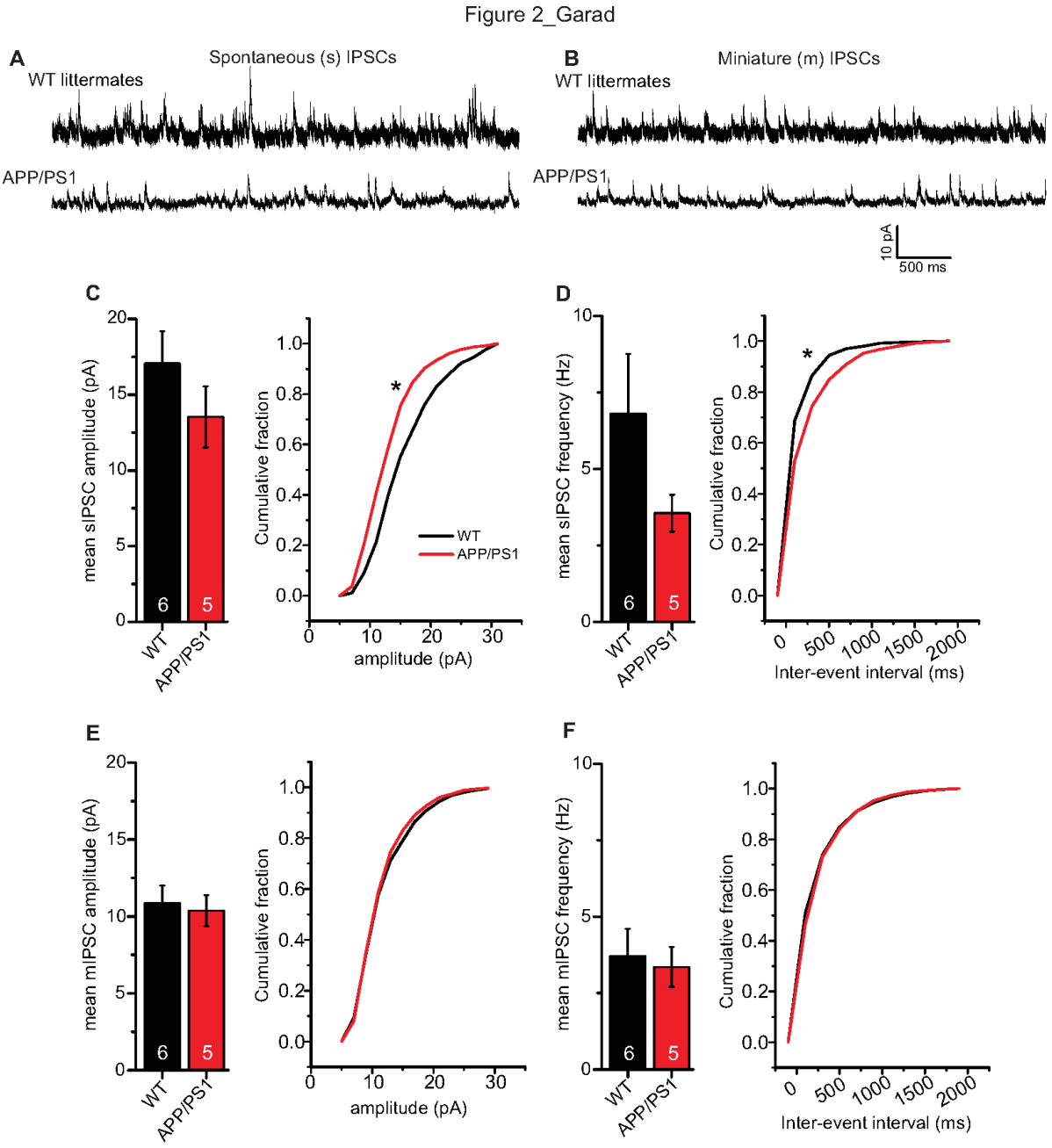

Figure 27: Spontaneous and miniature inhibitory synaptic transmission in CA1 neurons of adult APP/PS1 mice. Patch clamp recordings from hippocampal CA1 pyramidal cells at a holding potential of -30 mV in voltage clamp mode. APP/PS1 mice showed by red symbols, while WT mice designated by black symbols. **(A)** and **(B)** spontaneous (s) and miniature (m) IPSCs from WT littermate and APP/PS1 mice, respectively. Scale bars are displayed in the inset. **(C)** Hippocampal CA1 cells from APP/PS1 and WT mice expressed comparable mean sIPSC amplitudes (p=0.27), however significantly different cumulative sIPSC amplitude distribution (p<0.0001). **(D)** CA1 pyramidal neurons from APP/PS1 mice displayed comparable mean sIPSC frequencies (p=0.14), but significantly different distribution of sIPSC inter-event intervals (IEIs; p<0.0001) compared to WT littermates. **(E)** CA1 cells from WT littermate and APP/PS1 mice showed similar mean mIPSC amplitudes (p=0.58) and cumulative mIPSC amplitudes (p=0.13). **(F)** Hippocampal CA1 neurons from APP/PS1 animals displayed similar mean mIPSC frequencies (p=0.77), while different distribution of mIPSC IEIs (p=0.03)

compared to WT littermates. Digits in the bars represent the number of recorded neurons per condition, at least from two different animals per group. Data expressed as mean ± SEM. *: $p<0.05$, statistics were performed with two-tailed Student's t-test for parametric data and Mann-Whitney U-test for non-parametric data. Cumulative frequency distributions were analyzed with Kolmogorov-Smirnov test.

3.16 Adult APP/PS1 mice showed impaired intrinsic excitability in CA1 neurons and synaptic signal integration at SC-CA1 synapses

Since adult APP/PS1 mice expressed t-LTP deficits at hippocampal SC-CA1 synapses in an Aβ plaques distance-dependent manner and showed intact basal electrical and synaptic properties of CA1 pyramidal neurons (**Fig. 24, 25**); in this approach we used different stimulation paradigms (compare Methods) to study intrinsic excitability of CA1 neurons and also studied synaptic signal integration at SC-CA1 synapses. For these experiments, the temperature of extracellular aCSF in the recording chamber was maintained at 34-35^{o}C, which resembles body temperature of mice. Moreover, picrotoxin was excluded from the recording aCSF and acute hippocampal slices were used without CA3-CA1 cut (compare Methods). These recording conditions allowed us to study intrinsic excitability of CA1 neurons and synaptic signal integration at SC-CA1 synapses in physiologic conditions. The CA1 pyramidal neurons in the hippocampus of APP/PS1 mice displayed significantly decreased intrinsic excitability, measured in the form of somatic driven action potentials firing, (**Fig. 28A**; depolarization step 450 pA: WT: 43.7 ± 3.0 Hz (n=7/N=2); APP/PS1: 41.5 ± 2.1 Hz (n=11/N=3), ANOVA $F_{(1,160)}$=5.129 p=0.0249), and decreased hyperpolarization peak, though this effect did not reach statistical significance, in comparison to WT littermates (**Fig. 28B**; hyperpolarization peak (Ih) at hyperpolarization step 200 pA: WT: 29.6 ± 1.6 mV (n=7/N=2); APP/PS1: 27.1 ± 1.7 mV (n=11/N=3), ANOVA $F_{(1,80)}$=3.252 p=0.0751). Next, we studied spike probability as a measure of synaptic facilitation/synaptic signal integration at SC-CA1 synapses in the hippocampus of APP/PS1 and age-matched WT littermate mice. The hippocampal SC-CA1 synapses in APP/PS1 mice exhibited clear inability for synaptic facilitation/synaptic signal integration, measured in the form of spike probability, compared to WT littermates; though did not reach statistical significance (**Fig. 28C**; Spike probability at 50 Hz: WT: 0.24 ± 0.12 (n=6/N=2); APP/PS1: 0.07 ± 0.06 (n=10/N=3), ANOVA $F_{(1,84)}$=2.548 p=0.1142). Altogether, these results indicate under different recording conditions and stimulus paradigms, APP/PS1 mice showed clear deficits in intrinsic excitability as well as synaptic signal integration.

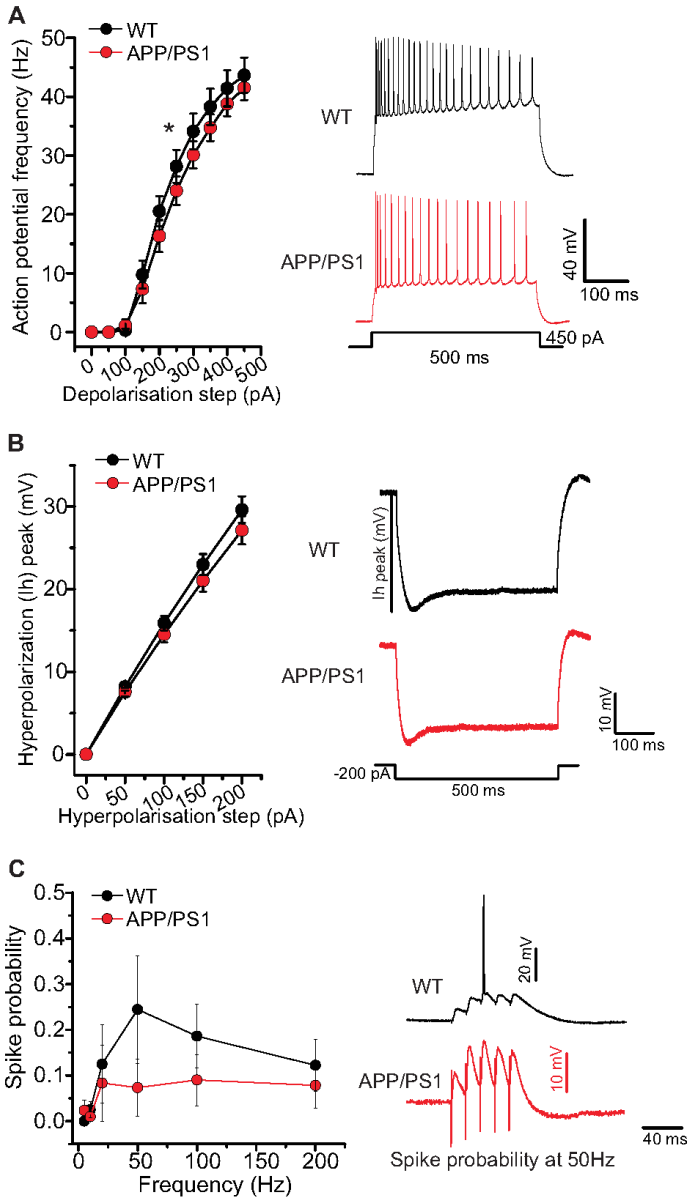

Figure 28: Six months old APP/PS1 mice showed deficits in intrinsic excitability of CA1 neurons and synaptic signal integration at SC-CA1 synapses. Patch clamp recordings from hippocampal CA1 pyramidal cells at endogenous resting membrane potential in current clamp mode. **(A)** The CA1 pyramidal neurons in the hippocampus of APP/PS1 mice (n=11/N=3) expressed decreased intrinsic excitability compared to WT littermates (n=7/N=2; p=0.02). Insets: action potentials firing in CA1 neurons in response to 450 pA (for 500 ms) somatic current injection from WT littermate and APP/PS1 animals. **(B)** The hippocampal CA1 cells in APP/PS1 mice (n=11/N=3) displayed reduced hyperpolarization peak, though not statistically significant, in comparison to WT littermates (n=7/N=2; p=0.07). Insets: The hippocampal CA1 pyramidal neurons response to 200 pA (for 500 ms) hyperpolarizing somatic current injection from both genotypes. **(C)** The hippocampal SC-CA1 synapses in APP/PS1 mice (n=10/N=3) exhibited impaired synaptic signal integration, though not statistically significant, compared to WT littermates (n=6/N=2; p=0.11). The CA1 neurons response to 5 pulse

train stimulation at frequency of 50 Hz in the hippocampus of WT littermate and APP/PS1 mice. Scale bars are shown in the respective insets. *: $p<0.05$, multiple comparisons were performed with ANOVA.

4 Discussion:

Compared with conventional high-frequency stimulation induced long-term potentiation (LTP), a traditional correlation based synaptic plasticity, spike timing-dependent plasticity (STDP) captures the importance of causality in determining the direction of synaptic modification (Hebb, 1949). Moreover, STDP, as a new learning paradigm, has rapidly gained interest, perhaps because of its combination of simplicity, physiological plausibility, and computational power. During development, STDP is a strong candidate for not only circuit remodeling but also learning and memory (see Feldman, 2012). In the present study, we assessed STDP in 6 months old adult mice (fully developed central nervous system) which had not been reported in previous studies (Carlisle et al., 2008; Edelmann et al., 2015; Frey et al., 2009; Pang et al., 2019; Pérez-Rodríguez et al., 2019). First, we described distinct recording conditions and STDP paradigms as equally efficient in the induction and maintenance of timing-dependent LTP (t-LTP) at the hippocampal Schaffer collateral (SC)-*Cornu Ammonis* (CA) 1 synapses in adults (**Fig. 11, 13 and 14**). Next, we illustrated altered t-LTP at hippocampal SC-CA1 synapses in 6 months old adult mice in a STDP paradigm-dependent manner compared to 1-month old mice (juveniles; **Fig. 16 and 17**). Moreover, adult animals expressed significantly decreased action potential frequency and amplitude (intrinsic excitability in CA1 cells and short-term plasticity at SC-CA1 synapses in the hippocampus in comparison to juveniles (see **Fig. 18)**. Overall, these results indicate that developmental maturation alters STDP at SC-CA1 synapses and basal electrical properties of CA1 pyramidal neurons in the hippocampus of 6 months old wildtype mice. In a further approach, we evaluated whether STDP and basal synaptic transmission at hippocampal SC-CA1 synapses are impacted in 6 months old APP/PS1 mice (Alzheimer's disease (AD) mouse model).

Several studies reported LTP deficits in the hippocampus as an early event in AD (Calella et al., 2010; Chang et al., 2006; Richards et al., 2003; Song et al., 2014; Trinchese et al., 2004), whereas the impact of AD pathology on STDP in the hippocampal formation remained unknown until today. In the current study, we assessed t-LTP at hippocampal SC-CA1 synapses in 6 months old adult amyloid precursor protein (KM670/671NL mutation) / presenilin 1 (L166P mutation) double transgenic AD mouse model (APP/PS1). We demonstrated intact t-LTP in adult APP/PS1 mice, when the amyloid beta (Aβ) plaques in the recorded slices were not considered (**Fig. 19, 20, 21**). On the other hand, 6x 1:4 t-LTP

induced by coordinated neuronal activity was significantly disrupted in adult APP/PS1 mice if the nearest Aβ plaque was <200 µm away from the recorded CA1 neuron (**Fig. 22**). Chronic fingolimod or voluntary running treatments were unable to restore the impaired t-LTP (**Fig. 23**). Further, we showed that APP/PS1 mice express intact basal electrical and synaptic properties of CA1 pyramidal neurons and normal spontaneous excitatory and inhibitory synaptic transmission (**Fig. 24-27**).

4.1 Establishing recording conditions to induce STDP at fully developed SC-CA1 synapses in the hippocampus of 6 months old wildtype mice

In an attempt to establish stable recording conditions to investigate STDP at SC-CA1 synapses in acute hippocampal slices from 6 months old mice, we tested distinct combinations of recording artificial cerebrospinal fluid (aCSF) and intracellular solution compositions. In this part, we discuss the possible factor(s) which could be responsible for inefficiency of different recording conditions in establishment of STDP in 6 months old adult animals.

4.1.1 Different STDP paradigms did not induce t-LTP under recording conditions with intact GABAergic inhibition

In this approach, we used acute hippocampal slices with no CA3-CA1 cut, recording aCSF without picrotoxin, i.e. we studied STDP properties with intact GABAergic (gamma aminobutyric acid) inhibition (see methods section 2.3; **Fig. 8**). Under these conditions we tested whether STDP can be induced with 100x 1:1 or 60x 1:1 stimulation successfully at fully developed hippocampal SC-CA1 synapses in 6 months old mice. We observed no STDP induction with these STDP paradigms (**Fig. 8**). In this experimental approach we did not use picrotoxin in the recording aCSF and studied STDP with intact GABAergic (gamma aminobutyric acid) system (**Fig. 8**). GABAergic inhibition and the properties of backpropagating action potentials (bAP) in dendrites are crucial factors for induction of STDP (Feldman, 2012; Kampa et al., 2007). Groen and coworkers (2014) described that 4-6 weeks old rats exhibited an increased GABAergic inhibition onto CA1 dendrites compared to 2-3 weeks old rats, which in turn impacted excitability of neurons, and bAP were detected at significantly less distances along dendrites of hippocampal CA1 neurons. Furthermore, it has been demonstrated that inhibitory synaptic transmission undergoes a markedly protracted postnatal maturation in CA1 pyramidal neurons in the hippocampus (Banks et al., 2002;

Cohen et al., 2000). Several studies reported STDP using similar induction paradigms used in the current study by using picrotoxin in the recording aCSF to block $GABA_A$ receptors thereby blocking $GABA_A$ receptor mediated inhibition (Cepeda-Prado et al., 2019, Corlew et al., 2007; Edelmann et al., 2015; Larsen et al., 2010; Paille et al., 2013). Henceforth, we argued that in the presence of intact GABAergic synaptic transmission in 6 months old mice, increased GABAergic inhibition through its impact on bAPs in dendrites and excitability of hippocampal CA1 neurons could be responsible for the lack of t-LTP by 100x 1:1 (2 Hz) or 60x 1:1 (0.14 Hz) stimulations in our study. However, further investigations are necessary to clearly distinguish the influence of fully matured GABAergic inhibition on STDP properties in adult mice.

4.1.2 The amount of free Ca^{2+} in the intracellular solution regulated induction and/or maintenance of t-LTP

The intracellular solution composition, in particular Ca^{2+} concentration, is decisive in induction and/or maintenance of STDP (Inglebert et al., 2021). As described in the respective methods and results part (**methods section 2.3 and results section 3.2-3.4**), in an endeavor to establish STDP at SC-CA1 synapses in the hippocampus of 6 months old mice, we tested four different compositions for the intracellular solution. In the series of STDP experiments, we tested the influence of Ca^{2+} -buffering capacity in intracellular solution on the efficiency of STDP induction and/or expression, with inclusion and/or exclusion of $CaCl_2$ and ethylene glycol-bis[β-aminoethyl ether]-N,N,N',N'-tetraacetic acid (EGTA; **Fig. 9-12**).

4.1.2.1 Six months old mice showed t-LTP with no added $CaCl_2$ in intracellular solution

With inclusion of $CaCl_2$ (0.75 μM) in intracellular solution; we observed spontaneous synaptic change/run-up as high as ~16% in negative controls (0:0, **Fig. 9, 10**), this run-up did not allow to observe significant t-LTP, in particular with t-LTP induction with 35x 1:4, 1.66 Hz or 70-100x 1:1 1.61 Hz stimulations in 6 months old adults (**Fig. 9**). However, earlier studies from our Lab observed efficient STDP and no run-up in non-stimulated negative controls with intracellular solution including $CaCl_2$ (0.75 μM) in 1 month old mice (Cepeda-Prado et al., 2019; Edelmann et al., 2015). The observed spontaneous run-up in negative controls in 6 months old mice with intracellular solution containing 0.75 μM $CaCl_2$ might be due to developmental maturation in fully matured 6 months old mice in comparison to 1-

month old mice (discussed in detail in section 4.2). Therefore, in our next approach we tested intracellular solution which excluded $CaCl_2$.

We observed successful induction and expression of STDP at hippocampal SC-CA1 synapses in 6 months old adult mice with intracellular solution which excluded $CaCl_2$ (**Fig. 11**). Importantly, we could observe effective STDP induction with low as well as high repeat, positive and negative spike timing STDP paradigms which was maintained for 30 min., using intracellular solution with no added $CaCl_2$ (**Fig. 11, 13 and 14**). For STDP as well as traditional correlation based synaptic plasticity, i.e. LTP (Larson & Munkácsy, 2015; Lynch et al., 1983; Park et al., 2018) and long-term depression (LTD) (Mahajan & Nadkarni, 2019; Mulkey & Malenka, 1992), the elevation of postsynaptic Ca^{2+}, in particular the amplitude and its time course of change in response to inducing stimulation, is essential. The elevated intracellular Ca^{2+} levels in turn act as a second messenger on downstream metabolic cascades that are responsible for the eventual modification of synaptic efficacy (Lisman, 1989; Puri, 2020). We propose that the presence of $CaCl_2$ in the intracellular solution could be responsible for spontaneous synaptic change/run-up in negative controls. Moreover, $CaCl_2$ inclusion in the intracellular solution likely influenced postsynaptic CA1 neurons ability to undergo spatiotemporal alterations in Ca^{2+}, which are crucial in STDP.

4.1.2.2 Added EGTA in intracellular solution disrupted t-LTP induction in adult mice

We observed no significant t-LTP with 100x 1:1 stimulation without added $CaCl_2$ and 0.5-1 mM EGTA inclusion in the intracellular solution (**Fig. 8, 12**). It has been reported that intracellular solution with EGTA, as a Ca^{2+} chelator with relatively slow binding kinetics, is efficient for STDP experiments in juvenile and young adult animals (3 months old; Banerjee et al., 2009; Bi & Wang, 2002; Buskila et al., 2013). EGTA is a slow equilibrating Ca^{2+} buffer and STDP induction is sensitive to loading of the postsynaptic cell with EGTA. The inclusion of EGTA at a concentration of 1 mM in the intracellular solution might interfere with binding kinetics of putative Ca^{2+} sensors, e.g. calmodulin in the postsynaptic cell. For STDP, calmodulin can activate Ca^{2+}/calmodulin-dependent protein kinase II (CaMKII), which translocates to the plasma membrane of spines and phosphorylates α-amino-3-hydroxy-5-methyl-4-isoxazolepropionic acid receptors (AMPARs) (Graupner & Brunel, 2007; Mihalas, 2011). The inefficient STDP with EGTA-based intracellular solution in 6 months old mice in the current study may also imply that Ca^{2+} should have plentiful time to diffuse away from the entry site prior to activating downstream signaling cascades responsible for STDP induction and expression. Further, both local and global Ca^{2+} signaling can play a crucial role in STDP.

For example, EGTA by reducing Ca^{2+} globally may disrupt Ca^{2+} -dependent binding or phosphorylation of secondary messengers within downstream signaling cascades required for STDP. Previous studies reported successful STDP with $CaCl_2$ inclusion (0.75 μM; Cepeda-Prado et al., 2019; Edelmann et al., 2015)) or EGTA (0.5-1 mM) -based intracellular solutions in juveniles or young adults (3 months old; Banerjee et al., 2009; Bi & Wang, 2002; Buskila et al., 2013). Moreover, there is the possibility that the 100x 1:1 stimulation induced elevation of Ca^{2+} in the postsynapse is not sufficient for t-LTP induction under specified recording conditions. Therefore, further investigations with different EGTA concentrations in intracellular solution and distinct STDP paradigms in adult animals would help to understand whether EGTA inclusion in the intracellular solution disrupts postsynaptic Ca^{2+} elevation and thereby inhibits the induction of t-LTP at hippocampal SC-CA1 synapses from adult mice.

4.2 Altered STDP at SC-CA1 synapses and basal properties of CA1 neurons in the hippocampus of 6 months old mice

Our study demonstrated that STDP can be induced at SC-CA1 synapses in acute hippocampal slices in adults by repeatedly pairing presynaptic stimulations with postsynaptic action potentials. To induce t-LTP, we used two STDP paradigms, the 1:1 (canonical) and a 1:4 (burst) protocol that mimics postsynaptic theta bursts of APs - a firing pattern that is observed during learning processes *in vivo* (Otto et al., 1991). Importantly, a small number of repeats (6 pairings of presynaptic EPSP with postsynaptic AP) at a low frequency (0.5 Hz) was sufficient to induce persistent changes in synaptic efficacy that lasted for 30 min (**Fig. 13, 14**). In addition, we observed significant t-LTP in adult mice with STDP paradigms executed at both positive and negative spike timings (Δt= + or -10 ms; **Fig. 13, 14**). Moreover, we showed that a high number of repeats (100 and 35 pairings for canonical and burst protocols, respectively) executed at 2 Hz were efficient in t-LTP induction and expression at hippocampal SC-CA1 synapses in adult mice (**Fig. 11**).

In comparison to 1 months old mice (juveniles; compare e.g. Cepeda-Prado et al., 2019; Edelmann et al., 2015; Frey et al., 2009; Pang et al., 2019; Pérez-Rodríguez et al., 2019), 6 months old mice expressed decreased t-LTP in response to 6x 1:1 (Δt= +10 ms) stimulation at hippocampal SC-CA1 synapses (**Fig. 16**). Further, 6x 1:1 (Δt= -10 ms) stimulation induced t-LTP in adults compared to no t-LTP in juveniles (**Fig. 17**). Moreover, adult mice displayed significantly decreased action potential frequency, action potential amplitude in CA1 neurons

(intrinsic excitability) and paired-pulse facilitation at SC-CA1 synapses compared to juveniles (**Fig. 18**). Significant increase in $GABA_B$ receptor inhibitory responses coinciding with the EPSP decay was also observed at hippocampal SC-CA1 synapses from adults (**Fig. 18J**).

4.2.1 Fully matured GABAergic inhibition and dendritic arborization in the hippocampus of 6 months old mice

The altered t-LTP results from adult mice are in agreement with earlier studies, which reported that the synaptic plasticity induction and/or expression mechanisms change significantly in the hippocampus with postnatal age (Buchanan & Mellor, 2007; Groen et al., 2014; Yasuda et al., 2003). Importantly, GABAergic inhibition and dendritic arborization changes significantly within the hippocampal CA1 region with increase in postnatal age (Banks et al., 2002; Cohen et al., 2000). An essential component for STDP is the backpropagating action potential (bAP). Backpropagation of APs along the dendrites can be modulated by morphology and ion channel composition of neurons, both of which change during development. Groen and coworkers (2014) have described that 4-6 weeks old rats display an increased GABAergic inhibition and APs back-propagated smaller distances in the dendrites of hippocampal CA1 neurons compared to 2-3 weeks old rats. We propose that increased GABAergic inhibition in 6 months old mice compared to 1-month old mice through its impact on bAPs along CA1 dendrites might be underlying altered t-LTP at SC-CA1 synapses and basal electrical properties of CA1 pyramidal neurons in the hippocampus. Indeed, we observed significantly increased $GABA_B$ receptor mediated inhibitory responses coinciding with the EPSP decay in the current study (**Fig. 18J**), highlighting the increased GABAergic inhibition in 6 months old adult mice. Developmental change in GABAergic inhibition likely impacts basal electrical and synaptic properties of CA1 neurons in 6 months old adult mice, and additional studies are necessary to clarify the role of this matured inhibition on STDP.

4.2.2 Postsynaptic Ca^{2+} sources and neuromodulator-dependent regulation of STDP at SC-CA1 synapses in fully matured 6 months old mice

We observed that N-methyl-D-aspartate receptors (NMDARs) act as Ca^{2+} source responsible for postsynaptic Ca elevation, which eventually mediated t-LTP induced by 6x 1:4 stimulation, in 6 months old mice (**Fig. 15**). Since postsynaptic N-methyl-D-aspartate receptors (NMDARs) are thought to be an important coincidence detector for t-LTP, developmental changes in NMDAR functions may be one of the modulators of the t-LTP properties. Furthermore, changes in calcium influx at the spine via postsynaptic voltage-gated

calcium channel expression or developmental regulation of protein kinases in postsynaptic structures that mediate hippocampal plasticity (Luchkina et al., 2014; Yasuda et al., 2003) could contribute to altered t-LTP in adults. Moreover, postnatal developmental changes in synaptic proteins and neuromodulators such brain-derived neurotrophic factor (BDNF) and dopamine may play a role in STDP induction and expression. The altered STDP and basal properties of CA1 pyramidal neurons observed in the current study could be the functional consequences of developmental factors in 6 months old mice.

4.2.3 Altered synaptic facilitation mechanisms and ion channel conductances in the hippocampus of 6 months old mice

Decreased paired-pulse facilitation at SC-CA1 synapses in the hippocampus of 6 months old adult mice (**Fig. 18**) may indicate the developmental change in spatiotemporal dynamics of Ca^{2+} in the presynaptic terminal, neurotransmitter release probability, the vesicle turnover and the gating of post-synaptic receptors, mechanisms underlying synaptic facilitation (Dutta Roy et al., 2014; Katz & Miledi, 1968; Zucker & Regehr, 2002). Moreover, alterations in different ionic conductance via changes in either the functional properties of Na^+, K^+ and Cl^- channels, or in their expression and distribution in CA1 neurons with increase in postnatal age could play a role in regulating basal properties.

Detailed studies are required to determine how changes in the postsynaptic NMDAR composition, downstream signaling cascades, GABAergic inhibition, bAP, and neuromodulators at different ages influence the expression, magnitude, and timing requirements for STDP. We propose that STDP is shaped by, but also modifies, synapses with development and thereby produces refinements in neuronal responses to synaptic inputs. In juvenile animals, STDP may facilitate synaptic connections to be established while in mature adults, perhaps it promotes potentiation and depression of connections in response to learning events. STDP might serve different roles according to the developmental stages.

STDP has been proposed as a mechanism for optimizing the tuning of neurons to sensory inputs, a process that underlies the formation of receptive field properties and associative memories (Feldman, 2012; Dan, 2006; Dan & Poo, 2004; Markram et al., 2011). Postnatal development/maturation can have a great influence on STDP rules. The STDP rules or learning curves must adjust during development to enable neurons to optimally tune their selectivity for environmental stimuli (Buchanan & Mellor, 2007; Groen et al., 2014; Yasuda et al., 2003), but these changes are poorly understood.

Next, we investigated whether AD pathology in 6 months old APP/PS1 mice affects STDP in the hippocampus.

4.3 Six months old APP/PS1 mice showed intact t-LTP at hippocampal SC-CA1 synapses when amyloid beta (Aβ) plaques location was not considered

Results from the current study showed that different STDP paradigms: low or high repeat, positive or negative spike timing interval; induced intact t-LTP in 6 months old APP/PS1 mice (**Fig. 19-21**). Contrary to our expectations, 6x 1:1 stimulation induced t-LTP in 6 months old APP/PS1 mice, while 6x 1:1 paradigm was unable to induce t-LTP in age-matched WT littermate mice (compare **Fig. 19B)**. Nonetheless, we observed significant t-LTP with 6x 1:1 stimulation in 6 months old C57Bl/6J mice, age-matched with APP/PS1 WT littermate mice, under similar recording conditions (**Fig. 13**). These results suggest that the presence of amyloid precursor protein (APP) and presenilin gene mutations randomly in WT littermates could interfere with t-LTP induction and/or expression. In addition, strain background differences could be responsible for 6x 1:1 t-LTP deficits in WT littermates compared to C57Bl/6J mice, though further investigations are necessary. On the other hand, studies have reported impaired conventional LTP in APP/PS1 mouse models of AD (compare Larson et al., 1999; see review Mango et al., 2019; Walsh et al., 2005).

As an early event in AD, synaptic dysfunctions such as impaired HFS induced conventional LTP of hippocampal synaptic transmission have been observed by several earlier studies (Calella et al., 2010; Chang et al., 2006; Richards et al., 2003; Song et al., 2014; Trinchese et al., 2004). All studies concerning conventional LTP or LTD (field potential measurements) typically employ presynaptic high frequency/theta burst stimulations for LTP induction or low frequency stimulations for LTD induction, compared to pairing of presynaptic and postsynaptic activations used for t-LTP induction in the current study (compare Methods). These fundamentally different induction paradigms are likely to recruit distinct signaling mechanisms in t-LTP compared to conventional LTP. Until today, AD pathology effects could be observed only in the form of LTP and LTD disruptions, an associative activity among larger groups of cells (measured on neuronal network level), compared to t-LTP which relies on plasticity at the single cell level. In addition, most of the conventional LTP and LTD studies were performed with intact GABAergic system, while in our STDP study we have

used $GABA_A$ receptor antagonist picrotoxin in the recording aCSF, typical in STDP experiments (Astori et al., 2010; Edelmann et al., 2015; Evans et al., 2012).

4.4 Impaired 6x 1:4 t-LTP in 6 months old APP/PS1 mice is correlated with distance of hippocampal CA1 neurons from Aβ plaques

We demonstrated that t-LTP, induced by distinct STDP paradigms at hippocampal SC-CA1 synapses in 6 months old adult APP/PS1 double transgenic mice was unaltered, when the amyloid-beta (Aβ) plaques location in the recorded slices was not considered (**Fig. 19-21**). Here, we argued that Aβ plaque levels in APP/PS1 mice at the age of 6 months might be correlated with impairments in t-LTP. Indeed, with methoxy-X04 staining of Aβ plaques in acute hippocampal slices, we witnessed low Aβ plaques density in CA1 region in 6 months old APP/PS1 mice (e.g., Kartalou et al., 2020a, b; Radde et al., 2006). Therefore, in blind conditions where Aβ plaques were not stained, recorded CA1 cells were mostly far away from plaques.

Moreover, APP/PS1 mice showed clear impairment of t-LTP in CA1 cells near to Aβ plaques (<200 µm, **Fig. 22A**). This indicates that the proximity of Aβ plaques is indeed decisive to observe clear t-LTP deficits under our recording conditions. Although the Aβ plaques have been identified as a principle component in AD histopathology a century ago, the pathogenic mechanisms of Aβ plaques are still unclear (see reviews Benilova et al., 2012; Castellani & Smith, 2011; Shea et al., 2019; Spires-Jones & Knafo, 2012; Zott et al., 2019). However, our results suggest that Aβ plaques and most likely associated soluble Aβ species, which are present at higher concentration around plaques, interfere with t-LTP in the CA1 pyramidal neurons in the proximity and thereby contributing to cognitive decline in AD pathology. In this respect it is important to note, that in CA1 pyramidal neurons farther away from Aβ plaques (>200 µm, **Fig. 22A**), t-LTP was unaltered and comparable to t-LTP in WT littermates. Furthermore, we observed a dependence of t-LTP magnitude from plaque distance (**Fig.22B**), which further supports an important role of plaque-associated toxicity for t-LTP. However, the detailed mechanism(s) by which Aβ plaques disrupts t-LTP at excitatory hippocampal SC-CA1 synapses and the time course of hippocampal synaptic impairment are not completely understood and demands further investigations. Furthermore, the results from the current study are inconclusive to understand whether changes in postsynaptic responsiveness, presynaptic neurotransmitter release or neurotransmitter uptake by neuroglial cells are underlying t-LTP deficits in the proximity of Aβ plaques.

4.5 Impaired 6x 1:4 t-LTP in APP/PS1 mice is insensitive to fingolimod and voluntary running treatments

Treatment with fingolimod (for 1 month) did not rescue impaired t-LTP in adult APP/PS1 mice (**Fig. 23A**). It has been described that some neuroprotective effects of fingolimod are mediated through the anti-inflammatory action on microglia and astrocytes (see e.g. Kartalou et al., 2020b) or through elevation of BDNF expression in the mouse brain (Deogracias et al., 2012; Doi et al., 2013; Fukumoto et al., 2014). Timing-dependent LTP induced with 6x 1:4 stimulation or 6x 1:1 stimulation was described to be BDNF independent in 1 month old mice (Cepeda-Prado et al., 2019). Therefore, 6x 1:4 t-LTP in 6 months old adult APP/PS1 mice is possibly insensitive to fingolimod mediated BDNF elevation. It has also been reported that fingolimod regulates neuroinflammation and may have a significant clinical impact in ameliorating or maybe delaying cognitive decline in AD (reviewed in Angelopoulou & Piperi, 2019). Interestingly, microglia are involved in neuroinflammation and has been reported to affect synaptic remodeling during activity-dependent synaptic plasticity (LTP) in the healthy adult brain (see review Innes et al., 2019; Pfeiffer et al., 2016). Moreover, Nazari and colleagues described a fingolimod mediated rescue of impaired conventional LTP in rats following focal cerebral ischemia (Nazari et al., 2016), while others reported fingolimod induced rescue of correlation based synaptic plasticity (LTP) in mouse models of Huntington's and Alzheimer's disease (Miguez et al., 2015; Kartalou et al., 2020b). It has been recommended that fingolimod increases the cyclic adenosine monophosphate (cAMP) levels and phosphorylation of cAMP response element-binding protein (CREB) in the hippocampus, preventing imbalance of BDNF receptors in the hippocampus (Miguez et al., 2015). These studies suggest an ameliorating effect of fingolimod on cognitive decline in AD, which could be successfully observed at neuronal network level (e.g. LTP), possibly mediated through elevated BDNF expression and/or regulation of neuroinflammation. However, our present study reveals no rescue of 6x 1:4 induced impaired t-LTP in the proximity of Aβ plaques in adult APP/PS1 mice (**Fig. 23A**). These disparate findings might indicate differences in signaling cascades involved in conventional LTP, which is based on the associative activity among larger groups of cells, compared to t-LTP, which relies on plasticity at the single cell level. This indicates that 6x 1:4 t-LTP in APP/PS1 mice is perhaps unresponsive to fingolimod mediated BDNF elevation as well as its effect on

neuroinflammation. Henceforth, further investigations are necessary, aimed towards STDP underlying signaling cascades in adult mice.

Voluntary running treatment (for 2 months) was unable to ameliorate disrupted t-LTP in adult APP/PS1 animals (**Fig. 23B**). It is well established that voluntary running increases BDNF gene and protein expression in the hippocampus and thereby protects hippocampal neurons against neurodegeneration (Farmer et al., 2004; Gómez-Pinilla et al., 2002; Lin et al., 2015). Cepeda-Prado et al. (2019) described 6x 1:4 t-LTP is independent of BDNF signaling in 1 month old mice (Cepeda-Prado et al., 2019). We suggest that 6x 1:4 t-LTP in adult APP/PS1 mice might be insensitive to BDNF and hence the failure of voluntary running to restore impaired t-LTP. Contrary to our expectations, following 2 months voluntary running, WT littermate mice expressed no t-LTP with 6x 1:4 stimulation. This suggests that voluntary running impairs t-LTP in WT control mice by an unknown mechanism. We propose that the voluntary running treatment might act as bidirectional synaptic plasticity regulator in WT littermates, suggesting that at the expense of impaired t-LTP, voluntary running treatment might have beneficial effect on t-LTD in WT littermate mice, though further investigations are necessary.

4.6 Six months old APP/PS1 mice displayed intact basal electrical properties of CA1 pyramidal neurons and its presynaptic Schaffer collateral input fibers

Since we observed t-LTP deficits only in the proximity of Aβ plaques in APP/PS1 mice, we also studied basal electrical and synaptic properties of CA1 pyramidal neurons as difference between genotypes (to observe general effects) as well as in Aβ plaque distance-dependent manner. A decreased input resistances, though not statistically significant, in 6 months old adult APP/PS1 mice (**Fig. 24G**) could be a result of alterations in K^+ conductance via changes in either the functional properties of these channels, or in their expression and distribution in CA1 neurons (Alier et al., 2011; Buskila et al., 2013; Ferreira & Klein, 2011). However, most of the studied basal properties of the hippocampal CA1 neurons, e.g. intrinsic excitability, paired-pulse facilitation, and resting membrane potential were intact in adult APP/PS1 mice (see **Fig. 24, 25**). These observations are consistent with findings from earlier studies (Briggs et al., 2013; Buskila et al., 2013). Although APP/PS1 mice displayed significantly higher mean excitatory postsynaptic currents (EPSC) amplitudes and a different cumulative distribution of EPSC amplitudes and inter-event intervals (IEI) for spontaneous EPSCs, we

observed largely unaltered properties of miniature EPSCs, indicating no gross changes in quantal synaptic transmission at hippocampal SC-CA1 synapses in adult APP/PS1 mice (EPSCs, **Fig.26**). In addition, CA1 pyramidal neurons in APP/PS1 mice expressed comparable non-evoked inhibitory synaptic transmission as WT littermate mice (IPSCs, **Fig.27**). Any changes in basal electrical and synaptic properties of CA1 pyramidal neurons and non-evoked synaptic transmission at SC-CA1 synapses in the hippocampus might be masked by compensatory mechanisms in APP/PS1 animals, a constitutive knock-in mouse model.

Overall, these data indicate that APP and PS1 mutations does not generally compromise CA1 pyramidal neurons' neuronal excitability and basal synaptic transmission at SC-CA1 synapses in 6 months old APP/PS1 mice.

4.7 Alzheimer pathology in 6 months old APP/PS1 mice showed inability for synaptic facilitation/signal integration

The CA1 pyramidal neurons in the hippocampus of 6 months old APP/PS1 mice expressed significant deficits in intrinsic excitability, estimated by number of action potentials fired by CA1 cell in response to different somatic current injections (0-450 pA for 500 ms, 50 pA increments) and with the measurement of hyperpolarization peak (Ih peak) in response to different somatic current injections/hyperpolarization steps (0-200 pA for 500 ms, 50 pA increments; **Fig. 28A, 28B**). This is at variance with the earlier described intact intrinsic excitability in 6 months old adult APP/PS1 mice (**Fig. 24, 25**), when we used somatic current injections with different stimulus paradigm (depolarization steps: 0-180 pA for 1000 ms, 20 pA increments). The stimulus strength and duration used for respective stimulations can possibly explain different intrinsic excitability results. The observed intact intrinsic excitability of CA1 pyramidal neurons in 6 months old APP/PS1 mice was studied under recording conditions where we included picrotoxin in the recording aCSF, acute hippocampal slices were used with CA3-CA1 cut, at 28-31^{o}C (**Fig. 24, 25**). In another approach where we observed impaired intrinsic excitability, we studied intrinsic excitability of CA1 pyramidal neurons in 6 months old APP/PS1 mice under more physiological recording conditions by excluding picrotoxin from the recording aCSF, intact acute hippocampal slices were used without CA3-CA1 cut, at 34-35^{o}C. The observed intact and impaired intrinsic excitability of CA1 neurons in in 6 months old APP/PS1 mice cannot directly compared due to difference in

recording conditions. Intrinsic excitability deficits in CA1 hippocampal pyramidal neurons from adult APP/PS1 mice findings are consistent with results from Eslamizade and colleagues (2015). These results imply that AD pathology, in particular Aβ plaques, can disrupt intrinsic excitability of CA1 pyramidal neurons in the hippocampus in part through enhancement of hyperpolarization activated channel currents and possibly via modification of transient receptor potential channel TRPV1 activity (Eslamizade et al., 2015). Furthermore, AD pathology likely changes GABAergic inhibition and different ionic conductance via the functional properties of Na^+, K^+ and Cl^- channels, or in their expression and distribution in CA1 neurons and thereby hampers intrinsic excitability. Although results from the current study are not conclusive to clearly identify underlying mechanisms for intrinsic excitability deficit in the hippocampal CA1 neurons of 6 months old APP/PS1 mice and demands further examination.

In another approach, we studied synaptic signal integration, by means of spike probability at different frequencies (5, 10, 20, 50, 100 and 200 Hz), at hippocampal SC-CA1 synapses in adult APP/PS1 mice. The stimulation paradigms designed to investigate synaptic signal integration are roughly based on paired-pulse facilitation (PPF); instead of two pulses, 5 pulses were used at different inter-stimulus intervals, i.e. 200, 100, 50, 20, 10 and 5 ms. We observed clear inability of synaptic facilitation/signal integration in APP/PS1 mice, though not reaching statistical significance compared to age-matched WT littermates (**Fig. 28C**). Synaptic facilitation is a form of activity-dependent transient change in synaptic effectiveness that last at most for a few minutes (Zucker & Regehr, 2002). The mechanisms such as spatiotemporal dynamics of Ca^{2+} in the presynaptic terminal, neurotransmitter release probability, the vesicle turnover and the gating of post-synaptic receptors underlie synaptic facilitation (Dutta Roy et al., 2014; Zucker & Regehr, 2002). Furthermore, residual Ca^{2+} hypothesis is widely accepted to explain synaptic facilitation (Katz & Miledi, 1968; Zucker & Regehr, 2002). Accordingly, in the presynaptic terminal leftovers from total Ca^{2+} influx occurred during the first stimulus adds nonlinearly to the calcium influx that occurs in subsequent stimulus. We suggest that AD pathology in adult APP/PS1 mice might disrupt one or more of these mechanism(s) underlying synaptic facilitation, i.e. spatiotemporal dynamics of Ca^{2+} in the presynaptic terminal, neurotransmitter release probability, the vesicle turnover and the gating of post-synaptic receptors to a certain extent and thereby impact synaptic signal integration at SC-CA1 synapses.

4.8 Conclusions

The current dissertation primarily addressed the influence of developmental maturation and Alzheimer's disease (AD) on spike timing-dependent plasticity (STDP) at fully developed hippocampal Schaffer collateral (SC)-CA1 synapses in 6 months old mice. STDP is a biologically plausible Hebbian plasticity rule at the single neuron level in contrast to traditional correlation based synaptic plasticity like conventional LTP or LTD. Moreover, we investigated the impact of developmental maturation and AD pathology on basal electrical properties of CA1 pyramidal neurons and spontaneous synaptic transmission at SC-CA1 synapses in the hippocampus of 6 months old mice (adults, fully developed system). The principle findings from the study are summarized as below

- Developmental maturation influences STDP at hippocampal SC-CA1 synapses in 6 months old mice compared to 1-month old mice (juveniles). In comparsion to t-LTP results in 1-month old mice, adults exhibited decreased t-LTP in response to 6x 1:1 (Δt= +10 ms) stimulation. Moreover, 6x 1:1 (Δt= -10 ms) stimulation induced t-LTP in adults compared to no t-LTP in juveniles.
- Moreover, the hippocampal CA1 pyramidal neurons in adults expressed decreased intrinsic excitability and SC-CA1 synapses showed decreased paired-pulse facilitation (PPF). These PPF results suggest that the developmental maturation affects presynaptic release probability. Moreover, APP/PS1 mice showed increased $GABA_B$ receptor mediated synaptic responses during the decaying phase of EPSPs, indicating a developmental change in GABAergic inhibition, compared to 1-month old juvenile animals.
- AD pathology did not significantly change STDP induced with low repeat as well as high repeat, positive and negative spike timing STDP paradigms when amyloid-β (Aβ) plaque location in the recorded slices was not resolved.
- Adult APP/PS1 mice, a well-acknowledged AD mouse model, showed significantly impaired timing-dependent LTP (t-LTP) in an Aβ plaque distance-dependent manner, which could not be restored with chronic fingolimod (1 month) or voluntary running (2 months) treatment.
- AD pathology did not impact basal electrical properties of CA1 pyramidal neurons and spontaneous synaptic transmission at SC-CA1 synapses in the hippocampus of 6 months old APP/PS1 mice.

4.9 Future Prospects

- In the current study, we observed significant t-LTP deficits at hippocampal SC-CA1 synapses in 6 months old APP/PS1 Alzheimer disease (AD) mouse model in the vicinity of Aβ plaques. Adult APP/PS1 mice expressed no significant impairments in t-LTP when Aβ plaques location or density in recorded slices was not resolved. Investigation of STDP in older, e.g. 9- or 12-months old APP/PS1 mice, which might exhibit higher Aβ plaques density in the hippocampal CA1, might be helpful to confirm Aβ plaque distance dependence of STDP in AD pathology.
- The molecular and cellular mechanisms underlying this t-LTP deficit in the Aβ plaques proximity in adult AD mouse models remain to be elucidated in future studies.
- Further investigations testing other STDP paradigms for induction and/or expression of t-LTP in Aβ plaques distance-dependent manner are necessary.
- We tested chronic fingolimod and voluntary running treatments separately to ameliorate impaired t-LTP, a phenotype, in adults APP/PS1 mice. These treatments strategies were tested based on their success in elevation of BDNF expression, rescue of impaired LTP and regulation of neuroinflammation. Since chronic fingolimod and voluntary running separately could not rescue the impaired t-LTP phenotype in APP/PS1 mice, combination of fingolimod and voluntary running in future investigations is necessary.
- Several studies report the molecular mechanism(s) underlying t-LTP in juveniles, while in adults the underlying mechanism(s) are not clear. Therefore, further investigations are necessary to unravel the molecular mechanisms underlying t-LTP in adults. It would be interesting to study which cellular changes occurring during developmental maturation influence these mechanisms compared to the mechanisms in juvenile animals. Furthermore, once the molecular mechanisms underlying t-LTP in adults will be identified, this might enable to tackle the disrupted t-LTP in Aβ plaques distance-dependent manner in APP/PS1 mice and design efficient treatment regimens to ameliorate AD pathology.

5 Bibliography:

2020 Alzheimer's disease facts and figures. (2020). *Alzheimer's and Dementia*, *16*(3), 391–460.

Abraham, W. C., & Bear, M. F. (1996). Metaplasticity: The plasticity of synaptic plasticity. *Trends in Neurosciences*, *19*(4), 126–130.

Abrahamsson, T., Lalanne, T., Watt, A. J., & Sjöström, P. J. (2016). Long-term potentiation by theta-Burst stimulation using extracellular field potential recordings in acute hippocampal slices. *Cold Spring Harbor Protocols*, *2016*(6), 564–572.

Alaei, H. A., Borjeian, L., Azizi, M., Orian, S., Pourshanazari, A., & Hanninen, O. (2006). Treadmill running reverses retention deficit induced by morphine. *European Journal of Pharmacology*, *536*(1–2), 138–141.

Alier, K., Ma, L., Yang, J., Westaway, D., & Jhamandas, J. H. (2011). Aβ inhibition of ionic conductance in mouse basal forebrain neurons is dependent upon the cellular prion protein PrP C. *Journal of Neuroscience*, *31*(45), 16292–16297.

Alzheimer A. (1907). Über eine eigenartige Erkrankung der Hirnrinde. Allgemeine Zeitschrift für Psychiatrie und phychish-Gerichtliche Medizin, (Berlin), *64*, 146–148.

Andersen, S. L. (2003). Trajectories of brain development: Point of vulnerability or window of opportunity? *Neuroscience and Biobehavioral Reviews*, *27*(1–2), 3–18.

Andrásfalvy, B. K., Makara, J. K., Johnston, D., & Magee, J. C. (2008). Altered synaptic and non-synaptic properties of CA1 pyramidal neurons in Kv4.2 knockout mice. *Journal of Physiology*, *586*(16), 3881–3892.

Angelopoulou, E., & Piperi, C. (2019). Beneficial Effects of Fingolimod in Alzheimer's Disease: Molecular Mechanisms and Therapeutic Potential. *NeuroMolecular Medicine*, *21*(3), 227–238.

Asl, S. S., Bergen, H., Ashtari, N., Amiri, S., Łos, M. J., & Mehdizadeh, M. (2019). Pelargonidin exhibits restoring effects against amyloid β-induced deficits in the hippocampus of male rats. *Med J Islam Repub Iran*.

Astori, S., Pawlak, V., & Köhr, G. (2010). Spike-timing-dependent plasticity in hippocampal CA3 neurons. *The Journal of Physiology*, *588*(22), 4475–4488.

Banerjee, A., Meredith, R. M., Rodríguez-Moreno, A., Mierau, S. B., Auberson, Y. P., & Paulsen, O. (2009). Double dissociation of spike timing-dependent potentiation and depression by subunit-preferring NMDA receptor antagonists in mouse barrel cortex. *Cerebral Cortex*, *19*(12), 2959–2969.

Banks, M. I., Hardie, J. B., & Pearce, R. A. (2002). Development of GABA $_{A}$ Receptor-Mediated Inhibitory Postsynaptic Currents in Hippocampus. *Journal of Neurophysiology*, *88*(6), 3097–3107.

Barria, A., & Malinow, R. (2002). Subunit-specific NMDA receptor trafficking to synapses. *Neuron*, *35*(2), 345–353.

Bear, M. F., & Malenka, R. C. (1994). Synaptic plasticity: LTP and LTD. *Current Opinion in Neurobiology*, *4*(3), 389–399.

Beason-Held, L. L., Shafer, A. T., Goh, J. O., Landman, B. A., Davatzikos, C., Viscomi, B., Ash, J.,

Bibliography

Kitner-Triolo, M., Ferrucci, L., & Resnick, S. M. (2020). Hippocampal activation and connectivity in the aging brain. *Brain Imaging and Behavior*, 1–16.

Bell, C. C., Han, V. Z., Sugawara, Y., & Grant, K. (1997). Synaptic plasticity in a cerebellum-like structure depends on temporal order. *Nature*, *387*(6630), 278–281.

Bender, V. A., Bender, K. J., Brasier, D. J., & Feldman, D. E. (2006). Two coincidence detectors for spike timing-dependent plasticity in somatosensory cortex. *Journal of Neuroscience*, *26*(16), 4166–4177.

Benilova, I., Karran, E., & De Strooper, B. (2012). The toxic Aβ oligomer and Alzheimer's disease: An emperor in need of clothes. *Nature Neuroscience*, *15*(3), 349–357.

Berchtold, N. C., Chinn, G., Chou, M., Kesslak, J. P., & Cotman, C. W. (2005). Exercise primes a molecular memory for brain-derived neurotrophic factor protein induction in the rat hippocampus. *Neuroscience*, *133*(3), 853–861.

Berron, D., Van Westen, D., Ossenkoppele, R., Strandberg, O., & Hansson, O. (2020). Medial temporal lobe connectivity and its associations with cognition in early Alzheimer's disease. *Brain*, *143*, 1233–1248.

Bi, G Q, & Poo, M. M. (1998). Synaptic modifications in cultured hippocampal neurons: dependence on spike timing, synaptic strength, and postsynaptic cell type. *The Journal of Neuroscience : The Official Journal of the Society for Neuroscience*, *18*(24), 10464–10472.

Bi, Guo Qiang, & Poo, M. M. (1998). Synaptic modifications in cultured hippocampal neurons: Dependence on spike timing, synaptic strength, and postsynaptic cell type. *Journal of Neuroscience*, *18*(24), 10464–10472.

Bi, Guo Qiang, & Wang, H. X. (2002). Temporal asymmetry in spike timing-dependent synaptic plasticity. *Physiology and Behavior*, *77*(4–5), 551–555.

Biel, M., Wahl-Schott, C., Michalakis, S., & Zong, X. (2009). Hyperpolarization-activated cation channels: from genes to function. *Physiological Reviews*, *89*(3), 847–885.

Bliss, T. V. P., & Lømo, T. (1973). Long-lasting potentiation of synaptic transmission in the dentate area of the anaesthetized rabbit following stimulation of the perforant path. *The Journal of Physiology*, *232*(2), 331–356.

Bliss, T. V, & Collingridge, G. L. (1993). A synaptic model of memory: long-term potentiation in the hippocampus. *Nature*, *361*(6407), 31–39.

Bosch, M., Castro, J., Saneyoshi, T., Matsuno, H., Sur, M., & Hayashi, Y. (2014). Structural and molecular remodeling of dendritic spine substructures during long-term potentiation. *Neuron*, *82*(2), 444–459.

Brickley, S. G., & Mody, I. (2012). Extrasynaptic GABA A Receptors: Their Function in the CNS and Implications for Disease. *Neuron*, *73*(1), 23–34.

Briggs, C. A., Schneider, C., Richardson, J. C., & Stutzmann, G. E. (2013). Beta amyloid peptide plaques fail to alter evoked neuronal calcium signals in APP/PS1 Alzheimer's disease mice. *Neurobiology of Aging*, *34*(6), 1632–1643.

Buchanan, K. A., & Mellor, J. R. (2007). The development of synaptic plasticity induction rules and the requirement for postsynaptic spikes in rat hippocampal CA1 pyramidal neurones. *J Physiol*, *585*, 429–445.

Bibliography

Buonomano, D. V., & Merzenich, M. M. (1998). Cortical plasticity: From synapses to maps. *Annual Review of Neuroscience*, *21*, 149–186.

Buskila, Y., Crowe, S. E., & Ellis-Davies, G. C. R. (2013). Synaptic deficits in layer 5 neurons precede overt structural decay in 5xFAD mice. *Neuroscience*, *254*, 152–159.

Calella, A. M., Farinelli, M., Nuvolone, M., Mirante, O., Moos, R., Falsig, J., Mansuy, I. M., & Aguzzi, A. (2010). Prion protein and Aβ-related synaptic toxicity impairment. *EMBO Molecular Medicine*, *2*(8), 306–314.

Campanac, E., & Debanne, D. (2008). Spike timing-dependent plasticity: a learning rule for dendritic integration in rat CA1 pyramidal neurons. *The Journal of Physiology*, *586*(3), 779–793.

Carlisle, H. J., Fink, A. E., Grant, S. G. N., & O'Dell, T. J. (2008). Opposing effects of PSD-93 and PSD-95 on long-term potentiation and spike timing-dependent plasticity. *The Journal of Physiology*, *586*(24), 5885–5900.

Castellani, R. J., & Smith, M. A. (2011). Compounding artefacts with uncertainty, and an amyloid cascade hypothesis that is "too big to fail." *Journal of Pathology*, *224*(2), 147–152.

Cepeda-Prado, E. A., Khodaie, B., Quiceno, G. D., Beythien, S., & Edelmann, E. (2019). Calcium-permeable AMPA receptors mediate timing-dependent LTP elicited by 6 coincident 1 action potentials at Schaffer collateral-CA1 synapses. bioRxiv preprint.

Chang, E. H., Savage, M. J., Flood, D. G., Thomas, J. M., Levy, R. B., Mahadomrongkul, V., Shirao, T., Aoki, C., & Huerta, P. T. (2006). AMPA receptor downscaling at the onset of Alzheimer's disease pathology in double knockin mice. *Proceedings of the National Academy of Sciences of the United States of America*, *103*(9), 3410–3415.

Chapman, P. F., White, G. L., Jones, M. W., Cooper-Blacketer, D., Marshall, V. J., Irizarry, M., Younkin, L., Good, M. A., Bliss, T. V. P., Hyman, B. T., Younkin, S. G., & Hsiao, K. K. (1999). Impaired synaptic plasticity and learning in aged amyloid precursor protein transgenic mice. *Nature Neuroscience*, *2*(3), 271–276.

Chen, X., & Johnston, D. (2004). Properties of single voltage-dependent K+ channels in dendrites of CA1 pyramidal neurones of rat hippocampus. *Journal of Physiology*, *559*(1), 187–203.

Chevaleyre, V., Takahashi, K. A., & Castillo, P. E. (2006). Endocannabinoid-mediated synaptic plasticity in the CNS. *Annual Review of Neuroscience*, *29*, 37–76.

Citri, A., & Malenka, R. C. (2008). Synaptic plasticity: Multiple forms, functions, and mechanisms. *Neuropsychopharmacology*. *Neuropsychopharmacology*, *33*, 18–41.

Cohen, A. S., Lin, D. D., & Coulter, D. A. (2000). Protracted Postnatal Development of Inhibitory Synaptic Transmission in Rat Hippocampal Area CA1 Neurons. *Journal of Neurophysiology*, *84*(5), 2465–2476.

Corlew, R., Wang, Y., Ghermazien, H., Erisir, A., & Philpot, B. D. (2007). Developmental switch in the contribution of presynaptic and postsynaptic NMDA receptors to long-term depression. *Journal of Neuroscience*, *27*(37), 9835–9845.

Cui, Y., Prokin, I., Xu, H., Delord, B., Genet, S., Venance, L., & Berry, H. (2016). Endocannabinoid dynamics gate spike- timing dependent depression and potentiation. *ELife*, *5*(Feb).

Dan, Y. (2006). Spike Timing-Dependent Plasticity: From Synapse to Perception. *Physiological Reviews*, *86*(3), 1033–1048.

Bibliography

Dan, Yang, & Poo, M. M. (2004). Spike timing-dependent plasticity of neural circuits. *Neuron*, *44*(1), 23–30.

Danglot, L., Triller, A., & Marty, S. (2006). The development of hippocampal interneurons in rodents. *Hippocampus*, *16*(12), 1032–1060.

Debanne, D., Gähwiler, B. H., & Thompson, S. M. (1998a). Long-term synaptic plasticity between pairs of individual CA3 pyramidal cells in rat hippocampal slice cultures. *The Journal of Physiology*, *507*(1), 237–247.

Debanne, D., Gähwiler, B. H., & Thompson, S. M. (1998b). Long-term synaptic plasticity between pairs of individual CA3 pyramidal cells in rat hippocampal slice cultures. *Journal of Physiology*, *507*(1), 237–247.

DeKosky, S. T., & Scheff, S. W. (1990). Synapse loss in frontal cortex biopsies in Alzheimer's disease: Correlation with cognitive severity. *Annals of Neurology*, *27*(5), 457–464.

Deng, W., Aimone, J. B., & Gage, F. H. (2010). New neurons and new memories: how does adult hippocampal neurogenesis affect learning and memory? *Nature Reviews. Neuroscience*, *11*(5), 339–350.

Deogracias, R., Yazdani, M., Dekkers, M. P. J., Guy, J., Ionescu, M. C. S., Vogt, K. E., & Barde, Y. A. (2012). Fingolimod, a sphingosine-1 phosphate receptor modulator, increases BDNF levels and improves symptoms of a mouse model of Rett syndrome. *Proceedings of the National Academy of Sciences of the United States of America*, *109*(35), 14230–14235.

Doi, Y., Takeuchi, H., Horiuchi, H., Hanyu, T., Kawanokuchi, J., Jin, S., Parajuli, B., Sonobe, Y., Mizuno, T., & Suzumura, A. (2013). Fingolimod Phosphate Attenuates Oligomeric Amyloid β–Induced Neurotoxicity via Increased Brain-Derived Neurotrophic Factor Expression in Neurons. *PLoS ONE*, *8*(4), e61988.

Duguid, I., & Sjöström, P. J. (2006). Novel presynaptic mechanisms for coincidence detection in synaptic plasticity. *Current Opinion in Neurobiology*, *16*(3), 312–322.

Dumas, T. C. (2005). Developmental regulation of cognitive abilities: Modified composition of a molecular switch turns on associative learning. *Progress in Neurobiology*, *76* (3), 189–211.

Dutta Roy, R., Stefan, M. I., & Rosenmund, C. (2014). Biophysical properties of presynaptic short-term plasticity in hippocampal neurons: insights from electrophysiology, imaging and mechanistic models. *Frontiers in Cellular Neuroscience*, *8*(MAY), 141.

Edelmann, E., Cepeda-Prado, E., Franck, M., Lichtenecker, P., Brigadski, T., & Lessmann, V. (2015). Theta Burst Firing Recruits BDNF Release and Signaling in Postsynaptic CA1 Neurons in Spike-Timing-Dependent LTP. *Neuron*, *86*(4), 1041–1054.

Edelmann, E., & Endres, T. Therapeutics for Ahzheimer disease: Behavior, Electrophysiology & Molecular Profiling. Progress report, CIRCPROT Symposium 2019, Nizza.

Edelmann, E., Cepeda-Prado, E., & Leßmann, V. (2017). Coexistence of Multiple Types of Synaptic Plasticity in Individual Hippocampal CA1 Pyramidal Neurons. *Frontiers in Synaptic Neuroscience*, *9*(March), 1–15.

Edelmann, E., & Lessmann, V. (2011). Dopamine modulates spike timing-dependent plasticity and action potential properties in CA1 pyramidal neurons of acute rat hippocampal slices. *Frontiers in Synaptic Neuroscience*, *3*(NOV), 1–16.

Bibliography

Eslamizade, M. J., Saffarzadeh, F., Mousavi, S. M. M., Meftahi, G. H., Hosseinmardi, N., Mehdizadeh, M., & Janahmadi, M. (2015). Alterations in ca1 pyramidal neuronal intrinsic excitability mediated by iH channel currents in a rat model of amyloid beta pathology. *Neuroscience*, *305*, 279–292.

Evans, R. C., Morera-Herreras, T., Cui, Y., Du, K., Sheehan, T., Kotaleski, J. H., Venance, L., & Blackwell, K. T. (2012). The effects of NMDA subunit composition on calcium influx and spike timing-dependent plasticity in striatal medium spiny neurons. *PLoS Computational Biology*, *8*(4), e1002493.

Farmer, J., Zhao, X., Van Praag, H., Wodtke, K., Gage, F. H., & Christie, B. R. (2004). Effects of voluntary exercise on synaptic plasticity and gene expression in the dentate gyrus of adult male sprague-dawley rats in vivo. *Neuroscience*, *124*(1), 71–79.

Feldman, D. E. (2000). Timing-based LTP and LTD at vertical inputs to layer II/III pyramidal cells in rat barrel cortex. *Neuron*, *27*(1), 45–56.

Feldman, D. E. (2012). The Spike-Timing Dependence of Plasticity. *Neuron*, *75*(4), 556–571.

Ferreira, S. T., & Klein, W. L. (2011). The Aβ oligomer hypothesis for synapse failure and memory loss in Alzheimer's disease. *Neurobiology of Learning and Memory*, *96* (4), 529–543.

Fino. (2010). Spike-timing dependent plasticity in the striatum. *Frontiers in Synaptic Neuroscience*, *2*(JUN), 6.

Fino, E., Paille, V., Cui, Y., Morera-Herreras, T., Deniau, J. M., & Venance, L. (2010). Distinct coincidence detectors govern the corticostriatal spike timing-dependent plasticity. *Journal of Physiology*, *588*(16), 3045–3062.

Flores, R. De, Mcmillan, C. T., Grossman, M., Wolk, D. A., Wisse, L. E. M., Das, S. R., Xie, L., Trojanowski, J. Q., Robinson, J. L., Lee, E., Irwin, D. J., & Yushkevich, P. A. (2020). Contribution of mixed pathology to medial temporal lobe atrophy in Alzheimer ' s disease. February, 3–5.

Fouquet, M., Desgranges, B., La Joie, R., Rivière, D., Mangin, J. F., Landeau, B., Mézenge, F., Pélerin, A., de La Sayette, V., Viader, F., Baron, J. C., Eustache, F., & Chételat, G. (2012). Role of hippocampal CA1 atrophy in memory encoding deficits in amnestic Mild Cognitive Impairment. *NeuroImage*, *59*(4), 3309–3315.

Frey, M. C., Sprengel, R., & Nevian, T. (2009). Activity pattern-dependent long-term potentiation in neocortex and hippocampus of GluA1 (GluR-A) subunit-deficient mice. *The Journal of Neuroscience*, *29*(17), 5587–5596.

Froemke, R. C., & Dan, Y. (2002). Spike-timing-dependent synaptic modification induced by natural spike trains. *Nature*, *416*(6879), 433–438.

Froemke, R. C., Poo, M. M., & Dan, Y. (2005). Spike-timing-dependent synaptic plasticity depends on dendritic location. *Nature*, *434*(7030), 221–225.

Froemke, R. C., Tsay, I. A., Raad, M., Long, J. D., & Dan, Y. (2006). Contribution of individual spikes in burst-induced long-term synaptic modification. *Journal of Neurophysiology*, *95*(3), 1620–1629.

Fuenzalida, M., De Sevilla, D. F., Couve, A., & Buño, W. (2010). Role of AMPA and NMDA receptors and back-propagating action potentials in spike timing-dependent plasticity. *Journal of Neurophysiology*, *103*(1), 47–54.

Bibliography

Fukumoto, K., Mizoguchi, H., Takeuchi, H., Horiuchi, H., Kawanokuchi, J., Jin, S., Mizuno, T., & Suzumura, A. (2014). Fingolimod increases brain-derived neurotrophic factor levels and ameliorates amyloid β-induced memory impairment. *Behavioural Brain Research*, *268*, 88–93.

Furcila, D., DeFelipe, J., & Alonso-Nanclares, L. (2018). A Study of Amyloid-β and Phosphotau in Plaques and Neurons in the Hippocampus of Alzheimer's Disease Patients. *Journal of Alzheimer's Disease*, *64*(2), 417–435.

Gaiarsa, J. L., Caillard, O., & Ben-Ari, Y. (2002). Long-term plasticity at GABAergic and glycinergic synapses: Mechanisms and functional significance. *Trends in Neurosciences*, *25*(11), 564–570.

Garad, M., Edelmann, E., & Leßmann, V. (2021). Impairment of spike timing-dependent plasticity at Schaffer collateral-CA1 synapses in adult APP/PS1 mice depends on proximity of Aβ plaques. Int. J. Mol. Sci., *22*(3), 1378.

Gerrow, K., & Triller, A. (2010). Synaptic stability and plasticity in a floating world. *Current Opinion in Neurobiology*, *20*(5), 631–639.

Gilbert, C. D. (1998). Adult cortical dynamics. *Physiological Reviews, 78* (2), 467–485.

Glazewski, S., Skangiel-Kramska, J., & Kossut, M. (1993). Development of NMDA receptor-channel complex and L-type calcium channels in mouse hippocampus. *Journal of Neuroscience Research*, *35*(2), 199–206.

Goedert, M., Wischik, C. M., Crowther, R. A., Walker, J. E., & Klug, A. (1988). Cloning and sequencing of the cDNA encoding a core protein of the paired helical filament of Alzheimer disease: Identification as the microtubule-associated protein tau. *Proceedings of the National Academy of Sciences of the United States of America*, *85*(11), 4051–4055.

Gómez-Pinilla, F., Ying, Z., Roy, R. R., Molteni, R., & Reggie Edgerton, V. (2002). Voluntary exercise induces a BDNF-mediated mechanism that promotes neuroplasticity. *Journal of Neurophysiology*, *88*(5), 2187–2195.

Götz, J., Chen, F., Van Dorpe, J., & Nitsch, R. M. (2001). Formation of neurofibrillary tangles in P301L tau transgenic mice induced by Aβ42 fibrils. *Science*, *293*(5534), 1491–1495.

Graupner, M., & Brunel, N. (2007). STDP in a bistable synapse model based on CaMKII and associated signaling pathways. *PLoS Computational Biology*, *3*(11), 2299–2323.

Groen, M. R., Paulsen, O., Pérez-Garci, E., Nevian, T., Wortel, J., Dekker, M. P., Mansvelder, H. D., van Ooyen, A., & Meredith, R. M. (2014). Development of dendritic tonic GABAergic inhibition regulates excitability and plasticity in CA1 pyramidal neurons. *Journal of Neurophysiology*, *112*(2), 287–299.

Grundke-Iqbal, I., Iqbal, K., & Tung, Y. C. (1986). Abnormal phosphorylation of the microtubule-associated protein τ (tau) in Alzheimer cytoskeletal pathology. *Proceedings of the National Academy of Sciences of the United States of America*, *83*(13), 44913–44917.

Gu, Q. (2002). Neuromodulatory transmitter systems in the cortex and their role in cortical plasticity. *Neuroscience*, *111*(4), 815–835.

Gustafsson, B., Wigstrom, H., Abraham, W. C., & Huang, Y. Y. (1987). Long-term potentiation in the hippocampus using depolarizing current pulses as the conditioning stimulus to single volley synaptic potentials. *Journal of Neuroscience*, *7*(3), 774–780.

Haass, C., & Selkoe, D. J. (2007). Soluble protein oligomers in neurodegeneration: Lessons from the

Bibliography

Alzheimer's amyloid β-peptide. *Nature Reviews Molecular Cell Biology*, *8*(2), 101–112.

Hashimotodani, Y., Ohno-Shosaku, T., Tsubokawa, H., Ogata, H., Emoto, K., Maejima, T., Araishi, K., Shin, H. S., & Kano, M. (2005). Phospholipase Cβ serves as a coincidence detector through its Ca 2+ dependency for triggering retrograde endocannabinoid signal. *Neuron*, *45*(2), 257–268.

Hashimotodani, Y., Ohno-shosaku, T., Watanabe, M., & Kano, M. (2007). Roles of phospholipase Cβ and NMDA receptor in activity-dependent endocannabinoid release. *Journal of Physiology*, *584*(2), 373–380.

Hebb, D. (1949). The Organization of Behavior. *A Neuropsychological Theory*. NewYork: Wiley.

Heneka, M.T.; Carson, M.J.; El Khoury, J.; Landreth, G.E.; Brosseron, F.; Feinstein, D.L.; Jacobs, A.H.; Wyss-Coray, T.; Vitorica, J.; Ransoho, R.M.; et al. (2015). Neuroinflammation in Alzheimer's disease. *Lancet Neurol.*, *14*, 388–405.

Hoffman, D. A., Magee, J. C., Colbert, C. M., & Johnston, D. (1997). K+ channel regulation of signal propagation in dendrites of hippocampal pyramidal neurons. *Nature*, *387*(6636), 869–875.

Holbro, N., Grunditz, Å., Wiegert, J. S., & Oertner, T. G. (2010). AMPA receptors gate spine Ca2+ transients and spike-timing-dependent potentiation. *Proceedings of the National Academy of Sciences of the United States of America*, *107*(36), 15975–15980.

Hoozemans, J. J. M., Veerhuis, R., Van Haastert, E. S., Rozemuller, J. M., Baas, F., Eikelenboom, P., & Scheper, W. (2005). The unfolded protein response is activated in Alzheimer's disease. *Acta Neuropathologica*, *110*(2), 165–172.

Hsieh, H., Boehm, J., Sato, C., Iwatsubo, T., Tomita, T., Sisodia, S., & Malinow, R. (2006). AMPAR Removal Underlies Aβ-Induced Synaptic Depression and Dendritic Spine Loss. *Neuron*, *52*(5), 831–843.

Huang, Y. Y., & Kandel, E. R. (1998). Postsynaptic induction and PKA-dependent expression of LTP in the lateral amygdala. *Neuron*, *21*(1), 169–178.

Hughes, J. R. (1958). Post-Tetanic Potentiation. *Physiological Reviews*, *38*(1), 91–113.

Inglebert, Y., Aljadeff, J., Brunel, N., & Debanne, D. (2021). Synaptic plasticity rules with physiological calcium levels. *Proceedings of the National Academy of Sciences of the United States of America*, *117*(52), 33639–33648.

Innes, S., Pariante, C. M., & Borsini, A. (2019). Microglial-driven changes in synaptic plasticity: A possible role in major depressive disorder. *Psychoneuroendocrinology*, *102*, 236–247.

Ito, M. (2005). Bases and implications of learning in the cerebellum - Adaptive control and internal model mechanism. *Progress in Brain Research*, *148*, 95–109.

Ju, T., Wang, X., Zhou, S., Zhao, T., Yang, M., Lin, J., Sun, L., Liu, T., Xu, Y., & Zhang, L. (2016). Streptozotocin inhibits synaptic transmission and edaravone attenuates streptozotocin-induced electrophysiological changes in CA1 pyramidal neurons of rat hippocampal slices. *NeuroToxicology*, *57*, 75–86.

Kampa, B. M., Letzkus, J. J., & Stuart, G. J. (2007). Dendritic mechanisms controlling spike-timing-dependent synaptic plasticity. *Trends in Neurosciences*, *30*(9), 456–463.

Karmarkar, U. R., & Buonomano, D. V. (2002). A model of spike-timing dependent plasticity: One or two coincidence detectors? *Journal of Neurophysiology*, *88*(1), 507–513.

Bibliography

Kartalou, G. I., Endres, T., Lessmann, V., & Gottmann, K. (2020a). Golgi-Cox impregnation combined with fluorescence staining of amyloid plaques reveals local spine loss in an Alzheimer mouse model. *Journal of Neuroscience Methods*, *341*.

Kartalou, G.-I., Rita, A., Pereira, S., Endres, T., Lesnikova, A., Casarotto, P., Pousinha, P., Delanoe, K., Edelmann, E., Castrén, E., Gottmann, K., Marie, H., & Lessmann, V. (2020b). Anti-inflammatory treatment with FTY720 starting after onset of symptoms reverses synaptic and memory deficits in an AD mouse model. *International Journal of Molecular Sciences*, *21*, 1–24.

Katz, B., & Miledi, R. (1968). The role of calcium in neuromuscular facilitation. *The Journal of Physiology*, *195*(2), 481–492.

Kayed, R., Head, E., Thompson, J. L., McIntire, T. M., Milton, S. C., Cotman, C. W., & Glabel, C. G. (2003). Common structure of soluble amyloid oligomers implies common mechanism of pathogenesis. *Science*, *300*(5618), 486–489.

Khlistunova, I., Biernat, J., Wang, Y., Pickhardt, M., Von Bergen, M., Gazova, Z., Mandelkow, E., & Mandelkow, E. M. (2006). Inducible expression of tau repeat domain in cell models of tauopathy: Aggregation is toxic to cells but can be reversed by inhibitor drugs. *Journal of Biological Chemistry*, *281*(2), 1205–1214.

Kip, S. N., Gray, N. W., Burette, A., Canbay, A., Weinberg, R. J., & Strehler, E. E. (2006). Changes in the expression of plasma membrane calcium extrusion systems during the maturation of hippocampal neurons. *Hippocampus*, *16*(1), 20–34.

Kirkwood, A., & Bear, M. F. (1994). Homosynaptic long-term depression in the visual cortex. *Journal of Neuroscience*, *14*(5 II), 3404–3412.

Klein, W. L., Krafft, G. A., & Finch, C. E. (2001). Targeting small A β oligomers: The solution to an Alzheimer's disease conundrum? *Trends in Neurosciences*, *24*(4), 219–224.

Klunk, W. E., Bacskai, B. J., Mathis, C. A., Kajdasz, S. T., McLellan, M. E., Frosch, M. P., Debnath, M. L., Holt, D. P., Wang, Y., & Hyman, B. T. (2002). Imaging Aβ Plaques in Living Transgenic Mice with Multiphoton Microscopy and Methoxy-X04, a Systemically Administered Congo Red Derivative. *Journal of Neuropathology & Experimental Neurology*, *61*(9), 797–805.

Kochlamazashvili, G., Henneberger, C., Bukalo, O., Dvoretskova, E., Senkov, O., Lievens, P. M. J., Westenbroek, R., Engel, A. K., Catterall, W. A., Rusakov, D. A., Schachner, M., & Dityatev, A. (2010). The extracellular matrix molecule hyaluronic acid regulates hippocampal synaptic plasticity by modulating postsynaptic L-type Ca2+ channels. *Neuron*, *67*(1), 116–128.

Koester, H. J., & Sakmann, B. (1998). Calcium dynamics in single spines during coincident pre- and postsynaptic activity depend on relative timing of back-propagating action potentials and subthreshold excitatory postsynaptic potentials. *Proceedings of the National Academy of Sciences of the United States of America*, *95*(16), 9596–9601.

Kramer, A. A., Ingraham, N. E., Sharpe, E. J., & Mynlieff, M. (2012). Levels of 1.2 L-Type Channels Peak in the First Two Weeks in Rat Hippocampus Whereas 1.3 Channels Steadily Increase through Development. *Journal of Signal Transduction*, 1–11.

Larsen, R. S., Smith, I. T., Miriyala, J., Han, J. E., Corlew, R. J., Smith, S. L., & Philpot, B. D. (2014). Synapse-Specific Control of Experience-Dependent Plasticity by Presynaptic NMDA Receptors. *Neuron*, *83*(4), 879–893.

Larsen, R. S., Rao, D., Manis, P. B., & Philpot, B. D. (2010). STDP in the developing sensory neocortex. *Frontiers in Synaptic Neuroscience*, *2*(9), 1–11.

Bibliography

Larson, J., & Munkácsy, E. (2015). Theta-burst LTP. *Brain Research*, *1621*, 38–50.

Larson, J., Lynch, G., Games, D., & Seubert, P. (1999). Alterations in synaptic transmission and long-term potentiation in hippocampal slices from young and aged PDAPP mice. *Brain Research*, *840*(1–2), 23–35.

Larson, J., & Munkácsy, E. (2015). Theta-burst LTP. *Brain Research*, *1621*, 38–50.

Levy, W. B., & Steward, O. (1983). Temporal contiguity requirements for long-term associative potentiation/depression in the hippocampus. *Neuroscience*, *8*(4), 791–797.

Lewis, J., Dickson, D. W., Lin, W. L., Chisholm, L., Corral, A., Jones, G., Yen, S. H., Sahara, N., Skipper, L., Yager, D., Eckman, C., Hardy, J., Hutton, M., & McGowan, E. (2001). Enhanced neurofibrillary degeneration in transgenic mice expressing mutant tau and APP. *Science*, *293*(5534), 1487–1491.

Liao, D., Hessler, N. A., & Malinow, R. (1995). Activation of postsynaptically silent synapses during pairing-induced LTP in CA1 region of hippocampal slice. *Nature*, *375*, 400–404.

Lin, T. W., Shih, Y. H., Chen, S. J., Lien, C. H., Chang, C. Y., Huang, T. Y., Chen, S. H., Jen, C. J., & Kuo, Y. M. (2015). Running exercise delays neurodegeneration in amygdala and hippocampus of Alzheimer's disease (APP/PS1) transgenic mice. *Neurobiology of Learning and Memory*, *118*, 189–197.

Lisman, J. (1989). A mechanism for the Hebb and the anti-Hebb processes underlying learning and memory. *Proceedings of the National Academy of Sciences of the United States of America*, *86*(23), 9574–9578.

Llorens-Martin, M., Blazquez-Llorca, L., Benavides-Piccione, R., Rabano, A., Hernandez, F., Avila, J., & DeFelipe, J. (2014). Selective alterations of neurons and circuits related to early memory loss in Alzheimerâ€™s disease. *Frontiers in Neuroanatomy*, *8*(MAY), 38.

Lohmann, C., & Kessels, H. W. (2014). The developmental stages of synaptic plasticity. *Journal of Physiology*, *592*(1), 13–31.

Lovett-Barron, M., Turi, G. F., Kaifosh, P., Lee, P. H., Bolze, F., Sun, X. H., Nicoud, J. F., Zemelman, B. V., Sternson, S. M., & Losonczy, A. (2012). Regulation of neuronal input transformations by tunable dendritic inhibition. *Nature Neuroscience*, *15*(3), 423–430.

Lu, H., Park, H., & Poo, M.-M. (2014). Spike-timing-dependent BDNF secretion and synaptic plasticity. *Philosophical Transactions of the Royal Society of London. Series B, Biological Sciences*, *369*(1633), 20130132.

Luchkina, N. V, Huupponen, J., Clarke, V. R. J., Coleman, S. K., Keinänen, K., Taira, T., & Lauri, S. E. (2014). Developmental switch in the kinase dependency of long-term potentiation depends on expression of GluA4 subunit-containing AMPA receptors. *Proc. Natl. Acad. Sci. USA*, *111*(11), 4321–4326.

Luque, M. A., Beltran-Matas, P., Marin, M. C., Torres, B., & Herrero, L. (2017). Excitability is increased in hippocampal CA1 pyramidal cells of Fmr1 knockout mice. *PLOS ONE*, *12*(9), e0185067.

Lynch, G., Larson, J., Kelso, S., Barrionuevo, G., & Schottler, F. (1983). Intracellular injections of EGTA block induction of hippocampal long-term potentiation. *Nature*, *305*(5936), 719–721.

Maejima, T., Oka, S., Hashimotodani, Y., Ohno-Shosaku, T., Aiba, A., Wu, D., Waku, K., Sugiura, T.,

& Kano, M. (2005). Synaptically driven endocannabinoid release requires Ca2+- assisted metabotropic glutamate receptor subtype 1 to phospholipase C β4 signaling cascade in the cerebellum. *Journal of Neuroscience*, *25*(29), 6826–6835.

Magee, J C, & Johnston, D. (1997). A synaptically controlled, associative signal for Hebbian plasticity in hippocampal neurons. *Science (New York, N.Y.)*, *275*(January), 209–213.

Magee, Jeffrey C. (1998). Dendritic hyperpolarization-activated currents modify the integrative properties of hippocampal CA1 pyramidal neurons. *Journal of Neuroscience*, *18*(19), 7613–7624.

Magee, Jeffrey C., & Johnston, D. (1997). A synaptically controlled, associative signal for Hebbian plasticity in hippocampal neurons. *Science*, *275*(5297), 209–213.

Mahajan, G., & Nadkarni, S. (2019). Intracellular calcium stores mediate metaplasticity at hippocampal dendritic spines. *Journal of Physiology*, *597*(13), 3473–3502.

Malenka, R. C., & Bear, M. F. (2004). LTP and LTD: An embarrassment of riches. *Neuron*, *44*(1), 5–21.

Maletic-Savatic, M., Lenn, N. J., & Trimmer, J. S. (1995). Differential spatiotemporal expression of K+ channel polypeptides in rat hippocampal neurons developing in situ and in vitro. *Journal of Neuroscience*, *15*(5 II), 3840–3851.

Mango, D., Saidi, A., Cisale, G. Y., Feligioni, M., Corbo, M., & Nisticò, R. (2019). Targeting Synaptic Plasticity in Experimental Models of Alzheimer's Disease. *Frontiers in Pharmacology*, *10*.

Mann, E. O., & Paulsen, O. (2007). Role of GABAergic inhibition in hippocampal network oscillations. *Trends in Neurosciences*, *30*(7), 343–349.

Markram, H., Gerstner, W., & Sjöström, P. J. (2011). A history of spike-timing-dependent plasticity. *Frontiers in Synaptic Neuroscience*, *3*(Aug), 1–24.

Markram H., Lübke J., Frotscher M., & Sakmann B. (1997). Regulation of Synaptic Efficacy by Coincidence of Postsynaptic APs and EPSPs. *Science*, *275*, 213–215.

Meredith, R. M., Floyer-Lea, A. M., & Paulsen, O. (2003). Maturation of Long-Term Potentiation Induction Rules in Rodent Hippocampus: Role of GABAergic Inhibition. *Journal of Neuroscience*, *23*(35), 11142–11146.

Miguez, A., García-Díaz Barriga, G., Brito, V., Straccia, M., Giralt, A., Ginés, S., Canals, J. M., & Alberch, J. (2015). Fingolimod (FTY720) enhances hippocampal synaptic plasticity and memory in Huntington's disease by preventing p75 NTR up-regulation and astrocyte-mediated inflammation. *Human Molecular Genetics*, *24*(17), 4958–4970.

Mihalas, S. (2011). Calcium messenger heterogeneity: A possible signal for spike-timing-dependent plasticity. *Frontiers in Computational Neuroscience*, *4*(JANUARY), 158.

Min, R., & Nevian, T. (2012). Astrocyte signaling controls spike timing-dependent depression at neocortical synapses. *Nature Neuroscience*, *15*(5), 746–753.

Mody, I. (2005). Aspects of the homeostaic plasticity of GABAA receptor-mediated inhibition. *Journal of Physiology*, *562*(1), 37–46.

Mulkey, R. M., & Malenka, R. C. (1992). Mechanisms underlying induction of homosynaptic long-

term depression in area CA1 of the hippocampus. *Neuron*, *9*(5), 967–975.

Nagahara, A. H., Merrill, D. A., Coppola, G., Tsukada, S., Schroeder, B. E., Shaked, G. M., Wang, L., Blesch, A., Kim, A., Conner, J. M., Rockenstein, E., Chao, M. V., Koo, E. H., Geschwind, D., Masliah, E., Chiba, A. A., & Tuszynski, M. H. (2009). Neuroprotective effects of brain-derived neurotrophic factor in rodent and primate models of Alzheimer's disease. *Nature Medicine*, *15*(3), 331–337.

Nazari, M., Keshavarz, S., Rafati, A., Namavar, M. R., & Haghani, M. (2016). Fingolimod (FTY720) improves hippocampal synaptic plasticity and memory deficit in rats following focal cerebral ischemia. *Brain Research Bulletin*, *124*, 95–102.

Neves, G., Cooke, S. F., & Bliss, T. V. P. (2008). Synaptic plasticity, memory and the hippocampus - a neural network aproach to causality. *Nature Reviews Neuroscience*, *9*(January 2008), 65–75.

Nevian, T., & Sakmann, B. (2004). Single Spine Ca2+ Signals Evoked by Coincident EPSPs and Backpropagating Action Potentials in Spiny Stellate Cells of Layer 4 in the Juvenile Rat Somatosensory Barrel Cortex. *Journal of Neuroscience*, *24*(7), 1689–1699.

Nevian, T., & Sakmann, B. (2006). Spine Ca2+ signaling in spike-timing-dependent plasticity. *Journal of Neuroscience*, *26*(43), 11001–11013.

Oddo, S., Caccamo, A., Shepherd, J. D., Murphy, M. P., Golde, T. E., Kayed, R., Metherate, R., Mattson, M. P., Akbari, Y., & LaFerla, F. M. (2003). Triple-transgenic model of Alzheimer's Disease with plaques and tangles: Intracellular Aβ and synaptic dysfunction. *Neuron*, *39*(3), 409–421.

Oddo, S., Vasilevko, V., Caccamo, A., Kitazawa, M., Cribbs, D. H., & LaFerla, F. M. (2006). Reduction of soluble Aβ and tau, but not soluble Aβ alone, ameliorates cognitive decline in transgenic mice with plaques and tangles. *Journal of Biological Chemistry*, *281*(51), 39413–39423.

Otto, T., Eichenbaum, H., Wible, C. G., & Wiener, S. I. (1991). Learning-related patterns of CA1 spike trains parallel stimulation parameters optimal for inducing hippocampal long-term potentiation. *Hippocampus*, *1*(2), 181–192.

Paille, V., Fino, E., Du, K., Morera-Herreras, T., Perez, S., Kotaleski, J. H., & Venance, L. (2013). GABAergic circuits control spike-timing-dependent plasticity. *Journal of Neuroscience*, *33*(22), 9353–9363.

Palmer, K., Berger, A. K., Monastero, R., Winblad, B., Bäckman, L., & Fratiglioni, L. (2007). Predictors of progression from mild cognitive impairment to Alzheimer disease. *Neurology*, *68*(19), 1596–1602.

Pang, K. K. L., Sharma, M., Krishna-K., K., Behnisch, T., & Sajikumar, S. (2019). Long-term population spike-timing-dependent plasticity promotes synaptic tagging but not cross-tagging in rat hippocampal area CA1. *Proceedings of the National Academy of Sciences*, *116*(12), 5737–5746.

Park, K., Lee, J., Jang, H. J., Richards, B. A., Kohl, M. M., & Kwag, J. (2020). Optogenetic activation of parvalbumin and somatostatin interneurons selectively restores theta-nested gamma oscillations and oscillation-induced spike timing-dependent long-term potentiation impaired by amyloid β oligomers. *BMC Biology*, *18*(1), 7.

Park, P., Kang, H., Sanderson, T. M., Bortolotto, Z. A., Georgiou, J., Zhuo, M., Kaang, B.-K., & Collingridge, G. L. (2018). The Role of Calcium-Permeable AMPARs in Long-Term

Bibliography

Potentiation at Principal Neurons in the Rodent Hippocampus. *Frontiers in Synaptic Neuroscience*, *10*(November), 42.

Pawlak, V., Wickens, J. R., Kirkwood, A., & Kerr, J. N. D. (2010). Timing is not everything: Neuromodulation opens the STDP gate. *Frontiers in Synaptic Neuroscience*, *12*(OCT), 146.

Pérez-Rodríguez, M., Arroyo-García, L. E., Prius-Mengual, J., Andrade-Talavera, Y., Armengol, J. A., Pérez-Villegas, E. M., Duque-Feria, P., Flores, G., & Rodríguez-Moreno, A. (2019). Adenosine Receptor-Mediated Developmental Loss of Spike Timing-Dependent Depression in the Hippocampus. *Cerebral Cortex*, *29*(8), 3266–3281.

Pfeiffer, T., Avignone, E., & Nägerl, U. V. (2016). Induction of hippocampal long-term potentiation increases the morphological dynamics of microglial processes and prolongs their contacts with dendritic spines. *Scientific Reports*, *6*.

Psotta, L., Rockahr, C., Gruss, M., Kirches, E., Braun, K., Lessmann, V., Bock, J., & Endres, T. (2015). Impact of an additional chronic BDNF reduction on learning performance in an Alzheimer mouse model. *Frontiers in Behavioral Neuroscience*, *9*, 58.

Puri, B. K. (2020). Calcium Signaling and Gene Expression. *Advances in Experimental Medicine and Biology*, *1131*, 537–545.

Querfurth, H. W., & Laferla, F. M. (2010). Mechanisms of Disease: Alzheimer's Disease. *N Engl J Med*, *362*, 329–373.

Radahmadi, M., Hosseini, N., & Alaei, H. (2016). Effect of exercise, exercise withdrawal, and continued regular exercise on excitability and long-term potentiation in the dentate gyrus of hippocampus. *Brain Research*, *1653*, 8–13.

Radde, R., Bolmont, T., Kaeser, S. A., Coomaraswamy, J., Lindau, D., Stoltze, L., Calhoun, M. E., Jäggi, F., Wolburg, H., Gengler, S., Haass, C., Ghetti, B., Czech, C., Hölscher, C., Mathews, P. M., & Jucker, M. (2006). Abeta42-driven cerebral amyloidosis in transgenic mice reveals early and robust pathology. *EMBO Reports*, *7*(9), 940–946.

Richards, J. G., Higgins, G. A., Ouagazzal, A. M., Ozmen, L., Kew, J. N. C., Bohrmann, B., Malherbe, P., Brockhaus, M., Loetscher, H., Czech, C., Huber, G., Bluethmann, H., Jacobsen, H., & Kemp, J. A. (2003). PS2APP transgenic mice, coexpressing hPS2mut and hAPPswe, show age-related cognitive deficits associated with discrete brain amyloid deposition and inflammation. *Journal of Neuroscience*, *23*(26), 8989–9003.

Ritter, L. M., Vazquez, D. M., & Meador-Woodruff, J. H. (2002). Ontogeny of ionotropic glutamate receptor subunit expression in the rat hippocampus. *Developmental Brain Research*, *139*(2), 227–236.

Rodríguez-Moreno, A., & Paulsen, O. (2008). Spike timing-dependent long-term depression requires presynaptic NMDA receptors. *Nature Neuroscience*, *11*(7), 744–745.

Rosenmund, C., Feltz, A., & Westbrook, G. L. (1995). Calcium-dependent inactivation of synaptic NMDA receptors in hippocampal neurons. *Journal of Neurophysiology*, *73*(1), 427–430.

Salon, M. L., Morelli, L., Castaño, E. M., Soto, E. F., & Pasquini, J. M. (2000). Defective ubiquitination of cerebral proteins in Alzheimer's disease. *Journal of Neuroscience Research*, *62*(2), 302–310.

Samorajski, T., Delaney, C., Durham, L., Ordy, J. M., Johnson, J. A., & Dunlap, W. P. (1985). Effect of exercise on longevity, body weight, locomotor performance, and passive-avoidance memory

of C57BL/6J mice. *Neurobiology of Aging*, *6*(1), 17–24.

Sarlus, H., & Heneka, M.T. (2017). Microglia in Alzheimer's disease. *J. Clin. Investig.*, *127*, 3240–3249.

Santacruz, K., Lewis, J., Spires, T., Paulson, J., Kotilinek, L., Ingelsson, M., Guimaraes, A., DeTure, M., Ramsden, M., McCowan, E., Forster, C., Yue, M., Orne, J., Janus, C., Mariash, A., Kuskowski, M., Hyman, B., Hutton, M., & Ashe, K. H. (2005). Medicine: Tau suppression in a neurodegenerative mouse model improves memory function. *Science*, *309*(5733), 476–481.

Santos, A. I., Wadman, W. J., & Costa, P. F. (1998). Sustained potassium currents in maturing CA1 hippocampal neurones. *Developmental Brain Research*, *108*(1–2), 13–21.

Scheff, S. W., Price, D. A., Schmitt, F. A., Dekosky, S. T., & Mufson, E. J. (2007). Synaptic alterations in CA1 in mild Alzheimer disease and mild cognitive impairment. *Neurology*, *68*(18), 1501–1508.

Selkoe, D. J. (2001). Alzheimer's disease: Genes, proteins, and therapy. *Physiological Reviews*, *81*(2), 741–766.

Selkoe, D. J. (2002). Alzheimer's disease is a synaptic failure. *Science*, *298* (5594), 789–791.

Semple, B. D., Blomgren, K., Gimlin, K., Ferriero, D. M., Noble-Haeusslein, L. J. (2013). Brain development in rodents and humans: Identifying benchmarks of maturation and vulnerability to injury across species. *Prog Neurobiol*, 1–16.

Seol, G. H., Ziburkus, J., Huang, S. Y., Song, L., Kim, I. T., Takamiya, K., Huganir, R. L., Lee, H. K., & Kirkwood, A. (2007). Neuromodulators Control the Polarity of Spike-Timing-Dependent Synaptic Plasticity. *Neuron*, *55*(6), 919–929.

Shankar, G. M., Bloodgood, B. L., Townsend, M., Walsh, D. M., Selkoe, D. J., & Sabatini, B. L. (2007). Natural oligomers of the Alzheimer amyloid-β protein induce reversible synapse loss by modulating an NMDA-type glutamate receptor-dependent signaling pathway. *Journal of Neuroscience*, *27*(11), 2866–2875.

Shea, D., Hsu, C. C., Bi, T. M., Paranjapye, N., Childers, M. C., Cochran, J., Tomberlin, C. P., Wang, L., Paris, D., Zonderman, J., Varani, G., Link, C. D., Mullan, M., & Daggett, V. (2019). α-Sheet secondary structure in amyloid β-peptide drives aggregation and toxicity in Alzheimer's disease. *Proceedings of the National Academy of Sciences of the United States of America*, *116*(18), 8895–8900.

Shouval, H. Z., Bear, M. F., & Cooper, L. N. (2002). A unified model of NMDA receptor-dependent bidirectional synaptic plasticity. *Proceedings of the National Academy of Sciences of the United States of America*, *99*(16), 10831–10836.

Siegelbaum, S. A., & Kandel, E. R. (1991). Learning-related synaptic plasticity: LTP and LTD. *Current Opinion in Neurobiology*, *1*(1), 113–120.

Sjöström, P. J., & Häusser, M. (2006). A Cooperative Switch Determines the Sign of Synaptic Plasticity in Distal Dendrites of Neocortical Pyramidal Neurons. *Neuron*, *51*(2), 227–238.

Sjöström, P. J., Turrigiano, G. G., & Nelson, S. B. (2001). Rate, timing, and cooperativity jointly determine cortical synaptic plasticity. *Neuron*, *32*(6), 1149–1164.

Sjöström, P. J., Turrigiano, G. G., & Nelson, S. B. (2003). Neocortical LTD via coincident activation of presynaptic NMDA and cannabinoid receptors. *Neuron*, *39*(4), 641–654.

Bibliography

Snyder, E. M., Nong, Y., Almeida, C. G., Paul, S., Moran, T., Choi, E. Y., Nairn, A. C., Salter, M. W., Lombroso, P. J., Gouras, G. K., & Greengard, P. (2005). Regulation of NMDA receptor trafficking by amyloid-β. *Nature Neuroscience*, *8*(8), 1051–1058.

Song, S., Wang, X., Sava, V., Weeber, E. J., & Sanchez-Ramos, J. (2014). In vivo administration of granulocyte colony-stimulating factor restores long-term depression in hippocampal slices prepared from transgenic APP/PS1 mice. *Journal of Neuroscience Research*, *92*(8), 975–980.

Spires-Jones, T., & Knafo, S. (2012). Spines, Plasticity, and Cognition in Alzheimer's Model Mice. *Neural Plasticity*, *2012*, 319836.

Spires-Jones, T. L., Meyer-Luehmann, M., Osetek, J. D., Jones, P. B., Stern, E. A., Bacskai, B. J., & Hyman, B. T. (2007). Impaired spine stability underlies plaque-related spine loss in an Alzheimer's disease mouse model. *American Journal of Pathology*, *171*(4), 1304–1311.

Squire, L. R., Stark, C. E. L., & Clark, R. E. (2004). The medial temporal lobe. *Annual Review of Neuroscience*, *27*(1), 279–306.

Tanaka, M.; Toldi, J.; Vecsei, L. (2020). Exploring the etiological links behind neurodegenerative diseases: Inflammatory cytokines and bioactive kynurenines. *Int. J. Mol. Sci.*, *21*, 1–33.

Tanzi, R. E., & Bertram, L. (2005). Twenty years of the Alzheimer's disease amyloid hypothesis: A genetic perspective. *Cell*, *120*(4), 545–555.

Terry, R. D., Masliah, E., Salmon, D. P., Butters, N., DeTeresa, R., Hill, R., Hansen, L. A., & Katzman, R. (1991). Physical basis of cognitive alterations in alzheimer's disease: Synapse loss is the major correlate of cognitive impairment. *Annals of Neurology*, *30*(4), 572–580.

Tong, G., Shepherd, D., & Jahr, C. E. (1995). Synaptic desensitization of NMDA receptors by calcineurin. *Science*, *267*(5203), 1510–1512.

Trinchese, F., Liu, S., Battaglia, F., Walter, S., Mathews, P. M., & Arancio, O. (2004). Progressive age-related development of Alzheimer-like pathology in APP/PS1 mice. *Annals of Neurology*, *55*(6), 801–814.

Turrigiano, G. G., & Nelson, S. B. (2004). Homeostatic plasticity in the developing nervous system. *Nature Reviews Neuroscience*, *5* (2), 97–107.

Tzounopoulos, T., Rubio, M. E., Keen, J. E., & Trussell, L. O. (2007). Coactivation of Pre- and Postsynaptic Signaling Mechanisms Determines Cell-Specific Spike-Timing-Dependent Plasticity. *Neuron*, *54*(2), 291–301.

Valtcheva, S., & Venance, L. (2016). Astrocytes gate Hebbian synaptic plasticity in the striatum. *Nature Communications*, *7*.

Vasilyev, D. V., & Barish, M. E. (2002). Postnatal development of the hyperpolarization-activated excitatory current Ih in mouse hippocampal pyramidal neurons. *Journal of Neuroscience*, *22*(20), 8992–9004.

Vos, T., Allen, C., Arora, M., Barber, R. M., Brown, A., Carter, A., Casey, D. C., Charlson, F. J., Chen, A. Z., Coggeshall, M., Cornaby, L., Dandona, L., Dicker, D. J., Dilegge, T., Erskine, H. E., Ferrari, A. J., Fitzmaurice, C., Fleming, T., Forouzanfar, M. H., … Zuhlke, L. J. (2016). Global, regional, and national incidence, prevalence, and years lived with disability for 310 diseases and injuries, 1990–2015: a systematic analysis for the Global Burden of Disease Study 2015. *The Lancet*, *388*(10053), 1545–1602.

Bibliography

Walsh, D. M., Townsend, M., Podlisny, M. B., Shankar, G. M., Fadeeva, J. V., El Agnaf, O., Hartley, D. M., & Selkoe, D. J. (2005). Certain inhibitors of synthetic amyloid β-peptide (Aβ) fibrillogenesis block oligomerization of natural Aβ and thereby rescue long-term potentiation. *Journal of Neuroscience*, *25*(10), 2455–2462.

Wang, H.-X., Gerkin, R. C., Nauen, D. W., & Bi, G.-Q. (2005). Coactivation and timing-dependent integration of synaptic potentiation and depression. *Nature Neuroscience*, *8*(2).

Watanabe, S., Hoffman, D. A., Migliore, M., & Johnston, D. (2002). Dendritic K+ channels contribute to spike-timing dependent long-term potentiation in hippocampal pyramidal neurons. *Proceedings of the National Academy of Sciences of the United States of America*, *99*(12), 8366–8371.

Wiesel, T. N., & Hubel, D. H. (1965). Extent of recovery from the effects of visual deprivation in kittens. *Journal of Neurophysiology*, *28*(6), 1060–1072.

Yang, S. N., Tang, Y. G., & Zucker, R. S. (1999). Selective induction of LTP and LTD by postsynaptic [Ca2+](i) elevation. *Journal of Neurophysiology*, *81*(2), 781–787.

Yasuda, H., Barth, A. L., Stellwagen, D., & Malenka, R. C. (2003). A developmental switch in the signaling cascades for LTP induction. *Nature Neuroscience*, *6*(1), 15–16.

Zhang, W., & Linden, D. J. (2003). The other side of the engram: Experience-driven changes in neuronal intrinsic excitability. *Nature Reviews Neuroscience*, *4*(11), 885–900.

Zhao, M., Choi, Y. S., Obrietan, K., & Dudek, S. M. (2007). Synaptic plasticity (and the lack thereof) in hippocampal CA2 neurons. *Journal of Neuroscience*, *27*(44), 12025–12032.

Zott, B., Simon, M. M., Hong, W., Unger, F., Chen-Engerer, H. J., Frosch, M. P., Sakmann, B., Walsh, D. M., & Konnerth, A. (2019). A vicious cycle of β amyloid−dependent neuronal hyperactivation. *Science*, *365*(6453), 559–565.

Zucker, R. S., & Regehr, W. G. (2002). Short-Term Synaptic Plasticity. *Annual Review of Physiology*, *64*(1), 355–405.

Publication and poster presentation list

Parts of this dissertation have been published under the following titles:

Publications:

Machhindra Garad, Elke Edelmann, Volkmar Leßmann (2021). Impairment of spike timing-dependent plasticity at Schaffer collateral-CA1 synapses in adult APP/PS1 mice depends on proximity of Aβ plaques. *Int. J. Mol. Sci.*, *22*(3), 1378. doi.org/ 10.3390/ijms22031378.

Machhindra Garad, Elke Edelmann, Volkmar Leßmann. Long-term depression at hippocampal mossy fiber-CA3 synapses depends on proBDNF but is not mediated by p75NTR signaling. (In revision, *Sci. Rep.*)

Poster and oral presentations:

Impairment of spike timing-dependent plasticity in the hippocampal CA1 area of an APP/PS1 Alzheimer disease mouse model (German Physiological Society, oral presentation, Ulm, Germany 2019)

Spike timing-dependent plasticity in hippocampal CA1 pyramidal neurons of 6 months old Alzheimer's disease mice. (Federation of European Neuroscience Societies, Berlin, Germany 2018).

Long-term depression (LTD) at hippocampal mossy fiber-CA3 synapses in rodents is independent of BDNF signaling unlike Schaffer collateral-CA1 synapses. (German Neuroscience Society, Göttingen, Germany 2017).

Aging and Alzheimer`s disease influence on spike timing-dependent plasticity and basal electrical properties of CA1 pyramidal neurons in rodent hippocampus. (Psychopharmacology winter school, Elevator pitch and poster, Crete, Greece 2017).

Declaration of Honor

„I hereby declare that I prepared this thesis entitled

Spike timing-dependent plasticity and basal synaptic transmission characterization at hippocampal Schaffer collateral -CA1 synapses of adult APP/PS1 Alzheimer's disease mice

without impermissible help of third parties and that none other than the indicated tools have been used; all sources of information are clearly marked, including my own publications.

In particular I have not consciously:
• Fabricated data or rejected undesired results
• Misused statistical methods with the aim of drawing other conclusions than those warranted by the available data
• Plagiarized external data or publications
• Presented the results of other researchers in a distorted way

I am aware that violations of copyright may lead to injunction and damage claims of the author and also to prosecution by the law enforcement authorities.
I hereby agree that the thesis may be reviewed for plagiarism by mean of electronic data processing.
This work has not yet been submitted as a doctoral thesis in the same or a similar form in Germany or in any other country. It has not yet been published as a whole."

(Place, Date)

(Signature)